

UNIVERSITY OF BELGRADE
FACULTY OF MEDICINE

Valentina S. Ćirković

**PHYLOGENETIC ANALYSIS OF
HANTAVIRAL MOLECULAR EVOLUTION
IN DIFFERENT RODENT SPECIES**

Doctoral Dissertation

Belgrade, 2018

UNIVERZITET U BEOGRADU
MEDICINSKI FAKULTET

Valentina S. Ćirković

**FILOGENETSKA ANALIZA
MOLEKULARNE EVOLUCIJE
HANTAVIRUSA U RAZLIČITIM VRSTAMA
GLODARA**

Doktorska disertacija

Beograd, 2018

INFORMATION ON PROMOTERS AND DISSERTATION COMMITTEE

Promoters:

Prof. dr Maja Stanojević, Institute of Microbiology and Immunology, Associate Professor at Faculty of Medicine, University of Belgrade, Belgrade, Serbia

Dr Gorana Stamenković, Senior Research Associate, Department of Genetic Research, Institute for Biological Research “Siniša Stanković”, University of Belgrade, Belgrade, Serbia

Dissertation committee:

Chair

Prof. dr Aleksandra Knežević, Associate Professor at Faculty of Medicine, University of Belgrade, Belgrade, Serbia

Committee members

Prof. dr Anna Papa-Konidari, full Professor at A' Department of Microbiology, Medical School, Aristotle University of Thessaloniki, Thessaloniki, Greece

Dr Sanja Glišić, Senior Research Associate, Vinča Institute of Nuclear Sciences, University of Belgrade, Belgrade, Serbia

Dr Snežana Tomanović, Senior Research Associate, Institute for Medical Research, University of Belgrade, Belgrade, Serbia

Prof. dr Ivana Lazarević, Associate Professor at Faculty of Medicine, University of Belgrade, Belgrade, Serbia

Ova doktorska disertacija je urađena na Institutu za mikrobiologiju i imunologiju Medicinskog fakulteta Univerziteta u Beogradu.

Prvo želim da izrazim posebnu zahvalnost mentorkama profesorki dr Maji Stanojević i Dr Gorani Stamenković na ukazanom poverenju i svestranoj pomoći tokom izrade ovog rada. Zahvalna sam vam što ste me uvele u predivni svet naučno istraživačkog rada i što ste svojom stručnošću i autoritetom odredile moje profesionalno opredeljenje.

Posebnu zahvalnost želim da iskažem pre svega iskrenoj prijateljici i kolegici Dr Marini Šiljić. Njeno angažovanje u svim fazama ovog rada, posvećeno vreme kao i sjajne ideje i korisni predlozi doprineli su u velikoj meri realizaciji ove doktorske disertacije.

Takođe bih se zahvalila i kolegicama dr Ini Gajić i dr Danijeli Karalić na stručnoj i pre svega prijateljskoj podršci.

Zahvaljujem se svim članovima komisije, koji su svojim stručnim sugestijama i dobronamernim savetima doprineli da ova doktorska disertacija ima ovakav oblik.

Θα ήθελα να εκφράσω τις πιο θερμές ευχαριστίες μου στην Καθηγήτρια Άννα Παπά-Κονιδάρη που ως μέλος της συμβουλευτικής επιτροπής συνέβαλλε σημαντικά στη επιτυχή διεξαγωγή της διατριβής μου

Zahvaljujem se kolegama sa Instituta za biološka istraživanja “Siniša Stanković” kao i kolegama sa Vojnomedicinske akademije u Beogradu koje su mi ustupile uzorke koji su bili predmet izučavanja u ovoj doktorskoj disertaciji.

Neizmernu zahvalnost dugujem svojoj porodici, svojim roditeljima i sestri, na beskrajnoj ljubavi i podršci. Dragi roditelji, hvala vam na svemu što ste učinili za mene i što ste od mene napravili vrednu i poštenu osobu.

Dejanu, mom suprugu i najboljem prijatelju, veliko hvala na iskrenoj ljubavi i bezrezervnoj podršci koju mi pruža. Mojoj ćerki Dunji hvala na najčistijoj ljubavi koja me je učinila boljom osobom i na beskrajnoj radosti koju mi pruža svakoga dana.

*Posvećeno
Mojim roditeljima*

SUMMARY

Phylogenetic analysis of hantaviral molecular evolution of in different rodent species

Introduction

Hantaviruses, members of the order *Bunyavirales*, family *Hantaviridae*, are enveloped viruses with a negative sense three-segmented RNA genome, consisting of large – L (6.5–6.6 kb), medium – M (3.6–3.7 kb) and small – S (1.7–2.0 kb) segments, coding for viral polymerase, viral glycoprotein precursor further processed into two separate envelope glycoproteins (Gn and Gc) and viral nucleocapsid protein, respectively. Hantaviruses are unique among the bunyaviruses in not being transmitted by an arthropod vector. These viruses are persistently active in their natural reservoirs including rodents, insectivores and bats. In nature, hantaviruses are circulating via horizontal transmission among infected natural reservoirs. Their primary natural hosts are rodents belonging to four different subfamilies, including *Sigmodontinae*, *Arvicolinae*, *Murinae* and *Neotominae*. Newly published data have extended hantavirus hosts to insectivores (families *Soricidae* and *Talpidae*) and bats (order *Chiroptera*). Hantaviruses are commonly divided into two groups: old world hantaviruses, present in Europe and Far East, mostly including pathogenic hantavirus species that cause hemorrhagic fever with renal syndrome (HFRS), and new world hantaviruses, present in the Americas, defined as etiological agents of hantavirus pulmonary syndrome (HPS). Mortality rates of these zoonotic diseases, caused by pathogenic hantaviruses, vary with up to 12%-18% for HFRS and 60% for HPS. Human infection occurs through respiratory exposure to contaminated secretions and excreta including urine, saliva, and feces. Humans are not among the natural hosts of hantaviruses and they are thought to be dead-end hosts, without further virus transmission, with the exception of few reported cases of human-to-human transmission of Andes virus (ANDV) in Argentina and Chile.

Hantaviruses, as segmented RNA viruses, are known to be highly variable with substitution rates of 10^{-2} to 10^{-4} substitutions/site/year. Genetic drift, homologous recombination and reassortment have been main proposed mechanisms for genetic diversity of hantaviruses. This thesis focuses on the evolutionary analyses of hantaviral sequence data. Multitude of phylogenetic methods, including phylodynamic and phylogeographic analyses, were employed to examine complex biological processes, such as evolutionary dynamics, natural selection, recombination and migration of hantaviruses.

The Aims of the Study

The aims of this study were to detect and genetically characterize hantavirus RNA recovered from different rodent reservoirs captured in Serbia. Moreover, the objectives included investigation of molecular evolution of hantaviruses by phylogenetic analysis of different genomic segments, including phylodynamic and phylogeographic analysis. Finally, the aim was to investigate the presence and properties of homologous recombination in hantavirus genomes.

Materials and Methods

The study was based on the sample pool from previous surveys conducted on the total of 350 rodents trapped in Serbia on several occasions during 5-year period (2007-2011). Of 350 rodents, 110 animals were genetically tested within the study of this thesis. The total RNA was extracted from tissues samples using the TRIZOL Reagent (GibcoBRL, Invitrogen, Karlsruhe, Germany). Nested-PCR (Polymerase chain reaction) method was used for amplification of the all three hantavirus segments. All obtained specific PCR products were directly sequenced and further analyzed by different phylogenetic and other bioinformatics approaches. For different purpose of phylogenetic analysis several data sets of partial L, M and S segments were made. The obtained L segment sequences were first analyzed by BLAST at NCBI (<http://blast.ncbi.nlm.nih.gov/Blast.cgi>) in order to determine similarity scores to specific hantaviruses. Further phylogenetic analysis was done under the best fit model of nucleotide substitution, obtained by jModelTest 0.1.1. Phylogenetic trees were inferred using different methods, including ML and Bayesian methods. Potential

recombination events were analyzed by BootScan method. In order to investigate the ancestral location and the spread of the virus, appropriate data set was analyzed using Bayesian framework with Markov Chain Monte Carlo (MCMC) method implemented in the Beast software package v 1.8.4.

Results

In total, encompassing all the tested rodent species, 6/110 (5.5%) genetically tested samples in the study were found positive for hantavirus. Positive samples were found in the species *A. flavicollis*, *A. agrarius*, *G. glis* and *M. arvalis*. Notably, *A. flavicollis* was the most abundant tested species, with hanta RNA positivity rate of 9.7% among the seropositive animals, 4.3% in total. According to the BLAST analysis, obtained isolates from three *A. flavicollis*, one *A. agrarius* and one *G. glis* were identified as Dobrava-Belgrade virus (DOBV) and the isolate recovered from *M. arvalis* was identified as Tula virus (TULV). Phylogenetic analysis based on partial L segment confirmed the results obtained by BLAST analysis. Namely, in the phylogenetic tree based on 37 L segment sequences, strains from Serbia clustered in a distinctive branch of Dobrava genotypes with strains from Greece, Slovenia and Turkey. In addition, partial M segment was recovered from all three samples of *A. flavicollis*. Overall nucleotide distance among all examined DOBV M segment sequences was 15.07% (SD±0.07). In the phylogenetic tree based on partial 16 M segment sequences all three Serbian sequences, isolated from *A. flaviollis*, were clustered together with other strains belonging to Dobrava genotype. Partial S segment was recovered from all samples, except one from *A. flavicollis*. Overall nucleotide diversity found in the partial S segment alignment was in the expected range of 7.95% (SD±0.06), with average distance between all Serbian strains of 2.21% (SD±0.09). In the phylogenetic tree based on 180 partial S segment sequences isolated from human and rodent samples all Serbian strains were also clustered together within Dobrava genotype. In the phylogenetic analysis of TULV S segment sequences were included two sequences from Serbia: TULV strain from *M. subterraneus* (AF017659) and the other one from *M. arvalis*, together with 64 sequences originating from different European and Asian countries. Phylogenetic tree based on 66 TULV S segment sequences of 570 nt (400-966 nt) showed the existence of different clusters matching to territory of sequences origin. Sequences from Serbia were closely related to those from East Slovakia (Y13980 and Y13979), forming clearly

separated cluster. Moreover, based on Bootscan recombination analysis, Serbian strains were detected as potential recombinants. Obtained results revealed the existence of two recombination peaks exceeding the cut-off of 70% bootstrap in both sequences from Serbia: one peak corresponding to S segment regions from positions around 600 to 750 nt that clustered together with TULV sequences from Czech Republic and West Slovakia; while the other clearly resolved peak, between positions 750 and 950 nt, clustered with TULV sequences from Russia. Reconstructed phylogenetic subtrees were in correlation with corresponding peaks proposed by bootscan analysis. Moreover, phylogeographic analysis results of TULV S segment sequences placed the root of origin in Kazakhstan, with posterior probability 1.

Conclusions

During the five-year study period (2007-2011) two hantaviruses, Dobrava-Belgrade virus (DOBV) and Tula virus (TULV), were genetically characterized in four different rodent species: *A. flavicollis*, *A. agrarius*, *G. glis* and *M. arvalis*. *Glis glis* species was found as the novel host and putative natural reservoir of DOBV, since this species, or any other species of the *Gliridae* rodent family, has not been previously associated with hantaviral infection. Potential DOBV spillover infection from *A. flavicollis* could not be excluded. Molecular screening of *A. flavicollis* from mountain Tara in western Serbia detected the presence of DOBV in tested animals, revealing this locality as a novel DOBV focus in the Balkans. Phylogenetic analyses of all three RNA segments (L, M and S) revealed that all Serbian DOBV strains from the novel focus belong to the DOBV-Dobrava genotype. Molecular screening of different rodent species in central Serbia detected TULV in *M. arvalis*. Phylogenetic analysis of both L and S segment sequences of the newly detected TULV strain was suggestive of geographically related clustering, as previously shown for the majority of hantaviruses. Exploratory recombination analysis, supported by phylogenetic and amino acid pattern analysis, revealed the presence of recombination in the S segment of the Serbian TULV, resulting in mosaic-like structure, similar to the one of Kosice strain originating from east Slovakia. Phylogeographic analysis of TULV S segment sequences placed the potential root and origin of TULV spread in central Asia, most probably in Kazakhstan. Phylogeographic analysis implied single introduction of TULV to Europe from central Asia, with the complex

pattern of local viral migration, including single introduction to Serbia with further spread locally and also to Slovakia.

Keywords: hantavirus, DOBV, TULV, rodents, phylogenetic analysis, recombination, phylogeography

Scientific field: Molecular Medicine / Virology

REZIME

Filogenetska analiza molekularne evolucije hantavirusa u različitim vrstama glodara

Uvod

Hantavirusi, taksonomski svrstani u red *Bunyavirales*, familija *Hantaviridae*, su virusi sa omotačem i negativnim jednolančanim RNK genomom koji je segmentiran i sastoji se od velikog – L (6.5–6.6 kb), srednjeg – M (3.6–3.7 kb) i malog – S (1.7–2.0 kb) segmenta. L segment kodira virusnu polimerazu, M segment kodira glikoproteinski prekursor od koga nastaju dva glikoproteina (Gn i Gc) i S segment kodira nukleokapsidni protein. Za razliku od ostalih bunjavirusa, transmisija hantavirusa se ne odvija putem artropodnog vektora. Ovi virusi trajno cirkulišu u svojim prirodnim rezervoarima koji obuhvataju glodare, insektivore i slepe miševе. U prirodi, hantavirusi se prenose putem horizontalne i vertikalne transmisije između zaraženih životinja. Najznačajniji rezervoari hantavirusa su glodari koji pripadaju različitim potfamilijama (*Sigmodontinae*, *Arvicolinae*, *Murinae* and *Neotominae*). Hantavirusi su podeljeni u dve grupe: hantavirusi starog sveta (prisutni u Evropi i na dalekom istoku) koji obuhvataju patogene vrste hantavirusa koji izazivaju hemoragijsku groznicu sa bubrežnim sindromom (HGBS) i hantavirusi novog sveta (prisutni u Americi) koji obuhvataju patogene vrste hantavirusa koji izazivaju hantavirusni pulmonarni sindrom (HPS). Stopa smrtnosti kod ovih zoonoza, uzrokovanih patogenim vrstama hantavirusa, varira od 12-18% za HGBS i do 60% za HPS. Čovek se inficira respiratornim putem u kontaktu sa izlučevinama zaraženih životinja (urin, feces, pljuvačka). S obzirom da čovek nije prirodni domaćin hantavirusa, dalji interhumani prenos hantavirusa nije moguć, sa izuzetkom nekoliko opisanih slučajeva prenosa Andes virusa (ANDV) u Čileu i Argentini. Hantavirusi, kao virusi sa segmentiranim RNK genomom, spadaju u visoko varijabilne mikroorganizme sa supstitucionom stopom od 10^{-2} - 10^{-4} izmena/mestu/godini. Genetički drift, homologa rekombinacija i izmena genskih segmenata su glavni mehanizmi koji leže u osnovi evolucije hantavirusa. U ovom istraživanju smo se fokusirali na analizu evolucije hantavirusa. Različite filogenetske metode, uključujući

filodinamsku i filogeografsku analizu, su primenjene u svrhu izučavanja bioloških procesa kao što su dinamika evolucije, prirodna selekcija, rekombinacija i kretanje hantavirusa.

Ciljevi

Ciljevi ove studije bili su detekcija i genetska karakterizacija hantavirusne RNK dobijene iz različitih prirodnih rezervoara. Istraživanje je takođe obuhvatilo analizu molekularne evolucije sva tri segmenta genoma hantavirusa primenom različitih filogenetskih metoda, uključujući filodinamsku i filogeografsku analizu. Poslednji cilj je bio ispitivanje prisustva homologe rekombinacije u okviru hantavirusnog genoma.

Materijali i metode

U okviru ove teze su molekularnim metodama testirani uzorci 110 glodara koji su bili dostupni za analizu iz ukupnog pula od 350 uzoraka dobijenih u više izlovljavanja tokom petogodišnjeg perioda (2007-2011), u okviru drugih istraživanja. Ukupna RNK iz tkiva je izolovana primenom TRIZOL-nog reagensa GibcoBRL, Invitrogen, Karlsruhe, Germany). Delovi sva tri segmenta su umnoženi metodom reakcije lančane polimerizacije u dva kruga (engl. „nested polymerase chain reaction“-nested PCR). DNK sekvence svih pozitivnih PCR produkata su analizirane filogenetskim i drugim bioinformatičkim metodama, uz formiranje odgovarajućih setova sekvencu za analizu uključivanjem postojećih u NCBI bazi podataka (<http://blast.ncbi.nlm.nih.gov>). Početna identifikacija dobijenih sekvenci L segmenta vršena je primenom BLAST alatke, poređenjem sa postojećim sekvencama u NCBI bazi podataka (<http://blast.ncbi.nlm.nih.gov/Blast.cgi>). Filogenetska analiza je rađena na osnovu nukleotidnog supstitucionog modela, određenog primenom jModelTest-a 0.1.1. Filogenetska stabla su konstruisana primenom metoda maksimalne verovatnoće i Bajesove statistike. Potencijalna rekombinacija je analizirana primenom BootScan metode. U cilju ispitivanja putanja širenja virusa, odgovarajući set sekvenci je analiziran primenom Bajesove statistike implementirane u Beast program v 1.8.4.

Rezultati

Pozitivan nalaz hantavirusne RNK nađen je u 6/110 (5.5%) ukupno testiranih uzoraka, uključujući sve testirane vrste glodara. Pozitivni uzorci su nađeni među vrstama: *A. flavicollis*,

A. agrarius, *G. glis* i *M. arvalis*. Najvbrojnija testirana vrsta bio je *A. flavicollis*, gde je procenat pozitivnih uzoraka na hanatvirusnu RNK bio 9,7% među seropositivnim životinjama (ukupno 4.3%). Na osnovu BLAST analize, pet dobijenih sekvenci, od kojih su tri izolovane iz *A. flavicollis*-a, jedna iz *A. agrarius*a i jedna iz *G. glis*a su identifikovane kao Dobrava-Beograd virus (DOBV). Šesta sekvenca, koja je izolovana iz *M. arvalis*-a, je identifikovana kao Tula virus (TULV). Filogenetska analiza seta sekvenci za L segment potvrdila je prethodno dobijene rezultate primenom BLAST analize. U filogenetskom stablu, konstruisanom na osnovu seta od 37 sekvenci za L segment, sve sekvence poreklom iz Srbije su se grupisale zajedno sa sekvencama iz Grčke, Slovenije i Turske koje su definisane kao Dobrava genotip. M segment je uspešno izolovan iz sva tri uzorka *A. flavicollis*-a. Ukupna nukleotidna distanca na nivou M segmenta iznosila je 15.07% (SD±0.07). U filogenetskom stablu, konstruisanom na osnovu 16 parcijalnih sekvenci za M segment, sva tri srpska izolata su svrstana u isti u okviru Dobrava genotipa. Sekvence za S segment su dobijene iz svih uzoraka koji su prethodno bili pozitivni na L segment, osim iz jednog uzorka *A. flavicollis*-a. Ukupna nukleotidna distanca na nivou S segmenta iznosila je 7.95% (SD±0.06), dok je prosečna nukleotidna distanca za sve isolate iz Srbije iznosila 2.21% (SD±0.09). U filogenetskom stablu konstruisanom na osnovu 180 parcijalnih sekvenci S segmenta, svi izolati iz Srbije su takođe svrstani u isti klaster u okviru Dobrava genotipa. U filogenetsku analizu sekvenci S segmenta TULV uključena su dva srpska izolata (sekvenca iz *M. arvalis*a dobijen u ovoj studiji i ranije publikovna izolat iz *M. subterraneusa*) zajedno sa još 64 sekvence preuzete sa NCBI baze podataka. U filogenetskom stablu konstruisanom na osnovu 66 sekvenci, dužine 570 nt (400-966 nt), jasno se vidi postojanje nekoliko klastera koji odgovaraju teritoriji sa koje su sekvence izolovane. Srpski izolati su se jasno klasterovali sa izolatima (Y13980 and Y13979) iz istočne Slovačke. Rekombinaciona bootscan analize ukazala je na postojanje rekombinacije u navedenim sekvencama iz Srbije. Dobijeni rezultati su pokazali postojanje dva rekombinaciona pika sa butstrep podrškom iznad 70% u oba srpska izolata: prvi pik, koji je odgovarao regionu S segmenta između pozicija 600 i 750, se klasterovao zajedno sa sekvencama iz Češke Republike i zapadne Slovačke, dok je drugi pik, koji je odgovarao regionu S segmenta između pozicija nt 750 i 950, se klasterovao zajedno sa sekvencama iz Rusije. Parcijalna filogenetska stabla („podstabla“), koja su konstruisana na osnovu dobijenih pikova bila su u jasnoj korelaciji sa rezultatima dobijenim bootscan analizom. Rezultati filogeografske analize, rađene na osnovu

sekvenci S segmenta TULV pokazali su da je najverovatnije mesto porekla ovog virusa Kazahstan sa posteriornom verovatnoćom od 1.

Zaključak

U uzorcima iz ispitivanog petogodišnjeg perioda (2007-2011.) genetički je dokazano prisustvo dva hantavirusa: Dobrava-Beograd virus (DOBV) i Tula virus (TULV), u četiri različite glodarske vrste: *A. flavicollis*, *A. agrarius*, *G. glis* i *M. arvalis*. Od navedenih, vrsta *Glis glis* do sada nije bila opisana kao domaćin i mogući DOBV rezervoar, kao ni bilo koja druga vrsta iz familije *Gliridae*. Nije isključeno potencijalno prelivanje infekcije iz vrste *A. flavicollis*. Molekularnim skriningom utvrđeno je prisustvo DOBV u uzorcima jedinki *A. flavicollis* izlovljenih u regiji planine Tare u zapadnoj Srbiji, što predstavlja novodokumentovano prirodno žarište DOBV infekcije na Balkanu. Filogenetskom analizom sva tri genomska segmenta utvrđeno je da svi novo-okarakterisani DOBV sojevi spadaju u DOBV-Dobrava genotip virusa. Molekularnim skriningom različitih uzoraka glodara iz centralne Srbije utvrđeno je prisustvo TULV u jedinki *M. arvalis*. Filogenetska analiza navedenog soja, uporedno sa postojećim sekvencama u bazi podataka, pokazala je grupisanje u skladu sa geografskim poreklom uzorka, kao što je od ranije poznao za većinu hantavirusa. Ekspolrativna analiza rekombinacije, uporedo sa filogenetskom analizom i analizom aminokiselinskih obrazaca, pokazala je postojanje rekombinacije u ispitivana 2 TULV soja iz Srbije. Slična struktura rekombinacije je ranije opisana kod TULV sojeva Košice, iz Slovačke. Filogeografskom analizom svih sekvenci TULV S segmenta u postojećim bazama podataka geografski izvor širenja TULV je lociran u srednjoj Aziji, najverovatnije u Kazahstanu, odakle je virus jednokratno uveden u Evropu, sa složenim daljim širenjem u okviru kog je jednokratno uveden u regiju Srbije odakle se najverovatnije proširio ka Slovačkoj.

Ključne reči: hantavirus, DOBV, TULV, glodari, filogenetska analiza, rekombinacija, filogeografija

Naučna disciplina: Molekularna medicina / Virusologija

TABELE OF CONTENTS

1. INTRODUCTION	1
1.1. HISTORICAL OVERVIEW	3
1.2. HANTAVIRUS CLASSIFICATION	4
1.3. VIRUS STRUCTURE AND LIFE CYCLE	6
1.3.1. Virion structure	6
1.3.2. Hantaviral life cycle	9
1.4. PATHOGENESIS OF HANTAVIRUS DISEASES	10
1.4.1. Hemorrhagic fever with renal syndrome (HFRS)	12
1.4.2. Hantavirus pulmonary syndrome (HPS)	13
1.5. HANTAVIRUS ECOLOGY	14
1.6. HANTAVIRUS EPIDEMIOLOGY	19
1.7. EVOLUTION OF HANTAVIRUSES	25
2. AIMS OF THE STUDY	38
3. MATERIALS AND METHODS	40
3.1. STUDY DESIGN AND ETHICAL APPROVAL	41
3.2. RODENT TRAPPING AND SPECIES IDENTIFICATION	41
3.3. RNA EXTRACTION FROM TISSUE SAMPLES	43
3.4. NESTED POLYMERASE CHAIN REACTION	43
3.5. AGAROSE GEL ELECTROPHORESIS	46
3.6. CYCLE SEQUENCING RECTION	47
3.6.1. Purification of pcr products	47
3.6.2. Cycle sequencing reaction	48
3.7. SEQUENCE DATASETS	49
3.8. PHYLOGENETIC ANALYSES	49
3.8.1. Identification and characterization of hantaviral RNA obtained from different animal reservoirs	50

3.8.2. Phylogenetic trees reconstruction	51
3.8.3. Selective pressure.....	52
3.8.4. Recombination analysis.....	53
3.8.5. Bayesian phylogenetic analysis of phylodynamics and phylogeography	54
4. RESULTS	57
4.2. HANTAVIRUS DETECTION AND IDENTIFICATION	59
4.3. COMPARATIVE PHYLOGENETIC ANALYSIS OF PARTIAL L, M AND S SEGMENT SEQUENCES OF DOBV	61
4.3.1. Phylogenetic analysis of partial DOBV L segment sequences	63
4.3.2. Phylogenetic analysis of partial DOBV M segment sequences.....	65
4.3.3. Phylogenetic analysis of partial DOBV S segment sequences	67
4.4. DETAILED PHYLOGENETIC ANALYSIS OF DOBV IN THE NEWLY FOUND NATURAL HOST	71
4.5. PHYLOGENETIC ANALYSIS OF DOBV FROM NEWLY DESCRIBED FOCUS IN THE BALKANS	73
4.6.1. Phylogenetic analysis of the partial TULV L segment sequences	76
4.6.2. Phylogenetic analysis of the partial TULV S segment sequences	78
4.7. RECOMBINATION ANALYSIS OF TULV STRAINS	81
4.8. BAYESIAN PHYLOGENETIC ANALYSIS OF TULV PHYLODYNAMICS AND PHYLOGEOGRAPHY	88
5. DISCUSSION.....	95
6. CONCLUSIONS.....	113
7. REFERENCES	116
APPENDIX	145

1. INTRODUCTION

Hantaviruses are endemically present in the Balkan region, particularly in Serbia, where sporadic cases and/or outbreaks of disease caused by these pathogens have been reported repeatedly. The first clinical and epidemiological evidence of hantaviral infection in Serbia date to the middle of the last century (Heneberg et al., 1964). In 1986, the first serological findings of hantaviral infection in both humans and small mammals in Serbia were made (Gligic et al., 1989a, 1989b). In 1989, the first isolation of Belgrade virus (subsequently named Dobrava–Belgrade virus) was made from a human sample in Belgrade, Serbia (Gligic et al., 1992). Moreover, in the Balkans, Serbia was the first country where Tula virus was detected, in European pine vole, *M. subterraneus* (Song et al., 2002). So far, serological findings imply circulation of multiple hantaviruses in Serbia, whereas molecular data about circulating hantaviruses in Serbia are lacking.

1.1. HISTORICAL OVERVIEW

Epidemic hemorrhagic fever was described for the first time among soldiers of the United Nations during the war between North and South Korea in 1951 (Smadel, 1953; Powel, 1953). Ever since, it has been known as Korean hemorrhagic fever (KHF) and it has remained endemic in the vicinity of the demilitarized zone between North and South Korea. The main symptoms were fever, headache, pain in the back and abdomen, a flushed face and various haemorrhagic manifestations with mortality rate of 5-10%. However, at the same time similar illness was also described in Sweden, whereas during 1930's Japanese physicians had met a disease with similar symptoms in Manchuria (Myhrman, 1951). At that time, illness was extensively investigated, but the etiological agent was not detected.

In former Yugoslavia, the first case with similar symptoms was recognized in 1951 (Simic, 1952). The patient was a soldier who got infected in the forest surrounding Fojnica in Bosnia and Herzegovina (B&H), a region where a few outbreaks with hundreds of HFRS cases have been noted further on (Hukic et al., 2011). In the following years clinical cases of hemorrhagic fever were also recognized in Albania (Eltari et al., 1987), Bulgaria (Verbevand Gabev, 1963), Greece (Antoniadis et al., 1984) and Romania (Manasia et al., 1977). The first documented epidemic was reported in a military camp in the forest of Fruska Gora in Serbia in 1961 (Heneberg et al., 1964). Subsequent epidemic occurred few years later, in 1967, located in B&H (region of Fojnica and Foca) and also in Croatia (Plitvice Lakes) (Vesenjok-Hirjan et al., 1971).

Throughout the following years there have been many failed attempts to isolate the causative agent of KHF. Finally, in 1978 Hantaan virus (HTNV) was isolated by Lee and collaborators, from field mouse *Apodemus agrarius* caught at the banks of the river Hantaan, located at the border between North and South Korea (Lee et al., 1978). Very soon after its' initial isolation, in 1982, the etiological agent of haemorrhagic fever was isolated in former Yugoslavia (Antonijevic and Gligic, 1982). Virus was isolated from a female patient, by propagating of human material into mouse brain.

Almost at the same time hemorrhagic fever with similar clinical symptoms had been recognized in Scandinavia where it was called Nephropathia Epidemica (NE) (Lahdevirta, 1971). In 1980 Puumala virus (PUUV), ethological agent of NE, was isolated from *Myodes glareolus* (bank vole) (Yanagihara et al., 1984). Both above mentioned diseases (KHF and NE)

are named hemorrhagic fever with renal syndrome (HFRS) and characterized by the same geographic distribution from Europe to Far East.

However, the first ever hantavirus was isolated in India in 1971, from shrew (*Suncus murinus*) (Carey et al., 1971). Relatedness of this Thottapalayam hantavirus to other hantaviruses was recognized many years later.

In the Americas, the first hantavirus was described in 1983. It was Prospect Hill (PHV) hantavirus, isolated from meadow vole (*Microtus pennsylvanicus*) (Yanagihara et al., 1984). However, this virus has never been associated with any disease, so it was the first model for a non-pathogenic hantavirus. In contrast to it, Sin Nombre (SNV) virus was isolated as ethological agent of hantavirus pulmonary syndrome (HPS), near the Four Corners point in the United States in 1993 (Childs et al., 1994).

1.2. HANTAVIRUS CLASSIFICATION

Hantaviruses are commonly divided into two groups: old world hantaviruses, present in Europe and Far East, mostly including pathogenic hantavirus species that cause HFRS, and new world hantaviruses, present in the Americas, defined as etiological agent of HPS. **Table 1** lists all known rodent- soricomorph- and chiroptera-borne hantaviruses together with their geographic distribution (Jonsson et al., 2010; Yanagihara et al., 2014).

Taxonomically, over 40 hantavirus species were grouped within the Hantavirus genus of the family *Bunyaviridae* (Heyman et al., 2009). The family *Bunyaviridae* also included four other genera *Tospovirus*, *Phlebovirus*, *Nairovirus* and *Orthobunyavirus* (Elliott et al., 2000). However, in the new classification proposed by International Committee on Taxonomy of Viruses (ICTV) the new order, *Bunyavirales*, has been established and further divided into three viral families: *Feraviridae*, *Fimoviridae* and *Hantaviridae* (https://talk.ictvonline.org/ictv-reports/ictv_online_report/). The family *Hantaviridae* includes one genus (*Orthohantavirus*) with 41 species.

The features encompassing all these viruses into a single family are similar morphology including envelope of the virus and tripartite single stranded RNA genome (Pringle, 1991). However, hantaviruses are unique in the former *Bunyaviridae* family in not being transmitted by an arthropod vector.

Phylogenetic analysis of hantaviral molecular
evolution in different rodent species

Table 1 Geographic distribution of rodent- soricomorph- and chiroptera-borne hantaviruses

Order	Family	Subfamily	Host species	Virus name	Geographic distribution		
<i>Rodentia</i>	<i>Muridae</i>	<i>Murinae</i>	<i>Apodemus agrarius</i>	Hantaan virus, Dobrava-Belgrade virus	China, South Korea, Russia, Europe		
			<i>Apodemus flavicollis</i>	Dobrava-Belgrade virus	Balkans		
			<i>Apodemus ponticus</i>	Dobrava-Belgrade virus	Russia		
			<i>Rattus</i> spp.	Seoul virus	Worldwide		
			<i>Apodemus agrarius</i>	Saarema virus	Europe		
			<i>Apodemus peninsulae</i>	Amur virus	Far East Russia		
			<i>Apodemus peninsulae</i>	Soochong virus	South Korea		
			<i>Arvicolidae</i>	<i>Arvicolinae</i>	<i>Myodes glareolus</i>	Puumala virus	Europe, Asia and America
					<i>Microtus fortis</i>	Khabarovsk virus	Far East Russia
					<i>Myodes regulus</i>	Muju virus	South Korea
					<i>Microtus pennsylvanicus</i>	Prospect Hill virus	Maryland
					<i>Microtus arvalis</i>	Tula virus	Russia and Europe
					<i>Microtus californicus</i>	Isla Vista virus	North America
					<i>Lemmus sibericus</i>	Topografov virus	Siberia
					<i>Cricetidae</i>	<i>Neotominae</i>	<i>Peromyscus maniculatus</i>
<i>Peromyscus leucopus</i>	Monongahela virus	North America					
<i>Peromyscus leucopus</i>	New York virus	North America					
<i>Peromyscus boylii</i>	Limestone Canyon virus	North America					
<i>Reithrodontomys mexicanus</i>	Rio Segundo virus	Cost Rica					
<i>Cricetidae</i>	<i>Sigmodontinae</i>	<i>Sigmodon hispidus</i>	Black Creek Canal virus	North America			
		<i>Oryzomys palustris</i>	Bayou virus	North America			
		<i>Oryzomys couesi</i>	Playa de Oro virus	Mexico			
		<i>Oryzomys couesi</i>	Catacamas virus	Honduras			
		<i>Oligoryzomys fulvescens</i>	Choclo virus	Panama			
		<i>Zygodontomys brevicauda</i>	Calabazo virus	Panama			
		<i>Sigmodon alstoni</i>	Cano Delgadito virus	Venezuela			
		<i>Oligoryzomys longicaudatus</i>	Andes virus	Argentina and Chile			
		<i>Oligoryzomys chocoensis</i>	Bermejo virus	Argentina			
		<i>Akodon azarae</i>	Pergamino virus	Argentina			
		<i>Oligoryzomys flavescens</i>	Lechiguanas virus	Argentina			
		<i>Necromys obscurus</i>	Maciel virus	Argentina			
		<i>Oligoryzomys longicaudatus</i>	Oran virus	Argentina			
		<i>Calomys laucha</i>	Laguna Negra virus	Paraguay, Bolivia, Argentina			
		<i>Holochilus chacoensis</i>	Alto Paraguay virus	Paraguayan Chaco			
<i>Akodon montensis</i>	Ape Aime virus	Eastern Paraguay					
<i>Oligoryzomys nigripes</i>	Itapúa virus	Eastern Paraguay					
<i>Oligoryzomys microtis</i>	Rio Mamore virus	Bolivia and Peru					

Phylogenetic analysis of hantaviral molecular
evolution in different rodent species

		<i>Necomys lasiurus</i>	Araraquara virus	Brazil
		<i>Oligoryzomys nigripes</i>	Juquitiba virus	Brazil
		<i>Akodon montensis</i>	Jabora virus	Brazil, Paraguay
<i>Soricomorpha</i>	<i>Soricidae</i>	<i>Suncus murinus</i>	Thottapalayam virus	India
		<i>Crocidura douceti</i>	Bowe virus	Guinea
		<i>Crocidura lasiura</i>	Imjin virus	Korea
		<i>Crocidura obscurior</i>	Azagny virus	Cote d'Ivoire
		<i>Crocidura shantungensis</i>	Jeju virus	Korea
		<i>Crocidura theresae</i>	Tanganya virus	Guinea
		<i>Myosorex geata</i>	Uluguru virus	Tanzania
		<i>Myosorex zinki</i>	Kilimanjaro virus	Tanzania
		<i>Anourosorex squamipes</i>	Cao Bang virus	Vietnam
		<i>Anourosorex yamashinai</i>	Xinyi virus	Taiwan
		<i>Blarina brevicauda</i>	Camp Ripley virus	United States
		<i>Blarina carolinensis</i>	Iamonia virus	United States
		<i>Neomys fodiens</i>	Boginia virus	Poland
		<i>Sorex araneus</i>	Seewis virus	Switzerland
		<i>Sorex caecutiens</i>	Amga virus	Russia
		<i>Sorex cinereus</i>	Ash River virus	United States
		<i>Sorex cylindricauda</i>	Qiandao Lake virus	China
		<i>Sorex isodon</i>	Yakeshi virus	China
		<i>Sorex minutus</i>	Asikkaia virus	Czech Republic
		<i>Sorex monticolus</i>	Jemez Springs virus	United States
		<i>Sorex roboratus</i>	Kenkeme virus	Russia
		<i>Sorex unguiculatus</i>	Sarufutsu virus	Japan
	<i>Talpidae</i>	<i>Talpa europaea</i>	Nova virus	Hungary
		<i>Urotrichus talpoides</i>	Asama virus	Japan
		<i>Neurotrichus gibbsii</i>	Oxbow virus	United States
		<i>Scaptonyx fuscicaudus</i>	Dahonggou Creek virus	China
		<i>Scalopus aquaticus</i>	Rockport virus	United States
<i>Chiroptera</i>	<i>Hipposideridae</i>	<i>Hipposideros pomona</i>	Xuan Son virus	Vietnam
	<i>Nycteridae</i>	<i>Nycteris hispida</i>	Magboi virus	Sierra Leone
	<i>Rhinolophidae</i>	<i>Rhinolophus sinicus</i>	Longquan virus	China
	<i>Vespertilionidae</i>	<i>Neoromicia nanus</i>	Mouyassue virus	Cote d'Ivoire
		<i>Pipistrellus abramus</i>	Huangpi virus	China

1.3. VIRUS STRUCTURE AND LIFE CYCLE

1.3.1. Virion structure

Hantaviruses are mainly round with 120-160 nm in diameter. These are enveloped viruses, with a negative sense three-segmented RNA genome, consisting of large – L (6.5–6.6 kb), medium – M (3.6–3.7 kb) and small – S (1.7–2.0 kb) segments, coding for viral polymerase, viral glycoprotein precursor further processed into two separate envelope

glycoproteins (Gn and Gc) and viral nucleocapsid protein, respectively (Plyusnin et al., 1996) (**Figure 1**). The lipid envelope of hantaviruses is spiked by peplomers consisting of Gn and Gc proteins. Each of the three segments contains non-coding sequences (NCR) on both the 5' and 3' ends (Plyusnin et al., 1996).

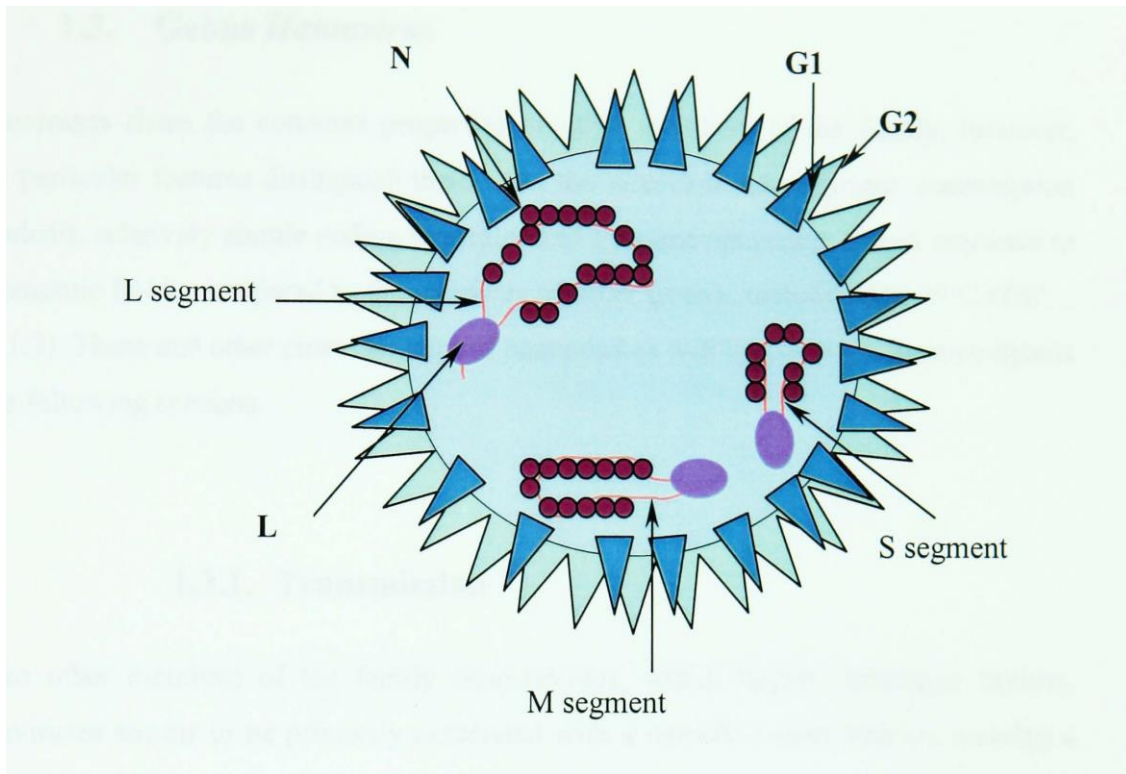


Figure 1. Schematic of the structure of *Bunyaviridae* family members. All three segments (L, M and S) are encapsidated by nucleocapsid protein N. Gn and Gc glycoproteins are embedded in lipid envelope. Modified from Minskaya, 2003.

As the result of existence of these conserved, complementary terminal structures on the ends of the L, M, and S segments, each segment can form circular structures called panhandles (**Figure 2**). They are thought to play an important role in viral transcription and in the proposed prime-and-realign mechanism of replication.

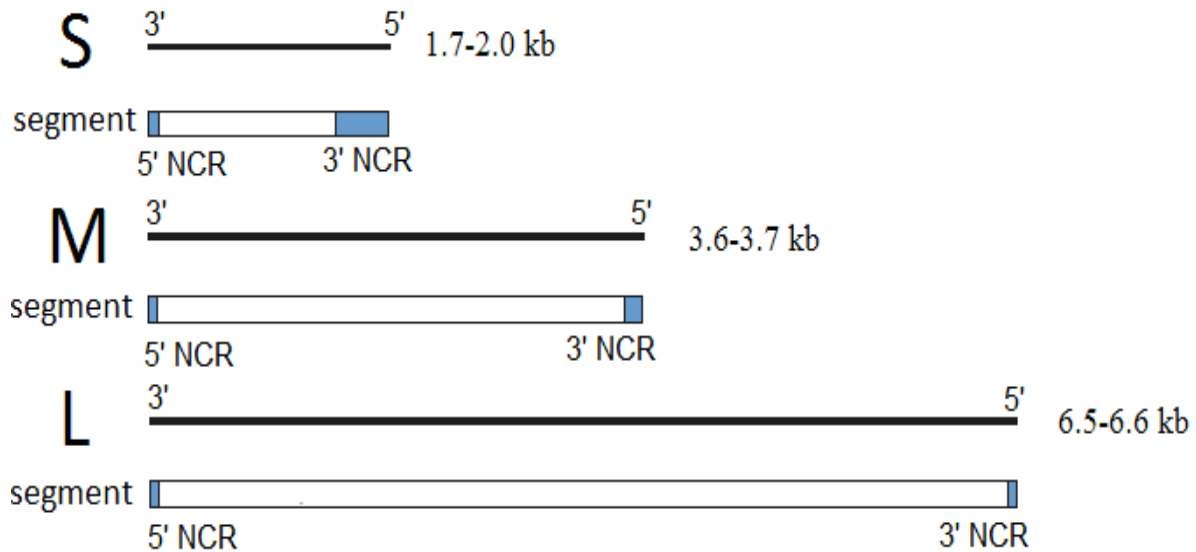


Figure 2. Structure and genome organization of hantaviruses

L segment encodes the viral RNA-dependent RNA polymerase (RdRp), consisting of approximately 2530 amino acid residues. Detailed analysis of amino acid alignment of all RNA-dependent RNA polymerases showed existence of five conserved motifs A, B, C, D, E (Poch et al., 1989). In addition to these motifs, pre-motif A and motif E were identified in viruses with segmented negative-strand RNA genome. Almost all these motifs are placed in the palm subdomain of the L segment and form an active site (Amroun et al., 2017).

M segment encodes glycoprotein precursor (GPC), consisting of approximately 1180 amino acid residues. Previous studies have shown that this protein is being cleaved to Gn and Gc glycoproteins which form a complex on the outer surface of the virion (Huiskonen et al., 2010; Battisti et al., 2011). Gn and Gc proteins form square-shaped surface spikes protruding from the viral membrane, with each spike complex made of four Gn and four Gc subunits. This Gn/Gc complex probably interacts with specific cellular surface proteins, β 3-integrins, facilitating cellular entry in target cells (Gavrilovskaya et al., 1998).

S segment codes for a nucleocapsid (N) protein of approximately 430 amino acids. It is highly conserved among different hantaviruses (Muyangwa et al., 2015). It has been shown that huge amount of this protein are expressed in early stages of infection and therefore the early immune response in patients infected by hantaviruses is directed mainly against the N protein

(Vapalahti et al., 1995). This protein has the most important role in RNA replication and encapsidation of each segment. It encapsidates each of the three genomic RNAs, thereby forming three ribonucleoproteins.

1.3.2. Hantaviral life cycle

Hantaviruses infect endothelial, epithelial, macrophage, follicular dendritic, and lymphocyte cells, by attaching viral glycoprotein to the receptor(s) on the host's cell surface (Jonsson et al., 2010). These viruses target polarized cells from the apical and basolateral membrane surfaces. The replicative cycle of hantaviruses occurs in the cytoplasm of infected cells (Plyusnin et al., 2012). Hantaviruses attach to several cellular receptors including β 3-integrins as receptors for pathogenic hantaviruses and β 1-integrins for non-pathogenic hantaviruses (Gavrilovskaya et al., 1999). Hantaviruses enter the cell via receptor mediated endocytoses (**Figure 3**). This process can be clathrin-dependent or not (Simon et al. 2009; Lozach et al. 2010). Primarily, virus is uncoated to release the three ribonucleoproteins into the cytoplasm. The next step is transcription by viral RdRp (vRdRp), producing the S, M, and L mRNAs. For initialization of this process, vRdRp needs primers which are obtained by a cap-snatching mechanism. N protein attaches to caps of host mRNAs and protects them from their own cellular RNA degradation machinery (Mir et al., 2008). Free ribosomes are the site of final translation of the S and L messenger RNAs (mRNAs), while translation of the M-segment transcript occurs on membrane-bound ribosomes. Namely, the glycoprotein precursor is proteolytically processed into Gn and Gc during import into the endoplasmic reticulum (ER) and further transported to the Golgi complex. The nucleocapsid protein is the most abundant viral protein and is synthesized early in the course of infection. Immediately after initial transcription, the RdRp switches from transcription to replication of all three genomic segments (L, M and S). Viral negative sense genomic RNAs (gRNAs) are converted by the action of RdRp to positive sense anti-genomic RNAs (agRNAs) and vice versa resulting in newly synthesized viral RNA segments. The newly formed viral RNAs are encapsidated by the N protein to form the ribonucleoproteins. The final step in virion maturation of bunyaviruses is assembling with the Golgi apparatus, followed by transport to cytoplasmic membrane via large

Golgi vesicles (Kuismanen et al. 1982; Salanueva et al. 2003). Enveloped virions are released to the extracellular space.

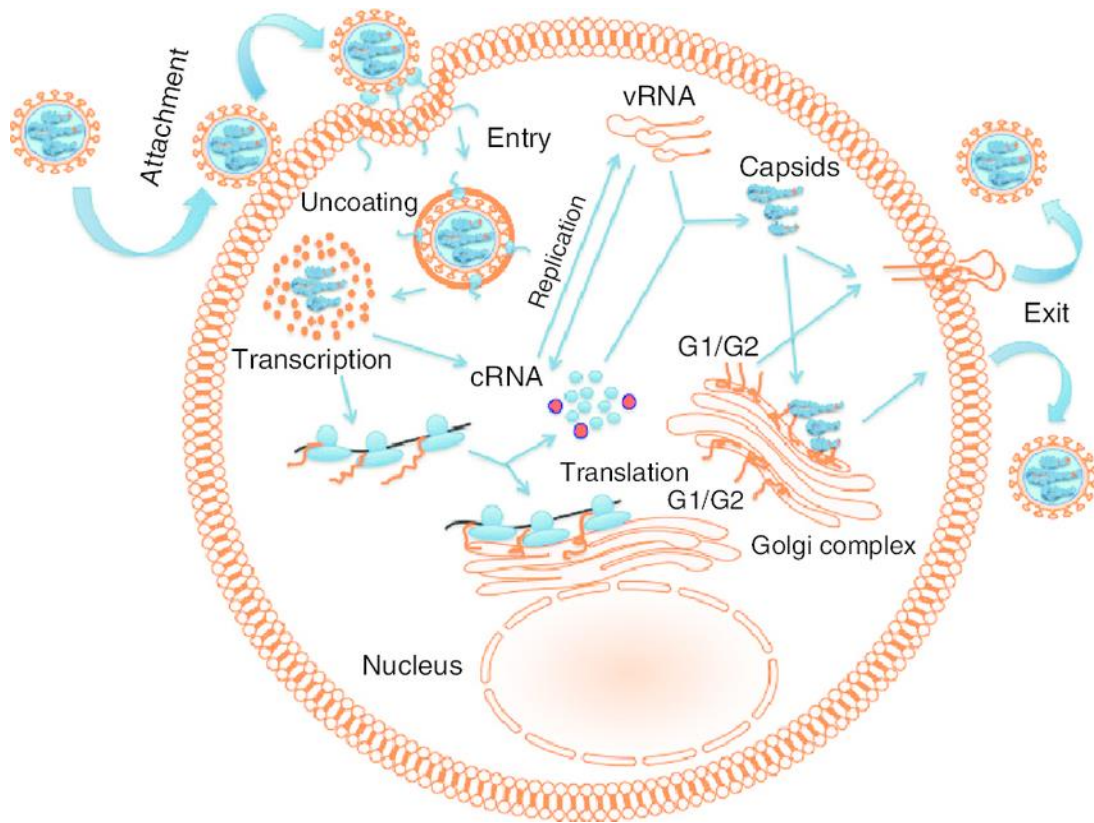


Figure 3. Replication cycle of hantaviruses Modified from Islam et al., 2011.

1.4. PATHOGENESIS OF HANTAVIRUS DISEASES

Hantaviruses proven to be human pathogens are mostly rodent borne, while hantaviruses found in shrews, moles and bats are still of undetermined pathogenicity for humans (Papa, 2012; Schlegel et al., 2012; Song et al., 2007). The geographic distribution of pathogenic hantaviruses and principal associated pathologies in humans are presented in **Figure 4**. Pathogenic hantaviruses are the causative agents of at least two human zoonotic diseases: hemorrhagic fever with renal syndrome (HFRS) and hantavirus pulmonary syndrome (HPS), with mortality rates of up to 12%-18% and 60%, respectively (Kovacevic et al., 2008; Jonsson et al., 2010 Papa, 2012).

Human infection occurs through respiratory exposure to contaminated rodent secreta and excreta. Incubation period is relatively long, 2-4 weeks. The symptoms of flu-like disease start suddenly and in some cases rapidly progress to severe or deadly forms of disease. The presence of hantavirus RNA in blood before disease onset has been described, however, IgG or IgM antibodies are not detected before the appearance of symptoms (Rasmuson et al., 2011; Ferres et al., 2007).

Upon viral entry through respiratory route, the first barrier for virus ingress to target cells is mucus covering respiratory epithelium. The trapped microbes, including hantaviruses, are subsequently being removed from the lungs to the throat by movements of ciliated cells through mucus (Flint et al., 2009). The lowest parts of the respiratory tract, the alveoli, lack both cilia and mucus and macrophages lining the alveoli are important for digestion of microbes (Flint et al., 2009). The next obstacle for virus entry is intact respiratory epithelium, which forms a particle-impermeable barrier. Once the virus surpasses these barriers, it spreads to the lung endothelium and further to other organs. The final target cells are endothelial cells of capillaries and small vessels in numerous organs and tissues (Nuovo et al., 1996). As mentioned above, β 3-integrins serve as receptors for pathogenic hantaviruses. Virus entry to endothelial cells induces the breakdown of their barrier function resulting in the so-called “vascular leak” mechanism (Manigold and Vial, 2014). Nevertheless, cytopathic effect (CPE) is not recognized in hantavirus infected endothelial cells. Therefore, illness and cell damage in hantaviral infection are the result of immunopathological mechanisms involving innate and adaptive immune responses (Schonrich et al., 2008).

In clinical practice, diagnostic tests most commonly used for diagnosis of hantavirus infection are based on enzyme-linked immunosorbent assay, indirect immunofluorescence or strip immunoblot (Manigold and Vial, 2014). All these tests aim to detect IgG/IgM antibodies against hantavirus nucleocapsid antigen (N-antigen), which is mostly conserved in hantaviruses. Moreover, almost all patients have IgM and IgG antibodies during the acute phase of the disease. Gn and Gc proteins are not considered of major diagnostic importance, since these proteins appear later in the clinical course and they are less conserved compared to the N protein.

Currently, there are no drugs approved by the Food and drug administration agency (FDA) for the treatment of patients infected with hantaviruses (Papa, 2012). Therefore, treatment is mainly symptomatic, including hydration, blood pressure regulation, oxygenation support and dialysis, if required. The use of ribavirin has been reported, which is a nucleoside analog with broad-spectrum antiviral activity.

1.4.1. Hemorrhagic fever with renal syndrome (HFRS)

HFRS is caused by Old World hantaviruses, present in Europe and in Far East (**Figure 4**) The causative hantavirus strains are Dobrava-Belgrade virus (DOBV), Saaremaa virus (SAAV), Seoul virus (SEOV), Puumala virus (PUUV) and Hantaan virus (HTNV).



Figure 4. Geographical distribution of pathogenic hantaviruses and principal associated pathologies in humans. HCPS = hantavirus cardiopulmonary syndrome; HFRS = haemorrhagic fever with renal syndrome; NE = nephropathia epidemica. Modified from Manigold and Vial, 2014.

Clinical course of HFRS usually develops in five distinctive phases: febrile, hypotensive, oliguric, diuretic and convalescent. Incubation period, ranging from 10 days to 6 weeks, is followed by flu-like symptoms in infected patients (Manigold and Vial, 2014). This febrile phase is characterized by myalgia, headache, abdominal pain and malaise, and also neurological, cardiovascular and gastrointestinal symptoms (Lednicky, 2013). The hypotensive phase is characterized by symptoms of vascular leakage, often associated to thrombocytopenia and shock. The oliguric phase lasts up to 5 days with risk for hypertension, pulmonary oedema and renal insufficiency. Consequently, half of fatalities due to HFRS occur during this phase. The initiation of the diuretic phase usually suggests the initiation of patients' recovery, and it is followed by a convalescent phase. Main laboratory findings are thrombocytopenia, leukocytosis or leucopenia, elevated levels of hematocrit (due to extravasation of fluid), serum urea and creatinine, and proteinuria. Depending on the hantavirus strain, both mild and severe forms of disease exist. Namely, DOBV and HTNV mostly cause severe forms of the disease with fatality rate of approximately 12-18% (Kovacevic et al., 2008; Vaheri et al., 2013). Mild forms of the disease are caused by SEOV and PUUV with fatality rates of 0.4%-2% (Vaheri et al., 2013).

1.4.2. Hantavirus pulmonary syndrome (HPS)

HPS is caused by New World hantaviruses, present in the Americas (Jonsson et al., 2010), as shown in **Figure 4**. Incubation period for these viral infections varies, ranging from 17 days for SNV to 38 days for Andes virus (ANDV) (Manigold and Vial, 2014). The febrile phase is characterized by the same symptoms as with HFRS and lasts up to 5 days. These symptoms are followed by thrombocytopenia, leucocytosis or leucopenia, elevated haematocrit, peripheral immunoblasts, abnormal liver function tests, mild increase in creatinine, hyponatraemia and proteinuria. In advanced stages of HPS, more specific symptoms appear, such as cough and dyspnoea, tachycardia and hypotension. Approximately 50% of infected patients develop cardiopulmonary phase characterized by dyspnoea, cough, tachycardia and hypotension, followed by rapidly progressive pulmonary oedema caused by capillary leakage and low cardiac output. Severity and case fatality rates of HPS vary depending on the strain

(circulating in the geographic regions), e.g. it is 25%-40% in Panama and 10% in Paraguay (Armein et al., 2013).

1.5. HANTAVIRUS ECOLOGY

Unlike other bunyaviruses, arthropod vectors are not involved in the transmission of hantaviruses. These viruses are persistently active in their natural reservoirs including rodents, insectivores and bats (Guo et al., 2013). In nature, hantaviruses are circulating via horizontal transmission among infected natural reservoirs. Hantaviruses are primarily rodent borne, with each species being mainly associated with particular rodent host (Maes et al., 2009; Jonsson et al., 2010). Rodents (order *Rodentia*, families *Muridae* and *Cricetidae*) of the *Murinae*, *Arvicolinae*, *Sigmodontinae* and *Neotominae* subfamilies serve as reservoir hosts for most hantavirus species. Nevertheless, the association of a particular hantavirus to specific rodent host species is not exclusive, hence they have also been detected in alternative rodent hosts, e.g. DOBV virus in *A. agrarius* and TULV in *Microtus agrestis*, *Microtus rossiaemeridionalis*, *Microtus subterraneus*, and *Arvicola amphibius* (Scharninghausen et al., 1999; Schlegel et al., 2012; Song et al., 2002). These findings might be the result of hantavirus spillover among sympatric species, which is promoted by complex biogeographic and anthropogenic pressures on the environment (Hjelle and Yates, 2001; Klingstrom et al., 2002; Zou et al., 2008).

Moreover, hantaviruses are also hosted by insectivores (families *Soricidae* and *Talpidae*) (Guo et al., 2013). Newly published data have extended hantavirus hosts to bats (order *Chiroptera*) (Sumibcay et al., 2012; Weiss et al., 2012; Guo et al., 2013).

Ecology and distribution of hantaviruses are directly related to the distribution of their natural hosts (**Figure 5**) (Jonsson et al., 2010).

Old World hantaviruses, which are circulating in Europe and Asia, are carried by species of four different rodent genera (*Apodemus*, *Microutus*, *Myodes*, *Rattus* and *Arvicola*) and two insectivore families (*Soricidae*, *Talpidae*).

Apodemus species (subfamily *Murinae*) are widely spread in Europe and Asia, underlying broad distribution of hantaviruses in this part of the World. *Apodemus*-borne hantaviruses, including HTNV and DOBV, are known to be the etiological agents of HFRS. HTNV and HTNV-like viruses were detected in three different *Apodemus* species (*A. agrarius*,

A. ponticus, and *Apodemus peninsulae*) in China, South Korea and Russia. In Europe, *Apodemus* species host various hantaviruses which are the etiological agents of HFRS.

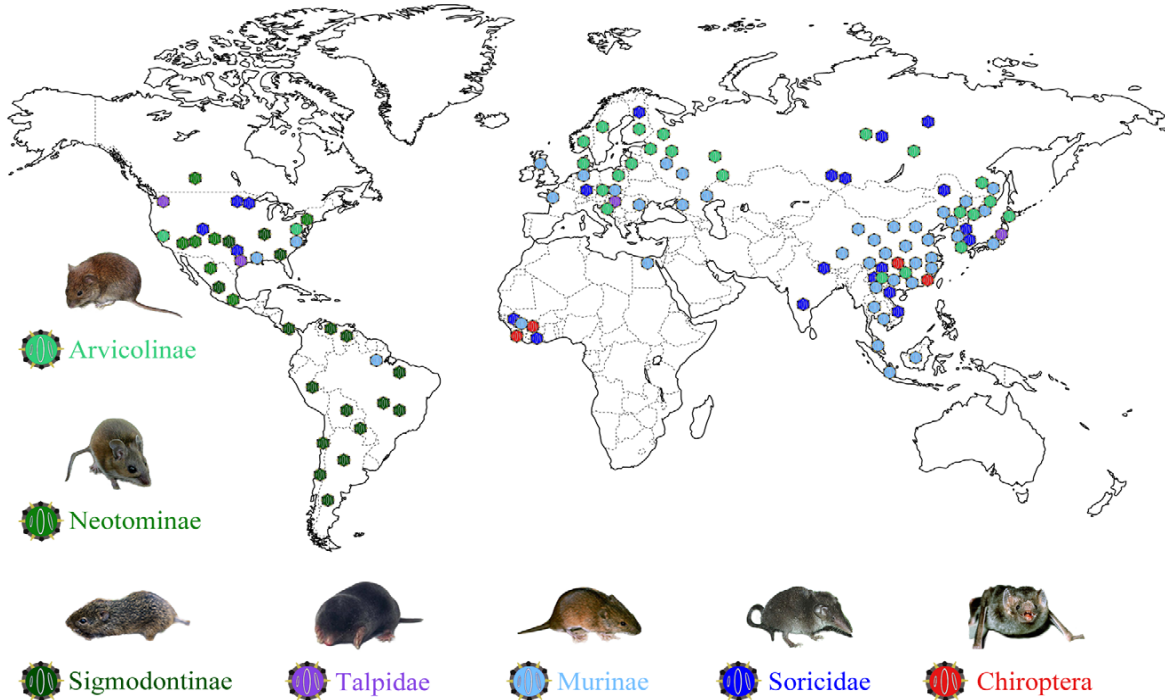


Figure 5. Map of the world illustrating the location of known hantaviruses by host group and associated mammalian hosts. Modified from Guo et al., 2013

Since its first description in Serbia in the past century, DOBV was detected throughout the Balkan Peninsula (Papa, 2012). Furthermore, it is associated with different rodent host species that are members of the subfamily *Murinae*. Earlier phylogenetic analysis revealed separate genetic lineages or genotypes of DOBV hosted by different *Apodemus* species (Papa, 2012). According to a new proposed classification, Dobrava-Belgrade virus species can be subdivided into four genotypes (Dobrava, Kurkino, Saaremaa and Sochi) in relation to their phylogeny, host reservoir, geographical distribution and pathogenicity for humans (Klempa et al., 2013; Vaheri et al., 2013). The Kurkino and Saaremaa genotypes are associated with the striped field mouse, *Apodemus agrarius*, Dobrava genotype with the yellow-necked field mouse, *A. flavicollis*, while Sochi genotype is associated with the Caucasian wood mouse, *Apodemus ponticus*. Among them, the Dobrava and Sochi genotypes are associated with more severe disease than that caused by Kurkino and Saaremaa.

Hantaviruses are also detected in different species of voles (*Arvicolinae*). Species of voles belonging to the genus *Microtus* are widely spread in Europe, North America and Asia. In Europe, TULV was firstly isolated in 1987 from *M. arvalis* and *M. rossiaemerdionalis* (Plyusnin et al., 1994). In the same year, TULV was also isolated in Russia from *Microtus arvalis*, and *Microtus levs* (previously *Microtus rossiaemerdionalis*). On the other hand, Khabarousk and Vladivostok viruses were isolated from *Microtus fortis* in Russia and Japan (Avšič-Županc et al., 2015). Moreover, *Microtus agrestes* was found to be the reservoir of TULV in Germany and Switzerland (Schlegel et al., 2012). In America, different hantavirus species were detected in *Microtus pennsylvanicus*, *Microtus californicus* and in *Microtus ochrogaster*.

Myodes glareolus (previously *Clethrionomys glareolus*), carrier of PUUV, is the most widespread mammal species. This bank vole species is widely spread in Europe (except of the Mediterranean region). In Asia, *Myodes rufocanus* and *Myodes regulus* are known hosts for Hokkaido virus (HOKV) in Japan, and Muju virus (MJUV) in Korea, respectively (Avšič-Županc et al., 2015).

Lately, *Arvicola amphibious* was also identified as carrier of TULV in Germany and Switzerland (Schlegel et al., 2012)

Different species of the *Rattus* genus are also hosts of hantaviruses. Seoul virus (SEOV) is harbored by *Rattus norvegicus* (Avšič-Županc et al., 2015). The worldwide distribution of SEOV is the consequence of the global distribution of its host reservoir.

New World hantaviruses, present in the Americas, are mostly associated with members of the rodent subfamilies *Neotominae* and *Sigmodontinae*. Since the first hantavirus detection in America (PHV), many additional hantaviruses have been isolated from different rodent species (Bi and Formenty, 2008; Yanagihara et al., 2014). SNV, the first etiological agent of HPS, was isolated from *Peromyscus maniculatus* (Childs et al., 1994). Moreover, the most important hantavirus in South America is ANDV, causative agent of HPS in Argentina (Calderon et al., 1999). In the following years different studies published data with newly detected hantavirus hosts. In Mexico, hantaviruses are in association with deer mice (*Peromyscus* spp.), harvest mice (*Reithrodontomys* spp.), and cotton rats (*Sigmodon* spp.) (Milazzo et al., 2012);

Oligoryzomys fulvescens is host of hantaviruses in Panama (Armién et al., 2016), while *Acodon azarae* is host of hantaviruses in Argentina (Maroli et al., 2015).

Rodents have been the only known hantavirus reservoirs for a long time. As already mentioned, the first ever hantavirus (Thottapalayam virus) was isolated in India (Carey et al., 1971). Moreover, the first hantavirus, detected in Africa (Guinea) was recovered from an insectivore (*Crocidura theresae*, family *Soricidae*) (Klempa et al., 2006). In the following years, *Sorex* spp. was detected as a common hantavirus host es in several European countries. So far, pathogenicity of these viruses is not elucidated (Kang et al., 2009; Yashina et al., 2010; (A) Schlegel et al., 2012). Several important scientific reports are connected with discovery of shrew-borne hantaviruses (Klempa, 2009). Shrew-borne hantaviruses have been found in widely separated parts of the world. Insectivores and rodents are evolutionary very divergent, leading to the assumption that other mammals may also harbor hantaviruses. Moreover, the pathogenicity of insectivore-borne hantaviruses has not been investigated yet. Finally, there is significant distinction between rodent- and shrew-borne hantaviruses at the amino acid level. This fact is the possible reason why these viruses were not detected for such long period.

Lately, hantaviruses have been detected in bats (Yanagihara et al., 2014; Zhang 2014; 2015). Namely, the first hantaviruses found in bats (families *Nycteridae* and *Vespertilionidae*) originated from a National park in Sierra Leone and near Mouyassué village in Côte d'Ivoire (Sumibcay et al., 2012; Weiss et al., 2012). Moreover, hantaviruses were found to be associated with different species of *Rhinolophus* genera in Asia (Guo et al., 2013). Hantaviruses were also detected in *Pipistrellus abramus* and *Hipposideros pomona*, originated from Asia and Vietnam, respectively (Guo et al., 2013; Arai et al., 2013). Although, hantaviruses were found only in few bat species, these species belong to both known suborders: suborder *Yinpterochiroptera*, which includes three families, *Hipposideridae*, *Rhinolophidae* and *Pteropodidae*, and suborder *Yangochiroptera*, which includes two families, *Nycteridae* and *Vespertilionidae*. The knowledge regarding the pathogenicity and role in the general evolution of hantaviruses isolated from bats is very limited and needs to be resolved in future.

Quite recently, the connection between hantavirus natural reservoirs and environmental and climate changes has been studied (Dearing and Dizney, 2010). Small mammals are very sensitive to climate and habitat changes. Climate changes influence food availability and winter

conditions may affect the distribution of small mammals. The example which decidedly confirms the association between climate and rodent population is the hantavirus outbreak in 1993 in the US Four Corners region (Klempa, 2009). Namely, a dramatic increase of rainfall associated with the 1992–1993 El Niño resulted in an increased abundance of rodent food, which led to 20-fold increase in rodent population resulting to a hantavirus outbreak. Later studies have also shown the influence of climate changes on increasing number of HFRS in some European countries (Clement et al., 2009; Linard et al., 2007). They showed that higher temperature during summer and autumn can influence on pathogen dynamics and subsequently increase the number of HFRS cases. In contrast, climate changes have negative effect on the vole population in Scandinavia (Klempa, 2009). It is known that voles, hosts of PUUV, have 3-4-year population cycles facilitating the transmission and spread of PUUV. Lately, these population cycles have been disturbed by climate fluctuations. Changes in climatic patterns of a phenomenon known as North Atlantic Oscillation (NAO), resulted in mild and wet winters, which have led to a decrease in vole population. Although it may seem illogical, this phenomenon can be explained by the fact that shorter period of protective snow cover combined with more frequent freezing and thawing periods, producing an ice rather than snow cover, resulted in decreased vole wintering success.

Landscape alternation during the past century resulted in transformation of land to farms, pastures, roads, and urban centers. Disturbed habitats are more convenient to generalist species, such as small mammals, able to tolerate and quickly adapt to ecological changes. In this way the scene was set for increased frequency of hantavirus transmission to humans (Mills, 2005).

Hantavirus infection of natural reservoirs is considered to be persistent and asymptomatic (Hardestam et al., 2008, Yanagihara et al., 1985; Bernshtein et al., 1999). However, some negative influence of hantaviruses on host's survival has been described, such as slower growth of infected animals and histopathological changes in infected tissues. As the result of persistent infection, animals transmit the viruses among themselves and shed virus in urine, saliva, and feces (Kruger et al., 2015). In the environment, virus particles remain infectious for several weeks – depending on environmental factors including humidity and temperature (Hardestam et al., 2007).

It has been shown that hantaviruses persist better in wet and cold environment compared to dry and warm conditions in laboratory experiments. All these changes can further influence the epidemiology of hantaviruses. A peak in viral load in rodents' excretions is detected few weeks after their initial contact with the virus. In the following prolonged chronic stage, the viral load is lower, resulting in significantly lower virus transmission potential (Hardestam et al., 2008; Yanagihara et al., 1985; Bernshtein et al., 1999).

Some previous studies have also shown the role of kinship in virus transmission between closely related animals. For example, investigation of TULV and PUUV spread in populations of *Cricetidae* species revealed that infected animals were more closely related to each other than non-infected ones, emphasizing the importance of virus transmission in hatches (Deter et al., 2008). On the other hand, in a study that examined the influence of kinship among rodents of *Apodemus flavicollis* species on hantavirus spread, the frequency of relatives was higher in seronegative in relation to seropositive group.

1.6. HANTAVIRUS EPIDEMIOLOGY

Human infection occurs through inhalation of contaminated secretions and excreta (urine, saliva, and feces). Virus transmission to humans has only rarely occurred directly by rodent bite (Douron et al., 1984). Risk factors increasing the possibility of hantavirus transmission to humans mostly include rural- and forest-related activities (Watson et al., 2013). Therefore, farmers, shepherds, forestry workers and soldiers are in highest risk for infection (Papa, 2012). Males are infected more often, with approximate 3:1 male to female ratio. Furthermore, the highest number of infected persons is detected among adults, and only few studies reported hantavirus infection in children (Peco-Antić et al., 1991; Bogdanovic et al., 1995; Eboriadou et al., 1999). Humans are not among the natural hosts of hantaviruses and they are thought to be dead-end hosts, without further virus transmission, with the exception of few reported cases of human-to-human transmission of ANDV in Argentina and Chile (Wells et al., 1997; Ferres et al., 2007). **Figure 6** shows the number of reported annual clinical cases of hantavirus infections since 2000.

The first HPS case was recognized in 1993 in the Four Corners area in USA, and it was caused by SNV (Childs *et al.*, 1994). In the following years HPS was spread through North and

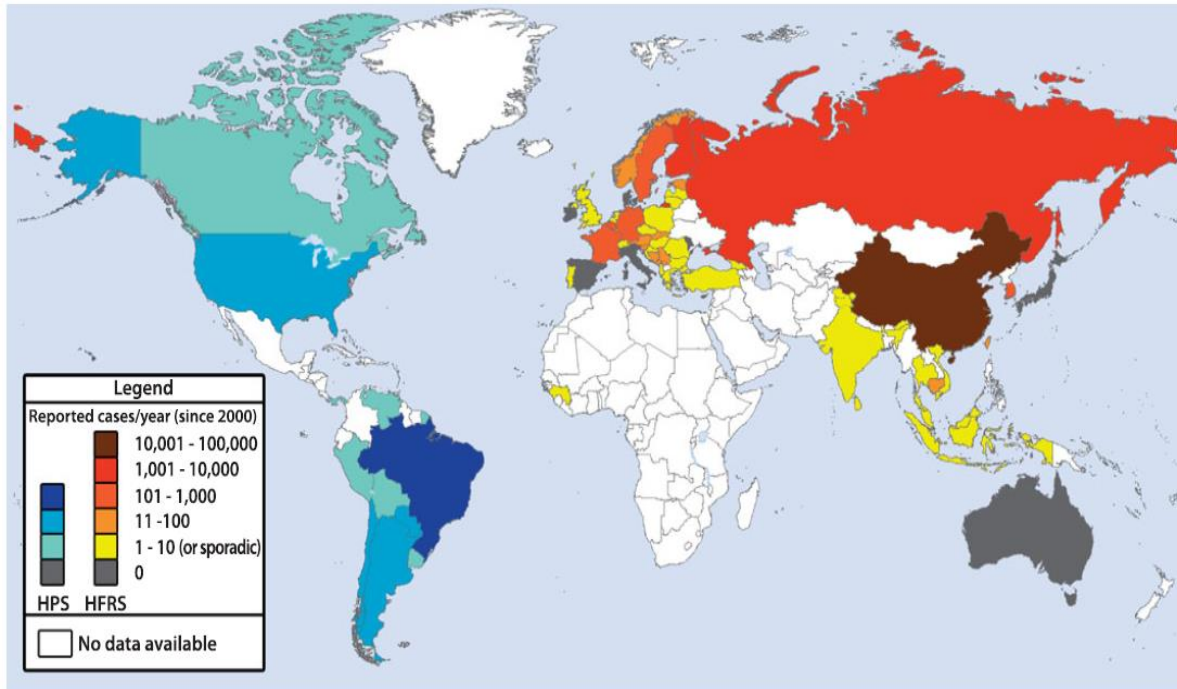


Figure 6. Reported clinical cases of hantavirus infections/year since 2000. Data included for each country is the average number of laboratory confirmed cases per year since 2000, with preference given to national/international registry reports. Imported cases are excluded. Modified from Watson et al., 2013.

South America with confirmed cases in Argentina, Bolivia, Brazil, Canada, Chile, Panama, Paraguay and Uruguay (Avšič-Županc et al., 2015). Currently over 15 different hantavirus species were identified as the etiological agents of HPS. Two different pathogenic strains of hantaviruses are predominant in the Americas, including SNV in North America and ANDV in South America. According to the results reported by Centers for Disease Control and Prevention, Atlanta, Georgia (USA) as of January 2017 until July 2017 a total of 728 cases of hantavirus Infections have been reported in the United States (<https://www.cdc.gov/hantavirus/surveillance/index.html>). However, the mortality rate is much higher compared to HFRS, around 40%. Moreover, in a study from Brazil, Araraquara virus (ARQV) has shown to be very virulent hantavirus, with 50% case fatality rate (Kruger et al., 2015). However, the presence of antibodies against HPS-causing hantaviruses has also been detected in asymptomatic infections or mild febrile cases (Watson et al., 2014). Brazilian

retrospective seroepidemiological study reported 2.3% seropositivity, while a study in Peru reported 0.3% seropositive individuals (Watson et al., 2014).

The first serologically confirmed cases in Africa were reported in 1984 in Benin, Burkina Faso, Central African Republic and Gabon (Gonzalez et al., 1984). However the first hantavirus, named Sangassou virus (SANGV), was found using a pan-hanta-PCR protocol in African wood mouse (*Hylomyscus simus*) trapped in a forest habitat in Guinea (Klempa et al., 2006). In the following years hantavirus infection was detected in Senegal, Nigeria, Egypt, Djibouti and Guinea (Avšič-Županc et al., 2015). Recently, independent studies reported 1-2% SANGV seroprevalence in Guinea and in the South African Cape Region (Witkowski et al., 2014; Klempa et al., 2010). Moreover, a study conducted in Sangassou village in Guinea reported seroprevalence of 4.4%. Reported data showed that this medical problem is underestimated in Africa, possibly because the lack of appropriate hantavirus antigens in diagnostic tests.

Asia is the continent where the epidemic hemorrhagic fever was firstly described. China is the country with the highest number of reported cases and deaths. During the period 1950-2007 more than 1.5 million cases were reported in China (Zhang et al., 2010). However, in 2007 after implementation of different preventive measures, 11248 cases were reported. Similar to other parts of the world, individual HFRS cases and outbreaks are influenced by ecological and occupational factors. More than 70% of HFRS cases are related to rural areas of China. These areas are characterized by poor housing conditions and high density of rodents' population. Severe forms of illness have been caused by HTNV and Amur/Soochong virus, with 15% fatality rate (Avšič-Županc et al., 2015). HTNV was first isolated from *A. agrarius* in 1978 (Lee et al., 1978). This hantavirus is known to be the causative agent in 70% of HFRS cases (Ryou et al., 2007). HTNV is the most important causative agent of HFRS in South Korea with high number of reported cases (Jonsson et al., 2010). Significant prevalence of anti-hantavirus antibodies has also been noted in other Asian countries, including Thailand, Indonesia and India (Jonsson et al., 2010). Although SEOV is present worldwide, the highest prevalence of SEOV infection was observed in Asia. This virus is the etiological agent of moderate form of disease with 1-2% of mortality rate. Unlike HTNV, SEOV is more

commonly found as a cause of HFRS in cities and urbanized areas, mainly due to the distribution of its natural host (*Rattus* spp).

Infections caused by hantaviruses are constantly present in European countries. During the period 2000-2009, the average number of annual reported cases was 3,138. Two different species of hantaviruses are known to cause HFRS in Europe: PUUV and DOBV. PUUV is widely present in central and northern Europe, since its natural reservoir (*M. glareolus*) is the most common rodent species in this part of the World. In some countries, such as Finland, Germany, Sweden and European part of Russia, thousands of PUUV cases occur in peak epidemic years. HFRS caused by PUUV is known as nephropathia epidemica (NE) and it mostly is characterized by mild symptoms. DOBV, on the other hand, is predominant in southeastern Europe (Balkan region). This virus causes severe forms of HFRS with mortality rate up to 12%. Individual cases and outbreaks are reported yearly, with approximately 40,000-60,000 cases annually in China as the most endemic country (accounting for 99% of all reported HFRS cases) (Avsic-Zupanc et al., 2016). Earlier phylogenetic analyses revealed separate genetic lineages or genotypes of DOBV hosted by different *Apodemus* species (Papa, 2012). However, new proposed classification subdivided DOBV species into four genotypes (Dobrava, Kurkino, Saaremaa and Sochi) in relation to their phylogeny, host reservoir, geographical distribution and pathogenicity for humans (Klempa et al., 2013; Vaheri et al., 2013). The Kurkino and Saaremaa genotypes are associated with *A. agrarius*, Dobrava genotype with *A. flavicollis*, and Sochi genotype with *A. ponticus*. DOBV genotypes induce HFRS with significant differences in case-fatality rate, from >10% in DOBV hosted in *A. flavicollis* to ≤1% in DOBV hosted in *A. agrarius* (Gligic, 2008; Papa, 2012).

DOBV is endemic in the Balkan region, where severe cases are reported every year. In Romania during the period of 1956-1977 the number of clinically confirmed HFRS cases was 27 (Manasia et al., 1977). Since 2008, when the laboratory diagnostic of hantaviruses was established in the National Reference Laboratory for Vector-Borne Infections, 17 additional HFRS cases have been diagnosed. All patients had severe form of the disease and all were exposed to occupation risk (Heyman et al., 2011; Maftai et al., 2012).

During the period of 1954-1986, 399 HFRS cases were diagnosed in Bulgaria, with serologically confirmed DOBV infection in 90% of all cases (Chumakov et al., 1988). From

2000-2010, 36 HFRS cases have been reported in the Rila-Pirin-Rodopa mountain ranges (Papa and Christova, 2011). All cases were clinically and serologically confirmed.

Cases of human infection caused by hantaviruses are also reported in Greece. The first serologically confirmed case was diagnosed in 1981 (Lee and Antoniadis, 1981). Up to 2001, 210 cases were reported in Greece (Heyman and Vaheri, 2008; Papa and Antoniadis, 2001). The most endemic regions are in the northwest and northeast parts of the country where 80% of total HFRS cases are observed. Two pathogenic hantaviruses are found in Greece: DOBV and PUUV and the predominant one is DOBV. As two viruses are present as causative agents of HFRS, the forms of HFRS vary from mild to severe, with average mortality rate 9% (Papa and Antoniadis, 2001).

In Albania, the first HFRS reports dated from 1987 (Eltari et al., 1987). From 2003-2006, 17.7% of cases clinically suspected as viral hemorrhagic fever, were confirmed as HFRS (Papa et al., 2008).

The first case of HFRS in former Yugoslav Republic of Macedonia was reported in 1987. In a 3-year study period (October 1987- July 1990), 10 patients were recognized as HFRS cases caused by DOBV (Polenakovic et al., 1995). The fatality rate was 10%.

The first clinical case of HFRS in Slovenia was reported in 1954 (Radosevic and Mohacek, 1954). Subsequently, the presence of few different hantavirus species (DOBV (genotypes Dobrava and Kurkino), PUUV, TULV and Seewis virus) were detected in Slovenia (Avsic-Zupanc et al., 2014). DOBV is known to cause severe forms of HFRS, since it was initially isolated in 1992 from *A. flavicollis* (Avsic -Zupanc et al., 1992). On the other hand, PUUV is causative agent of mild and moderate forms of HFRS, with significantly lower mortality rate. From 1999-2008, 208 clinically and laboratory confirmed cases were reported in Slovenia (Kraigher et al., 2012). DOBV was detected in 134 patients and PUUV was detected in 377 patients. The overall fatality rate was 4.5%.

Hantaviruses are endemic throughout Croatia with some exceptions, including the coastal region and the islands. In this country, HFRS is caused by DOBV or PUUV, but two-third of cases are caused by PUUV (Markotic et al., 1996). The first documented clinical case was reported in 1952 (Radosevic and Mohacek, 1954). Since then, sporadic cases have been reported annually with few outbreaks. Dinara region, first recognized as endemic during an

outbreak in 1995, was the region with the highest proportion of DOBV infections (Kuzman et al., 1997). During an outbreak in 2001, 401 HFRS cases were reported. DOBV IgM antibodies were detected in 17% patients (Kuzman et al., 2003).

Bosnia & Herzegovina (B&H) is known to be highly endemic country for hantaviruses. The first clinical case was reported in 1967 and since then 732 HFRS cases were diagnosed (Heyman et al., 2011). Three different hantaviruses, including PUUV, DOBV and SEOV are known to circulate in B&H (Clement et al., 1994; Hukic et al., 2011). However, almost 50% of HFRS cases are caused by PUUV (Hukic et al., 2011). In general population, surveilled seroprevalence to PUUV was 6%, while the seroprevalence to DOBV was 1.5%. Some large outbreaks have been documented in the past (Hukic et al., 2010). The first large epidemic occurred in 1989 with an overall fatality of 6.6% (Gligic et al., 1992b). The next epidemic was recognized during the war in 1995, with mortality rate of 7.3% (Markotic et al., 1996). Most patients were soldiers; 190 patients with symptoms compatible with HFRS were admitted in the hospital, and HFRS was confirmed in 128 patients (Lundkvist et al., 1997).

Recognition of HFRS cases in Montenegro dates from 1967. Ever since, four outbreaks were reported in Montenegro. High number of cases was detected in the northeast part of the country (Berane, Plav, Mojkovac, Pluzine and Kolasin). DOBV is the most common causative agent of HFRS (90%). The average mortality of DOBV cases is 4.8% (Gledovic et al., 2008).

Epidemiological studies from Serbia described sporadic individual human cases or episodic outbreaks of HFRS induced by hantavirus infection. The first isolation of Dobrava–Belgrade virus was made from an HFRS patient in Belgrade, Serbia, in 1992 (Gligic et al., 1992). Soon thereafter, a new hantavirus strain was isolated from *A. flavicollis* captured in Dobrava, Slovenia, and its genome was analyzed (Avsic-Zupanc et al., 1992). In 1993, based on a 420-bp sequence of the S fragment, the Belgrade virus and the Dobrava virus were found to be genetically highly similar (Taller et al., 1993). Therefore, both viruses are now considered to be the same and were named Dobrava–Belgrade virus (DOBV). The first serologically confirmed HFRS case in Serbia was reported in 1979 (Diglisic et al., 1994). Up to now, many serologically confirmed HFRS cases were observed annually, with outbreaks occurring in 1986, 1989 and 1995–96 (Gligic et al., 1988, 1989, 1992; Diglisic et al., 1994; Avsic-Zupanc et al., 2000). The most recent available data about HFRS patients in Serbia refer to 2002, during a

large epidemic in Serbia and Montenegro with 128 confirmed cases, including genetic detection of DOBV (Papa et al., 2006). Moreover, Puumala-like virus and TULV were also detected in Serbia (Diglisic et al., 1994; Song et al., 2002). PUUV-like virus was isolated during the epidemic in Pozarevac in 1988. The disease was diagnosed in four children and one adult; one child died. The PUU-like virus was isolated from *Mus musculus* captured in Pozarevac, suggesting that *M. musculus* can play important role in hosting and transmitting hantaviruses causing severe form of HFRS. In a study conducted during 1983-1989, rodents were captured in former Yugoslavia (Bosnia, Croatia, Montenegro, Slovenia and Serbia); the captured rodents were *A. agrarius*, *A. flavicollis*, *Apodemus sylvaticus*, *M. subterraneus*, *M. arvalis* and *Microtus multiplex*, and TULV was detected in *M. subterraneus* using molecular methods, captured in Serbia in 1987. TULV was first isolated from *M. arvalis* and *M. rossiaemeridionalis* captured in the Tula region in Russia (Plyusnin et al., 1994). At the same time, TUV was also detected in Slovakia, near the town Malacky; virus was recovered from *M. arvalis* (Sibold et al., 1995). In the following years, TULV was detected in various European countries (Bowen et al., 1997; Heyman et al., 2002; Plyusnin et al., 1995; Sibold et al., 1999). Moreover, TULV was also isolated from *Arvicola amphibious* trapped in Germany and Switzerland, representing the first detection of TULV in Eurasian water vole (Schlegel et al., 2012). For a long time TULV was considered as non-pathogenic hantavirus. However, human infections caused by TULV have been recently reported in at least two occasions in Czech Republic and in France (Zelena et al., 2013; Reynes et al., 2015). It has been suggested that TULV has the possibility of recombination (Sibold et al., 1999a).

1.7. EVOLUTION OF HANTAVIRUSES

The study of evolution and relatedness of genes and organisms may be performed using different approaches - for example, morphological characteristics are still important for taxonomy. However, increasing number of molecular data (nucleotide and amino acid sequences) are nowadays used to explore phylogenetic relationships. Sometimes, the only way to examine relatedness among organisms is the use of morphological characteristics, as is the case for mummies and fossils. Since viruses do not leave fossil records, the only way to study their past is through phylogenetic relationships of existing viruses.

Currently, the characteristics of the viral genome are important source of information. Understanding the processes that lie behind genetic diversity and access to an early evolutionary history is important for understanding the current properties of pathogens and for designing preventive, therapeutic and public health measures. Phylogenetic analysis includes reconstruction of the evolutionary history based on genomic data and represents fundamental element in molecular and epidemiological studies. Reconstruction of phylogenetic trees provides insights into the evolutionary relationships of viral strains combined with the possibility to investigate anyepidemiological links.

Based on evolutionary theory, all organisms have evolved from a single common ancestor. However, different molecular mechanisms are responsible for variations in genomes of each organism which results in biodiversity. The mechanism to infer relationships among genes is by analyzing mutations. Namely, phylogenetic methods assume the appropriate level of similarity between examined sequences that share a common ancestor. This means that sequences can be analyzed together using phylogenetic methods only if they have not accumulated too much variation. Therefore, the term “homology” is used only when the common ancestor is recent enough for the sequence information to have retained enough similarity for it to be used in phylogenetic analysis. Taxonomic comparison showed that related species are limited in a number of mutations, which are usually found on the third codon position of an open reading frame (ORFs), therefore, the evolution in proteins is lower than that in nucleotides.

Evolutionary relatedness between genes can be approached using phylogeny, therefore showing which genes are most related. The best way to illustrate evolutionary relationships among genes is to construct phylogenetic tree, a graphical representation resembling the structure of a tree, hence the name. In order to construct a phylogenetic tree, it is necessary homologous sites of examined sequences to be compared with each other (positional homology). This can be achieved by aligning the homologous sequences in such way that homologous sites form columns in the alignment.

Various models can be applied to infer phylogeny based on a set of viral sequences. These models are used to reconstruct the evolutionary history of a population of gene sequences based on sequence similarity in the form of a phylogenetic tree with individual nodes

on a tree representing a hypothetical most recent common ancestor of the observed gene sequences located at the tips of the tree. Two broadly used methodical approaches are distance-based and criterion-based or algorithmic. Distance-based methods [Neighbor-joining (NJ), Fitch–Margoliash (FM), and Unweighted Pair Group Method with Arithmetic Means (UPGMA)] are based on the pair-wise distance matrix, which means the degree of differences between sequence pairs. These methods cluster taxa according to a pre-defined set of rules. When a fast method for inferring relationships between taxa is required, NJ trees have been shown to provide a good approximation to the minimum evolution tree, particularly for large datasets.

Criterion based methods are Maximum Likelihood (ML), Bayesian and Maximum Parsimony (MP) method. ML method, under the best fitting model of evolution, searches the likelihood of all trees and the tree with the highest likelihood becomes chosen as the best tree. Bayesian method also uses concept of likelihood, but it does not search only one best tree. In contrast to ML, this method calculates posterior probability of trees and chooses the one with the highest probability. Disadvantage of this algorithm is that it is computationally demanding, especially for large data sets. Prior to analysis, Bayesian method requires the researcher to specify model parameters (prior distribution). In Bayesian phylogenetic inference posterior probabilities are obtained by exploring tree space using a sampling technique, called Markov chain Monte Carlo (MCMC). The collection of post-burn-in samples obtained after convergence to the stationary distribution is an approximation to the posterior distribution of the parameter under consideration. The advantage of this method compared to ML is the possibility of comparison of two alternative hypotheses. After MCMC analysis, it should be summarize tree samples from a Bayesian phylogenetic analysis. In this tree the sum of the posterior probabilities of clades is maximized [the maximum clade credibility (MCC) tree]. Bayesian phylogenetic inference programs, such as BEAST (Bayesian Evolutionary Analysis by Sampling Trees, Drummond and Rambaut, 2007), utilize genetic sequence data and time-structured sampling information under a strict or relaxed evolutionary clock model to infer past population dynamics, including substitution rate, divergence times, and demographic growth, and returns a posterior set of rooted, time-structured trees. Using a Bayesian MCMC algorithm,

the analysis returns the rate of nucleotide substitution and the time to the most recent common ancestor (TMRCA) at the root and at each of the nodes.

MP method infers the best tree topology for a set of aligned sequences that can be explained with the smallest number of character changes. This method infers the minimum number changes required along its branches for each nucleotide position in sequence to explain the observed states at the terminal nodes. The sum of this score for all positions is called parsimony length of the tree and it is computed for different tree topologies.

Molecular mechanisms which play important role in evolution of each organism are mutations, recombination, reassortment, natural selection and genetic drift.

Recombination is a widespread mechanism of molecular evolution. Populations of many different organisms have experienced this genetic exchange. Changes in genome created by this mechanism generally result in major evolutionary leaps, including acquired resistance against drugs. In general, recombination affects evolutionary history by changing it and therefore it can not be neglected. Moreover, there are several potential scenarios for recombination which should be mentioned. The first one is the situation when homologous region of nucleotide sequence is being replaced from donor to acceptor sequence. The result of this event is homologous recombination. The other scenario results in crossovers at non-homologous sites. The outcome of this event is non-homologous recombination. Additionally, exchange can be detected in both sequences (symmetrical recombination), or one sequence can be the donor and the second to be the acceptor (non-symmetrical recombination).

Since viruses are the obligate cellular parasites, recombination is only possible if two different viral strains co-exist in the same cell. Genetic exchange can occur in both DNA and RNA viruses, with either segmented or non segmented genomes. However, the occurrence of recombination is facilitated in viruses with segmented genome. Actually, during co-infection, different segments can be easily exchanged in the same host cell. The result of this process is called reassortment (Lemey and Posada, 2009).

Recombination, as one of molecular mechanisms responsible for genetic diversity has been described in different families within RNA viruses (Worobey and Holmes, 1990). However, for a long period of time it was thought that recombination was absent in RNA viruses except polioviruses (Copper et al., 1974). The most likely mechanism proposed for this

process is copy-choice model, primarily described for poliovirus (Copper et al., 1974). This process requires jumping of RNA-dependent RNA polymerase (RdRp) from one RNA molecule to another, during RNA replication. During this process polymerase remains bound with nascent nucleic acid chain allowing formation of genetically distinct viral strains (Simon-Loriere and Holmes, 2011). However, it was documented to occur with very low frequency in negative stranded RNA viruses (Chare et al., 2003). Actually, the best evidence of recombination among negative stranded RNA viruses is seen in hantaviruses (Han and Worobey, 2011). Genome structure and life cycle of viruses may play important role in occurrence of recombination in these viruses.

Exchange of genes or parts of genes through the process of recombination results in mosaic genomes consisting of parts with different evolutionary history.

Recombination and reassortment can be analyzed on the level of nucleotide sequences, but also on the amino acid level. Therefore, several programs have been developed for recombination analysis. The most commonly used is the Recombination Detection Program (RDP) (Salminen and Martin 2009).

Natural selection is the most powerful evolutionary mechanism and the best explanation of the complexity of life forms and organisms. It is exerted through different effects on organisms. The first one is positive selection, which increases the frequency of a beneficial mutation until it becomes fixed in the population. The other effect is negative selection which decreases the frequency of a deleterious mutation until it is eliminated. Additionally, selection does not affect the frequency of neutral mutations. Several approaches have been developed in order to detect possible selection, including those which detect selection in single genomic regions within a single population and comparative approaches which extend basic methods, either to multiple loci within a genome or to multiple populations. The methods which can be applied on single genomic regions are summary statistic methods and dN/dS methods (Pybus and Shapiro, 2009).

Summary statistic methods represent the simplest methods to detect the presence of selection. Using these methods, statistics that summarize the relative frequency of polymorphic sites are been calculated from studied alignment. Obtained statistics are then compared against the values expected to occur under a “null model” of neutral evolution. If the statistics are

considerably different from their expected values, then the neutral null model can be rejected (Pybus and Shapiro, 2009).

In protein coding sequences, mutations can be classified as synonymous (silent) or non-synonymous (replacement). dN/dS methods reflect the difference in the selective forces acting on silent versus replacement changes, where d_N and d_S are considered as per replacement or silent site, respectively, thereby indicating that random mutations create more replacement changes than silent changes due to the structure of the genetic code. If all replacement fixations are neutral, the ratio dN/dS is equal to one. If $dN/dS < 1$, the rate of replacement fixation is slower, indicating that negative selection has acted more strongly on replacement changes. In case $dN/dS > 1$, means that positive selection must have occurred, because no other obvious process can result in a faster fixation rate for replacement changes. The most common used dN/dS methods are single likelihood ancestor counting (SLAC) method and the fixed-effects likelihood (FEL) method (Pybus and Shapiro, 2009).

Genetic drift is a variation in the relative frequency of mutations which fluctuate randomly through time, with no net tendency towards increase or decrease, until the mutations become either fixed or eliminated. These fluctuations are very small in large populations, however they are very important because new mutations begin at very low frequencies and therefore they are highly susceptible to elimination. Important consequence of genetic drift is that mutations are fixed significantly slower compared to selection (Vandamme, 2009).

Continual increase of genetic data and advances in statistical inference allow for new opportunities for phylodynamic studies of infectious diseases (Faria et al., 2011). Rapid evolution of viruses as etiological agents of infectious diseases means that the epidemiological and ecological processes that shape their genetic diversity act on approximately the same time scale as mutations fixed in viral populations (Holmes, 2008). The result of this interaction is a spatial phylodynamic process that can be recovered from genomic data using phylogeographic analyses. The relevance of this analysis is multiple, including prediction of emergence of infectious diseases by detecting the key host species and the geographic areas from which pathogens spread and prediction of the impact of movement of natural reservoirs on the spread of viral diseases.

Phylogenetic reconstruction provides initial insight into the origin of viral strains. Phylogenetic trees embed spatial diffusions as evidence of transitions among locations (Faria et al., 2011). Herein, spatial diffusion can be treated as a process of trait evolution where the particular trait — in this case, geographic location, is considered as an inherited property of the virus. The next step is to estimate ancestral locations using appropriate method, which are categorized according to the criterion used to choose between alternative hypothesis and according to the process used to model the traits change across the tree. Namely, each process can be specified for traits distributed discretely, e.g., in cases when viruses originate from different countries or cities. On the other hand, process can be specified for traits which are distributed continuously, for example, when latitude and longitude coordinates are used as spatial locations for viral samples. Indeed, Bayesian statistical framework is probably the best due to flexibility in hypothesis testing.

Spatiotemporal reconstructions can be assessed by two different phylogeography approaches; phylogeographic inference in discrete space and phylogeography in continuous space and time (Lemey et al., 2009; Lemey et al., 2010). If sequence sampling locations are considered as discrete states, a continuous-time Markov chain (CTMC) can be used to model diffusion between locations (Lemey et al., 2009). Because all rates are generally not required to explain adequately the diffusion process, the estimation procedure would gain efficiency through focusing on a limited set of well-supported migration pathways. Therefore, this problem can be resolved by introducing Bayesian stochastic search variable selection (BSSVS) model which enables to construct a Bayes factor test that identifies the most parsimonious description of the phylogeographic diffusion process.

However, such discrete transitions do not explicitly model the diffusion process in continuous space (Lemey et al., 2010). For continuous geographic coordinates (latitude and longitude), Brownian diffusion (BD) finds analogues to the CTMC. This random-walk model allows fully exploring two-dimensional space, and delivering a more realistic representation of the diffusion process, particularly for continuously distributed samples.

Genetic drift and reassortment have been proposed as the main mechanisms explaining genetic diversity of hantaviruses as segmented negative-sense RNA viruses (Plyusnin et al., 2002). Genetic drift represents the fixation of variation through random processes resulting in

changes over generations (Bennett et al., 2014). This mechanism is the underlying force of hantavirus diversification upon transmission to a new host. Namely, possible scenario of hantavirus diversification has involved a host switch from a shrew ancestor into bats, and, subsequently, into rodents, followed by additional cross-species transmission events within some of these orders.

Reassortment is generally defined as an exchange of genetic segment(s) between parental viruses. Since the genome of hantaviruses consists of three segments, reassortment is one of the important mechanisms in hantavirus evolution. Moreover, reassortment between closely related viruses appears to occur frequently when their hosts share the same niche, but infrequently between genetically distinct hantaviruses, especially for the viruses whose hosts have no opportunity to contact each other (Zhang, 2014). This evolutionary force has been detected in both Old World and New World hantaviruses. Results of molecular phylogenetic analyses have indicated possible reassortment between S and M segments of DOBV-Af (Dobrava genotype) and DOBV-Aa (Kurkino genotype) (Klempa et al., 2003). Reassortment was also detected in HTNV lineages originated from Republic of Korea (Kim et al., 2016). Jabora and Juquitiba hantaviruses, isolated in Paraguay, were also defined as reassortants (Chu et al., 2011).

Natural selection is known important mechanism for hantavirus evolution (Bennett et al., 2014). Diversity of hantaviruses has been shaped by negative selection, resulting in proportionally less substitutions affecting phenotype than expected. However, positive selection has not been proven yet. It is possible that positive selection plays an episodic role, for example following a host switch.

Hantaviruses represent possibly the best example of long-term association between RNA viruses and their hosts. Hantaviruses were considered to had strongly cospeciated with rodents and insectivores as their hosts, since these mammals shared last common ancestor approximately 100 million years ago (Ramsden et al., 2009). This fact was also based on phylogenetic inference of members of the Hantavirus genus which revealed three constantly well-defined clades, each associated with only one of the three subfamilies of Muroid rodents: Arvicolinae, Murinae, and Sigmodontinae (Plyusnin et al. 1996). Nevertheless, since the hantaviruses were at that time also isolated from insectivores, overall phylogenetic inference of

both rodent- and insectivore-borne hantaviruses revealed that neither one of these formed monophyletic clade (Arai et al., 2008). Following the assumption of codivergence, the rate of molecular evolutionary change in hantaviruses has been estimated at approximately 10⁻⁷ nucleotide substitutions per site, per year (Hughes and Friedman, 2000; Sironen et al., 2001). Additionally, substitution rates obtained for other RNA viruses are 10⁻² to 10⁻⁴ substitutions/site/year, which are several orders of magnitude higher than that reported for hantaviruses (Jenkins et al. 2002; Hanada et al. 2004). Based on these findings, hantaviruses would be considered among the slowest evolving viruses. However, since the hantaviruses use an RNA-dependent RNA polymerase for replication with error rates in the region of one mutation per genome replication, a low rate of nucleotide substitution is inconsistent. Few years later, it was confirmed that these viruses exhibit short-term substitution rates of 10⁻² to 10⁻⁴ substitutions/site/year (Ramsden et al. 2008). According to this result it was strongly suggested that hantaviruses are evolving significantly faster than it was predicted based on shared divergence times with their rodent hosts.

Phylogenetic analyses of the available S or M sequences revealed that all known hantaviruses form four ‘phylogroups’ (**Figure 7** and **Figure 8**). The phylogroup I includes hantaviruses isolated from insectivores. This group engaged a basal position in the phylogenetic tree, according to the Bayesian Maximum Clade Credibility (MCC) tree (which is automatically rooted on the assumption of a molecular clock such that basal viral lineages can be identified) (Guo et al., 2013). Hantaviruses placed in phylogroup II originate from bats and the more divergent Nova virus (NVAV) identified in the European common mole (*Talpa europaea*) in Hungary (Kang et al., 2009). Phylogroup III consists of all other known insectivore-associated hantaviruses together with all known *Murinae*-associated hantaviruses, forming two distinct clades. Phylogroup IV includes two monophyletic groups corresponding to hantaviruses sampled from *Arvicolinae*, *Neotominae*, and *Sigmodontinae* rodent subfamilies. Similar results were obtained when the phylogenetic analysis was based on M segment, except that the second phylogroup was placed in the basal position, followed by phylogroups I, III, and IV (Guo et al., 2013). These phylogenetic data imply that the ancestor of the extant hantaviruses might have first appeared in Chiroptera and/or Soricomorpha (Guo et al., 2013).

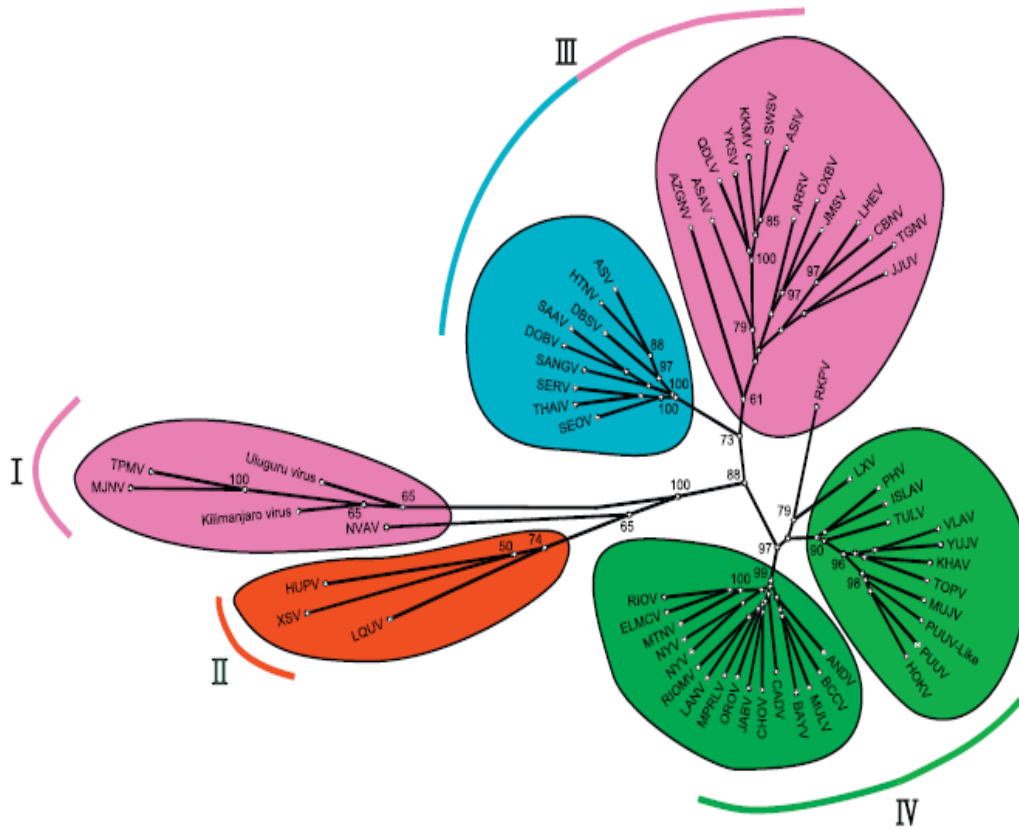


Figure 7. Phylogenetic tree based on the available entire coding regions of the hantavirus S segment estimated using the Maximum Likelihood (ML) method. The numbers above or below branches indicate bootstraps. Colors indicate *Chiroptera*-borne viruses (red), *Soricomorpha*-borne viruses (purple), *Murinae*-borne viruses (blue), *Arvicolinae*-borne viruses (light green), and *Sigmodontinae/Neotominae*-borne viruses (dark green). Modified from Zhang, 2014.

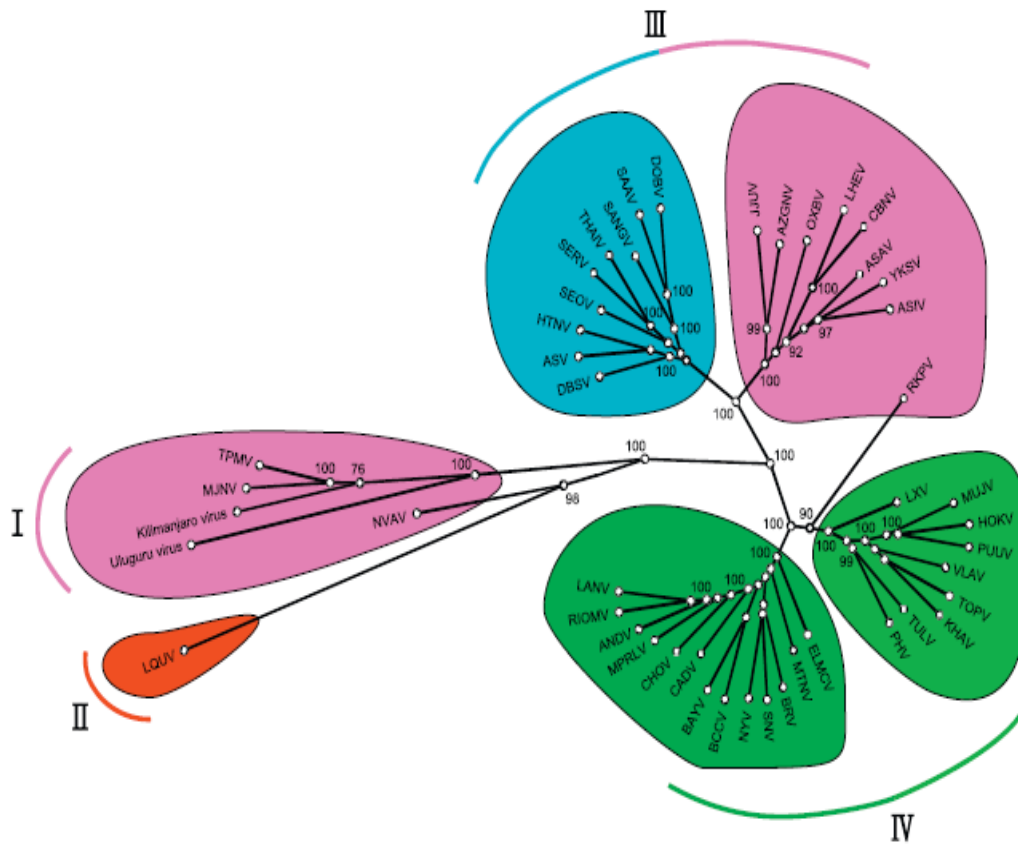


Figure 8. Phylogenetic tree based on the available entire coding regions of the hantavirus M segment estimated using Maximum Likelihood (ML) method. The numbers above or below branches indicate bootstraps. Colors indicate *Chiroptera*-borne viruses (red), *Soricomorpha*-borne viruses (purple), *Murinae*-borne viruses (blue), *Arvicolinae*-borne viruses (light green), and *Sigmodontinae/Neotominae*-borne viruses (dark green). Modified from Zhang, 2014.

Up to now, spatial diffusion of hantaviruses represent an unexplored scientific field. In general, phylogeography has played an important role in the evolution of hantaviruses and therefore has strongly influenced the hantavirus diversification. Geographic structure of hantaviruses is strongly affected by host distribution (**Figure 9**). For example, DOBV and SAAV are restricted to Europe, since the distribution of their natural reservoirs is limited to Europe; TULV and Seewis virus (SWSV) are in circulation throughout Europe and Russia, while PUUV is known to be present in Europe and Asia. Likewise, exchange of hantaviruses between more or less distinct hosts is also possible (Sschlegel et al., 2012; Guo et al., 2013).

Phylogenetic analysis of hantaviral molecular evolution in different rodent species

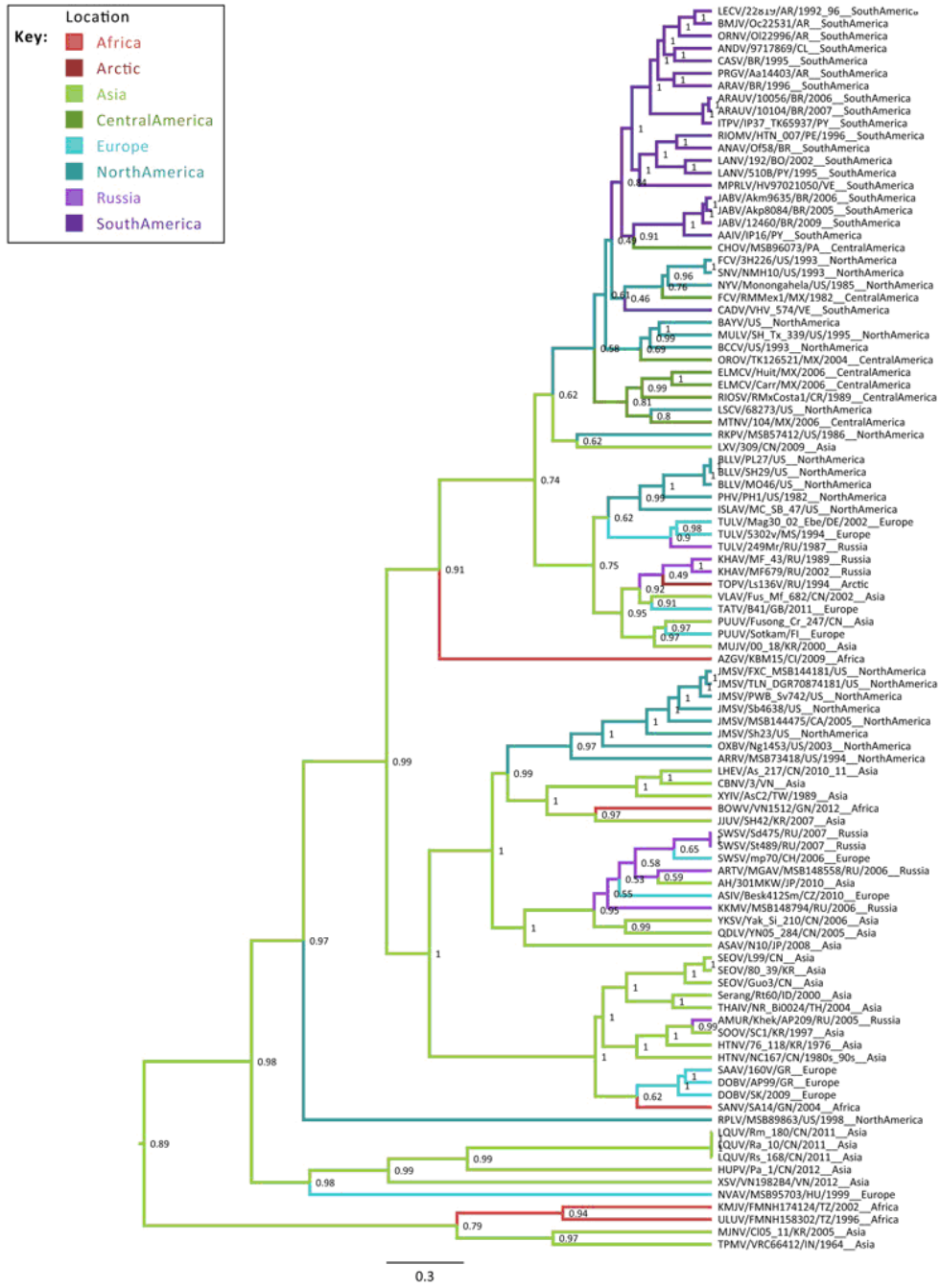


Figure 9. Phylogeography of hantaviruses. Maximum clade credibility tree based on the S segment using BEAST v1.8 (MCMC run for 50 million generations), with estimates of node geographic state indicated by color of the descending branch and probability at node. The scale bar indicates number of substitutions per site. Modified from Bennett, 2014.

The phylogenetic data showed that Asia represents possible geographic origin of the major lineages of hantaviruses, from where they spread to the Americas separately in shrews and rodents (Bennett et al., 2014).

The currently unresolved questions are related to the discovery of new species of small mammals serving as natural hosts of hantaviruses and their importance as a sources of zoonoses, as well as the role of changes in the host, the degree of co-evolution of hantaviruses with their hosts, and the molecular mechanisms of hantaviral genome evolution. The questions may be answered as additional whole genome sequences will be available in the NCBI database.

2. AIMS OF THE STUDY

The current thesis focuses on the evolutionary analysis of hantaviral sequence data. Multiple phylogenetic methods, including phylodynamic and phylogeographic analysis, were employed to examine complex biological processes, such as evolutionary dynamics, natural selection, recombination and migration of hantaviruses.

Specific aims of the study were:

1. To investigate the presence of hantaviral genome in various rodents trapped in Serbia by molecular methods and to genetically characterize the hantavirus RNA,
2. To study the molecular evolution of hantaviruses applying phylogenetic, phylodynamic and phylogeographic analyses on the three hantaviral RNA segments.
3. To explore and characterize the occurrence of homologous recombination in the hantavirus genome.

3. MATERIALS AND METHODS

3.1. STUDY DESIGN AND ETHICAL APPROVAL

The study was designed as molecular and phylogenetic investigation of hantaviruses detected in different animal reservoirs. It was performed at the Institute of Microbiology and Immunology, Faculty of Medicine, University of Belgrade in collaboration with the Institute for Biological Research Sinisa Stankovic, University of Belgrade and the Military Medical Academy, Belgrade. Before the study initiation, the protocol was approved by the Ethical Committee of the School of Medicine, University of Belgrade.

3.2. RODENT TRAPPING AND SPECIES IDENTIFICATION

The study sample was based on animal tissues of 350 rodents trapped on several occasions during a 5-year period (2007-2011) at eight different trapping sites in Serbia, by collaborating researchers from the Institute for Biological Research Sinisa Stankovic, University of Belgrade and the Military Medical Academy, Belgrade (**Table AI, Appendix**). These trappings had been performed within different studies not related to hantavirus research. However, the trapping sites corresponded to the vicinity of hantavirus natural hosts and humans, thus the resulting pool of samples could be used for hantavirus research.

The included trapping sites were situated in central, west and south Serbia (**Figure 10**). Avala Mountain (511 meters above sea level) and Kosutnjak park-forest are popular recreational sites located near Belgrade, the capital city of Serbia. The region of the Ravanica River, at altitude ranging between 580 and 716 meters, is located in central Serbia; this location is characterized by hilly and wooded terrain of mixed deciduous forest (beech, oak, oak, hazel, hornbeam) with wild pear and apple trees on the fringes. Cer and Tara mountains are located in western Serbia; Cer Mountain with altitude of 689 meters above sea level is located 100 km west of Belgrade, while Tara Mountain with altitude 1000-1500 meters above sea level is a popular tourist center. Vranje is a city in southern Serbia, known as potential focus of hantaviruses, with high number of reported HFRS cases. Lisine is a waterfall in eastern Serbia situated at an altitude of 380 meters. Zajecar is a city in eastern Serbia.

For the purpose of this research, rodents belong to different families (*Murine*, *Arvicolinae* and *Glirinae*) were studied. Blood and tissue (liver, kidney or lung) samples were taken from each captured animal and stored at -80°C until use. The animals trapped in the

region of Ravanica River and Zajecar (165/350) were identified to species level according to morphological characteristics. All other animals (185/350) had previously been identified to species level by a recently developed ISSR-PCR (Inter Simple Sequence Repeat-Polymerase Chain Reaction) analysis (Bugarski-Stanojevic et al., 2011).

From this pool of animal samples, 110 tissue specimens of different animals were available for hantavirus genetic analysis and characterization within the current study. Forty-six out of 110 sampled animals had been previously found serologically positive to either hantaviral antigens or antibodies, whereas 64/110 samples were tested using molecular approach only.



Figure 10. Map of trapping sites in Serbia

3.3. RNA EXTRACTION FROM TISSUE SAMPLES

Total RNA was extracted from tissues samples using the TRIZOL Reagent (GibcoBRL, Invitrogen, Karlsruhe, Germany). Applied procedure is based on the acid guanidine isothiocyanate-phenol-chloroform method (Chomczynski and Sacchi, 1987). Namely, TRIZOL reagent is suitable for rapid isolation of total RNA from different tissues. During the homogenization and cell lysis step of the sample, TRIZOL reagent maintains the integrity of RNA and at the same time degrades the cells and cellular components. Addition of chloroform leads to splitting the mixture into the aqueous and organic phase. RNA remains exclusively in the aqueous phase of which it is recovered by precipitation with isopropanol. This technique is particularly suitable in working with small amount of samples.

Briefly, small pieces of analyzed tissues, approximately 10 mg, were homogenized in liquid nitrogen using a mortar and pestle. The mixture was then transferred to a 1.5 ml sterile tube containing 1 ml of TRIZOL. After 5 min of incubation at room temperature, 200 µl of chloroform was added. Obtained mixture was then mixed by vortexing for 10-15 sec and incubated at room temperature for 3 min. Homogenate was further centrifuged at 12,000 g for 15 min at 4°C and the aqueous phase was transferred in a new sterile tube. In order to precipitate RNA, 500 µl of cold isopropyl alcohol was added and the mixture was incubated at room temperature for 10 min, followed by centrifugation at 12,000 g for 10 min at 4°C. Obtained supernatant was removed and the pellet was washed twice with 1 ml of 75% ethanol, using centrifugation at 7,500 g for 5 min at 4°C after every step. The pellet was then air-dried and dissolved in 25 µL of RNase-free water with 5 U of RNase inhibitor.

3.4. NESTED POLYMERASE CHAIN REACTION

Total RNA was used as the starting template for reverse transcriptase polymerase chain reaction (RT-PCR). All samples were initially tested using a pan-hanta protocol which amplifies a 412-bp fragment of the L RNA segment of all known hantaviruses (**Table 2**). All reagents used for the PCR reaction mix, were thawed in refrigerator and put on ice during the mix preparation. For the first round of the PCR assays (outer PCR), RNA was reverse transcribed using the One Step RNA PCR Kit (Qiagen, Hilden, Germany). Reaction mix was prepared according to manufacturer's instructions. Cycling parameters were also optimized

according to manufacturer's instructions with some changes of annealing temperature, when necessary.

Table 2. Primer pairs used in nested PCR and cycle sequencing reaction.

Primer	Sequence (5'-3')	Hantavirus species	Segment	Reference
HAN-L-F1	ATGTAYGTBAGTGCWGATGC	all	L	Klempa et al., 2006
HAN-L-R1	AACCADTCWGTCCRTCATC	all	L	Klempa et al., 2006
HAN-L-F2	TGCWGATGCHACIAARTGGTC	all	L	Klempa et al., 2006
HAN-L-R2	GCRTCRCWGARTGRTGDGCAA	all	L	Klempa et al., 2006
DOB-S-F1	GTAGTAGGCTCCCTAAAAAGC	DOBV	S	this study
DOB-S-R1	GGGATTACATAAAGCATGGGA	DOBV	S	this study
DOB-S-F2	CACTACACTAAAGATGGCAA	DOBV	S	this study
DOB-S-R2	GGATAATGCAACAAATACAATTA	DOBV	All	this study
OSM55	TAGTAGTAKRCTCC	DOBV	All	Kang et al., 2010
RT-DOB	TAG TAG TAK RCT CCC TAA ARA G	DOBV	All	Sibold et al., 2001
D1162C	AGT TGI AT(I+C) CCC ATI GA(I+C) TGT	DOBV	S	Sibold et al., 2001
D955C	ACC CAI ATT GAT GA(I+C) GGT GA	DOBV	S	Sibold et al., 2001
D113	GAT GCA GAI AAI CAI TAT GAR AA	DOBV	S	Sibold et al., 2001
D357	GA(I+C) ATT GAT GAA CCI ACA GG	DOBV	S	Sibold et al., 2001
M1470c	CCI GGI TTI CAT GGI TGG GC	DOBV	M	Klempa, 2004
M2029R	CCA TGI GCI TTI TCI KTC CA	DOBV	M	Klempa, 2004
M1674c	TGT GAI RTI TGI AAI TAI GAG TGT GA	DOBV	M	Klempa, 2004
M1990R	TCI GCI STI GCI GCC CA	DOBV	M	Klempa, 2004
PPT334C	TAT GGI AAT GTC CTT GAT GT	TULV	S	Bowen et al., 1997
PPT986R	GCA CAI GCA AAI ACC CA	TULV	S	Bowen et al., 1997
PPT376C	CCI AGT GGI CAI ACA GC	TULV	S	Bowen et al., 1997
PPT716R	AAI CCI ATI ACI CCC AT	TULV	S	Bowen et al., 1997
S5	TACAGAGCAGCAGATTACCTGA	TULV	S	Song et al., 2002

Standard conditions were:

- 8 µl of 5x OneStep RT-PCR Buffer
- 1,6 µl of dNTP mix
- 1.6 µl of forward primer in 0.6 µM final concentration (Invitrogen by Life Technologies, Carlsbad, California, USA) (**Table 2**)
- 1.6 µl of reverse primer in 0.6 µM final concentration (Invitrogen by Life Technologies, Carlsbad, California, USA) (**Table 2**)

- 15.6 µl of RNase-free water
- 10 µl of RNA template.

Final reaction volume was 40µl.

Prepared PCR reaction mix was further proceeded in the thermal cycler “Eppendorf Mastercycler ep gradient S”. Samples were initially reverse transcribed at 50°C for 40 minutes followed by denaturation at 94°C for 15 minutes. After an initial denaturation step the cycling was further consisted of three steps (94°C for 30; primers were annealed for 1 minute at an appropriate temperature; 72 °C for 3 minute) repeated 40 times and followed by a final elongation step for 10 minutes at 72 °C.

Second round (inner PCR) was prepared using Thermo scientific dream taq PCR master mix (2X) (Applied Biosystem, Foster City, California).

Standard conditions were:

- 25 µl of DreaMountainaq PCR Master Mix (2X)
- 2 µl of Fw primer in 0.6 µM final concentration (Invitrogen by Life Technologies, Carlsbad, California, USA) (**Table 2**)
- 2 µl of Rev primer in 0.6 µM final concentration (Invitrogen by Life Technologies, Carlsbad, California, USA) (**Table 2**)
- 16 µl of nuclease free water
- 5µl of outer DNA template

Final reaction volume was 50µl.

Prepared PCR reaction mix was further proceeded in the thermal cycler “Eppendorf Mastercycler ep gradient S”. Samples were initially denaturated at 94°C for 15 minutes. After an initial denaturation step the cycling was further consisted of three steps (94°C for 30; primers were annealed for 1 minute at an appropriate temperature; 72 °C for 3 minute) repeated 40 times and followed by a final elongation step of 10 minutes at 72 °C.

For both rounds of PCR, positive and negative controls were tested along with the samples, in order to check whether the procedure is working and to determine any possible contamination.

The initial PCR for all examined samples was done using degenerated primers for detection partial L segment of all known hantaviruses. All samples which were positive for the presence of partial L segment were further analyzed by using different pairs of primers for amplification of fragments of S and M segments (Table 2). DOBV S segment sequences isolated from *A. flavicollis* were amplified and sequenced using DOB-S-F1, DOB-S-F2, DOB-S-F2 and DOB-S-S2 primers, while DOBV S segment sequences isolated from *A. agrarius* and *G. glis* were amplified and sequenced using OSM55, RT-DOB, D1162C, D955C, D113 and D357 primers. DOBV M segment sequences were amplified and sequenced using M1470c, M2029R, M1674c, M1990R primers. TULV S segment sequence was amplified and sequenced using PPT334C, PPT986R, PPT376C, PPT716R and S5 primers. PCR protocols were prepared in the same way as described above with appropriate annealing temperatures.

In addition to the primers described in literature, a number of hantavirus specific primers were designed within the current study (DOB-S-F1, DOB-S-F2, DOB-S-F2, DOB-S-S2), using the appropriate tool at the NCBI database (www.ncbi.nlm.nih.gov/tools/primer-blast/).

All lyophilized primers were diluted in sterile distilled water to a stock concentration of 100 pmol/μl and stored at -20°C until required. Prior to the PCR testing, primers were equilibrated to working concentrations of 20 pmol/μl and also stored at -20 °C. Annealing temperature of each primer was calculated according to the melting temperature of primers, which was calculated using PerlPrimer (<http://perlprimer.sourceforge.net>).

3.5. AGAROSE GEL ELECTROPHORESIS

Analysis of the PCR products was performed by electrophoresis in 2% agarose gel. The basic principle of this method is based on the fact that charged particles of different masses, under the influence of the electric field, passes different paths in agarose gel. The same TAE (Tris-acetate-EDTA) buffer was used for both, gel and electrophoreses (Sambrook et al., 1989). The 50x stock of TAE was diluted 50:1 with distilled water to prepare the working solution, containing 40mM Tris, 20mM acetic acid, and 1mM EDTA. 2% agarose gel was prepared by dissolving 2g of agarose in 100ml TAE buffer and heating to the melting point. Ethidium

bromide (EtBr 25 µg/ml, Serva Electrophoresis GmbH, Heidelberg, Germany) was added in the solution for visualization of the DNA bands. 5 µl of samples were mixed with 2 µl of the gel loading dye (0.125% Bromophenol blue, 40% Sucrose) and approximately 7 µl of mixture was loaded per lane on agarose gel. The Gene Ruler™ 1 kb DNA ladder (DNA Standard 100bp - Serva Electrophoresis GmbH, Heidelberg,) was used as a molecular length size marker. Electrophoresis reactions were run at 120 V. Visualization of the DNA was performed under UV light with a wavelength between 280 and 320 nm.

3.6. CYCLE SEQUENCING RECTION

3.6.1. Purification of pcr products

Amplified PCR products (which were defined as positive on the agarose gel), were further purified with MinElute Purification Kit (Qiagen, Hilden, Germany) kit, following the manufacturer's instructions. The purification protocol based on silica membrane spin was used, which allows binding of nucleic acids to a silica membrane inside a spin column (Sambrook *et al.*, 1989).

General protocol was as follows:

- Firstly, 200 µl of Buffer PB and 40 µl product of the nested PCR reaction were roughly mixed and applied to MinElute column and centrifuge for 1 min at 18,000 x g. Flow-through was discarded and the MinElute column was put back into the same collection tube.
- Then, 750 µl Buffer PE was added to the MinElute column and centrifuged twice for 1 min at 18,000 x g. Flow-through was discarded and the MinElute column was put back into the same collection tube. The column was centrifuged for an additional 1 min at maximum speed.
- At last, MinElute column was placed in a clean 1.5 ml microcentrifuge tube. 10 µl Buffer EB (10 mM Tris·Cl, pH 8.5) was added to the center of the membrane, let the column stand for 1 min, and then, centrifuge for 1 min at 18,000 x g.

Obtained filtrate was used for the cyclic sequencing reaction.

3.6.2. Cycle sequencing reaction

Purified PCR products were subjected to direct sequencing of both the sense (forward) and antisense strands (reverse). DNA sequencing was carried out using the Sanger cycle sequencing method. Sanger sequencing is based on the selective incorporation of chain-terminating dideoxynucleotides by DNA polymerase during in vitro DNA replication (Sanger et al, 1977). Chain termination sequencing reactions were set up in house, using BigDye Terminator v3.1. Cycle Sequencing kit (Applied Biosystems Incorporated, Foster City, CA) according to manufacturer's instructions. Fluorescently labeled dyes are attached to ACGT extension products in DNA sequencing reactions. The dyes come in four colors red (for thymidine), blue (for cytosine), black (for guanine) and green (for adenine). The dyes are incorporated using either 5'-dye label primers or 3'-dye label dideoxynucleotide terminators. For each sample two cycle sequencing reactions were set, using inner PCR primers described in **Table 2**.

General protocol was as follows:

- 1µl each primer 5 µM working concentration
- 1µl of purified RT-PCR product,
- 2µl 5× Cycle sequencing dilution buffer
- 2µl BigDye
- 4µl ultrapure water.

Final reaction volume was 10µl.

The sequencing PCR included 40 cycles of 96 °C for 30 s, 50 °C for 7 s and 60°C for 4 min. After running the sequencing reaction, non-incorporated dideoxynucleoside triphosphates were removed by 75% isopropyl alcohol precipitation and the pellet was resuspended in 20µl High Density Formamide (Applied Biosystems Incorporated, Foster City, CA) for denaturation and detected in an ABI Prism 310- Genetic Analyzer capillary electrophoresis system (Applied Biosystem, Foster City, CA, USA). Results were analyzed with the Sequencing analysis software v.5.2 (Applied Biosystem, Foster City, USA).

3.7. SEQUENCE DATASETS

Several datasets of hantavirus L, M and S segment sequences of the studied hantaviruses were used in phylogenetic analyses. Each dataset contained the newly detected DOBV and/or TULV sequences together with sequences downloaded from the NCBI database (<http://www.ncbi.nlm.nih.gov/nucleotide>).

The studied data set for DOBV L segment contained 37 sequences of 260 nt in length. One data set of 16 sequences was created for the M segment analyses of DOBV (434 nt in length). In course of different phylogenetic analyses 4 different data sets of DOBV S segment were made, consisting of: 180 sequences of 494 nt in length for general phylogenetic exploration; 68 sequences of 528 nt in length and 36 sequences of 789 nt in length for defining the novel HFRS focus, and 67 sequences of 501 nt in length for exploring novel host reservoir.

Four different data sets were constructed for TULV. Two sets, for general phylogenetic L and S segment analyses, were made of 21 sequences (322 nt in length) for L, and 66 sequences (570 nt in length) for the S segment. Moreover, in order to analyze possible recombination events, a set of 22 S segment TULV sequences comprising 928 nt (position 400-1324 nt according to the S segment reference strain NC005227) were aligned.

For the purpose of phylogeographic analysis, one dataset for TULV S segment sequences was made with two inclusion criteria for each sample: knowledge of the exact place of origin and collection date. The data set was made of 137 S segment sequences of 543 nt in length.

Complete list of all sequences with the NCBI accession numbers and relevant data is shown in **Table AII, Appendix**.

3.8. PHYLOGENETIC ANALYSES

Phylogenetic analysis requires multiple sequences need to be formatted in a single file. However, different phylogenetic software packages use different formats resulting in about 18 common used formats. Therefore, all formerly prepared sequence datasets were firstly converted in different sequence formats, including FASTA, NEXUS and PHYLIP (http://phylogeny.lirmm.fr/phylo.cgi/data_converter.cgi). Sets of previously formatted sequences were aligned in appropriate software package. This step is very important for further

phylogenetic analysis, because the quality of alignment directly affects the results obtained in further analysis.

In this study sequence alignment was done using ClustalW software with progressive multiple sequence alignment approach. ClustalW, implemented in Molecular Evolutionary Genetics Analyses (MEGA version 5.1) software, took a set of input sequences and carried out the entire progressive alignment procedure automatically (Tamura et al., 2011). After aligning sequences in pairs, program generated distance matrix that can be used to make a simple initial tree of the sequences. Obtained guide tree generated using the Neighbor-Joining method, was used to lead the multiple alignment.

Manual editing is the next step in the analysis and it is needed to be done in order to correct obvious alignment errors and to remove gaps. To be precise, there is no need to delete all positions with gaps, because they also contain some useful information. If the columns in the alignment are not overly gapped (less than 50%), they can be kept in the alignment.

Since phylogenetic reconstruction is a problem of statistical inference, the use of a model of nucleotide substitution (evolutionary model) becomes obligatory. Therefore, in order to construct phylogenetic tree it is necessary to carry out the best-fit model of nucleotide substitution. jModelTest 0.1.1 is suitable tool to calculate statistical selection of best-fit models of nucleotide substitution (Posada 2008). It implements five different model selection strategies: hierarchical and dynamical likelihood ratio tests (hLRT and dLRT), Akaike and Bayesian information criteria (AIC and BIC), and a decision theory method (DT). All models were selected according to the Akaike Information Criterion (AIC) using all 88 proposed models.

3.8.1. Identification and characterization of hantaviral RNA obtained from different animal reservoirs

The obtained L segment sequences were first analyzed by BLAST at NCBI (<http://blast.ncbi.nlm.nih.gov/Blast.cgi>) in order to determine similarity scores to specific hantaviruses. After initial identification of hantavirus species using BLAST, all positive samples were further analyzed for the amplification of partial M and S segment fragments

using appropriate pairs of primers (**Table 2**). Final confirmation of species was done based on phylogenetic clustering.

3.8.2. Phylogenetic trees reconstruction

Different evolution mechanisms (mutations, recombination and natural selection) play important role in divergence of sequences. The measure of this divergence is called genetic distance. An essential requirement for computing genetic distances is the prior definition of a model of substitution, which provides a statistical description of this stochastic process. Therefore, after the sequence alignments were made and the best fitting model of evolution for each alignment was defined, genetic distance can be inferred. In this study PAUP software package was employed to calculate genetic distance under the best fitting evolutionary model (Swofford, 2003).

The next step in phylogenetic analysis is inferring the phylogenetic trees. Phylogenetic tree is a diagram that depicts the relationships between sequences including in analysis. Phylogenetic trees were inferred using different methods, including ML and Bayesian methods. PHYML program was used for ML inference of phylogenies (Guindon et al., 2010). The input sequence format for this program is PHYLIP. BEAST and MrBayes programs were employed to infer phylogenetic trees using Bayesian method (Tamura et al., 2011; Drummond and Rambaut, 2007; Ronquist and Huelsenbeck, 2003). The input sequence file for these programs was NEXUS file.

Bootstrapped replicates of phylogenies were sampled to assess support for clades. Bootstrap analysis is a simple and effective technique to test the relative stability of groups within a phylogenetic tree. Briefly, for an alignment of sequences where the rows represent different taxa and the columns are sites along the genome, columns of sites are randomly sampled with replacement to create a new alignment of the same size as the original. For the random sample a tree is then inferred. This resampling process is usually repeated many times (usually 1000 times). Overall, under normal circumstances, considerable confidence can be given to branches or groups supported by more than 70%. This technique can be applied together with almost all methods for construction of phylogenetic trees.

The final trees, together with bootstrap values, were visualized and edited by FigTree (<http://tree.bio.ed.ac.uk/software/figtree/>).

Each sequence contained certain amount of evolutionary information and the maximum-likelihood approach can be used to study it. Likelihood-mapping method, implemented in TreePuzzle, can be employed to investigate the phylogenetic signal of each sequence. Briefly, this program analyzed sequences using likelihood-mapping method of 10,000 randomly chosen quartets (set of four sequences), under the best fitting substitution models described above (Strimmer & von Haeseler, 1997). A likelihood map was consisted of dots placed on the triangle surface. Each dot placed in the corners of triangle represent fully resolved phylogenies in which one tree is clearly better than the others, unlike the dots placed in the center of the triangle which represent star-like signal. The results of this analysis showed whether the data are suitable for a further phylogenetic reconstruction.

Prior to further phylogenetic analysis all datasets were studied using this program. Firstly, sets were converted in appropriate format (PHYLIP) for this program. Likelihood-mapping analyses were done under the appropriate sets of parameters, including best fitting model for each set and 10000 randomly chosen quartets.

3.8.3. Selective pressure

Considering natural selection as one of the important molecular mechanisms for virus evolution and therefore it is very important to asses the potential presence of selection pressure. Codon-based models of molecular evolution are able to infer signatures of selection from sequence alignments by estimating the mean ratio of synonymous (dS) and non-synonymous substitutions (dN). Overall selection pressure was estimated using the single likelihood ancestor counting (SLAC) method from the HyPhy package, a computational phylogenetics software package intended to perform maximum likelihood analyses of genetic sequence data and equipped with tools to test various statistical hypotheses (Pond and Frost, 2005), available at <http://www.datamonkey.org>.

3.8.4. Recombination analysis

Since recombination is not rare event in highly variable viruses, detection of this evolutionary mechanism is very important for further phylogenetic analysis. Therefore, after alignments of all datasets have been generated and the best fitting models were determined, sequences were examined using different recombination detection programs.

Initially, Recombination Detection Program version 4 (RDP4) was employed to examine potential recombination events in all datasets (<http://web.cbio.uct.ac.za/~darren/rdp.html>). RDP4 is very potential program containing several different recombination detection methods to both detect and characterize the recombination events. In addition to original RDP method, it includes the BOOTSCANning, the GENECONV, the Maximum Chi Square, the CHIMAERA, the Sister Scanning, the 3SEQ and the BURT methods (Martin et al., 2015). After loading the sequence FASTA file, under the button Option it is possible to adjust parameters for all methods. All above mentioned methods were used in our study and the results were interpreted according to manual instructions for each method.

BootScan method, implemented in SimPlot, is also broadly used method for identification of recombination (<https://sray.med.som.jhmi.edu/scroftware/simplot/>) (Lole et al., 1999). This method compares query sequence (potential recombinant) to a set of known non-recombinants (reference sequences) and identifies whether the query sequence is recombinant, but also the locations of potential breakpoint positions and the probable origins of different tracts of sequence within a recombinant. Different parameters, such as window size, step size and bootstrap value, can be set using the BootScan options. The result is shown in the form of curve, which represents comparison between the sequence being analyzed and reference sequence(s).

In order to analyze possible recombination events a set of 22 S segment TULV sequences 928-nt long (position 400-1324 nt according to S segment reference strain NC005227) were aligned. The TULV sequences were grouped according to clustering taken from the S phylogenetic tree; it contained four groups: one, consisted of sequences from Czech Republic and West Slovakia; a second with sequences from Germany and Poland; a third with sequences from Russia, while two sequences from Serbia were the (forth) query group.

Bootscan analysis was performed with Kimura (2-parameter) distance model, with window size of 160 bp and a step size of 20 bp, while 70% bootstrap value was defined as the cutoff level.

Identification of signature amino acid (AA) sequence differences between the examined strains was performed using VESPA (viral epidemiology signature pattern analysis) program (Korber and Myers, 1992). VESPA identifies site specific signature residues, defined as positions for which the most common AA differs between a query and a reference alignment. The sequences which were suggested to be potential recombinants have been set as query sequences in this analysis and they were compared to two reference data sets consisted of 62 sequences 190 aa long (used for reconstruction of S segment phylogenetic tree), and 18 full length S segment sequences (309 aa long) (scanned for recombination testing). In addition, the pattern of amino acid substitutions in Slovakian and Serbian strains were manually compared to those from Russia and Czech Republic.

3.8.5. Bayesian phylogenetic analysis of phylodynamics and phylogeography

BEAST is a program for Bayesian analysis of molecular sequences using a Markov Chain Monte Carlo (MCMC) method. It can be used as a method of choice for reconstructing phylogenies, but also for phylodynamic and phylogeographic analyses. A set of 137 TULV S segment sequences was analyzed using BEAST v 1.8.4.

Estimation of demographic growth, substitution rate and phylogeographic distribution was performed in a Bayesian framework using the MCMC method implemented in BEAST for viral dataset that exhibited sufficient temporal structure, as tested using root-to-tip regression analyses in TempEst (Rambaut et al., 2016).

Changes in effective population size through time were estimated using Bayesian Skyline Plot analysis, implemented in BEAST. Log-normal molecular clock and Bayesian Skyline as the tree prior were set in analysis. Moreover, 3 partitions: codon positions “1, 2 and 3 option” was selected so that each codon position has its own rate of evolution. Bayesian skyline plot was reconstructed in Tracer v1.6. using tree files obtained in BEAST analyses.

The substitution rate was calculated under the Log-normal molecular clock model together with the constant population demography as tree prior in two separate runs in

50,000,000 steps each, with sampling at every 5000 steps and the results were combined using LogCombiner 1.8.4 (implemented in BEAST) with 10% burn-ins removed from each run.

Phylogeographic analysis is very useful tool to trace the historical dispersal and migration patterns of pathogens. In order to investigate the ancestral location in viral spread, the alignment was made of 137 sequences of S segment TULV (543 nt in length). Each included sequences fulfilled two inclusion criteria: availability of exact place of origin and collection date. Assessment of TULV ancestral locations was done in continuous space by activating the Homogenous Brownian model. Additionally, a model was applied that allows for branch-specific rate variation in the diffusion process (termed 'relaxed random walks', RRWs) in order to test the rate of TULV spread. This model is known as Cauchy RRW model. Comparison of both applied models, Homogenous Brownian model and Cauchy RRW model, was done by estimating marginal likelihoods (MLE) using path sampling (PS) and stepping stone sampling (SS), which have recently been implemented in BEAST (Baele et al., 2012, 2013). Typically, PS/SS model selection is performed after doing a standard MCMC analysis. Log-normal molecular clock model together with the constant population demography was found to be best fit for our dataset. All runs were consisted of 10^8 generations and sampled every 10,000 steps.

Tracer v 1.6 (<http://tree.bio.ed.ac.uk/software/tracer/>) was used to analyze the output of BEAST for each analysis. This software assessed the convergence of the Markov chain calculating the effective sample size (ESS) for each parameter, representing the number of independent samples that would be the equivalent to the autocorrelated samples produced by the MCMC. For this analysis ESS values higher than 100 were considered sufficiently robust.

Maximum clade credibility tree (MCCT) was generated by TreeAnnotator, also implemented in BEAST package. This tool takes a single target tree and annotates it with the summarized information including, the average node ages, the posterior support and the average rate of evolution on each branch. The final tree was visualized and edited by FigTree (<http://tree.bio.ed.ac.uk/software/figtree/>).

In order to analyze the output from Bayesian phylogeographic analysis, Spread3 (Spatial Phylogenetic Reconstruction of Evolutionary Dynamics) program was used

(https://rega.kuleuven.be/cev/ecv/software/Spread3_tutorial#sectionOne). This is a tool for analyzing and visualizing discrete and continuous trait evolutionary histories associated with phylogenies. Namely, the MCC tree is converted to a java script object (JSON) file. Next the JSON file is then used for rendering the visualization using a Data Driven Document (D3) library.

Analysis of temporal structure of sequences is very important step in phylogeographic analysis. Widely used software for this analysis is TempEst program (Rambaut et al., 2016). Briefly, this program is designed to examine dated-tip trees (where sequences have been collected at different dates) and contemporaneous trees (where all sequences have been collected at the same time). The input data for this program is a phylogenetic tree previously generated in appropriate program under the maximum likelihood (ML) approach. The correlation coefficient, obtained as result of the program, indicates whether analyzed sequence data are suitable to be inferred under a molecular-clock assumption. If the correlation coefficient is <0.2 , the dataset is not suitable for further phylogenetic analysis; $0.2-0.4$ means weak temporal structure of examined sequences; >0.4 means that the analyzed dataset is suitable for phylogenetic analysis. For the purpose of this analysis, the phylogenetic trees were initially constructed in PHYML program. Obtained trees together with sampling date were input information for analysis in TempEst program. Obtained results were presented as chart of the distribution of root-to-tip distances (a regression against sampling date for dated tips).

4. RESULTS

4.1. RODENT POPULATION UNDER STUDY

Tissue samples from 110 animals were genetically tested for hantavirus RNA within the current study, as shown in **Table 3**, depicting also the trapping sites and year of trapping. Forty-six out of 110 sampled animals had previously been found serologically positive to either hantaviral antigens or antibodies, whereas 64/110 samples had been tested using molecular approach only (**Table 4**).

Table 3. List of animals tested within the current study. Location and year of trapping are shown.

Host species	Number of animals	Trapping site	Year of trapping
<i>Apodemus flavicollis</i>	9	Ravanica River	2007
<i>Apodemus flavicollis</i>	6	Tara Mountain	2008
<i>Apodemus flavicollis</i>	30	Zajecar	2009
<i>Apodemus flavicollis</i>	4	Tara Mountain	2009
<i>Apodemus flavicollis</i>	1	Avala Mountain	2009
<i>Apodemus flavicollis</i>	5	Kosutnjak	2010
<i>Apodemus flavicollis</i>	3	Avala Mountain	2010
<i>Apodemus flavicollis</i>	3	Vranje	2010
<i>Apodemus flavicollis</i>	8	Ravanica River	2011
<i>Apodemus sylvaticus</i>	2	Ravanica River	2007
<i>Apodemus sylvaticus</i>	9	Zajecar	2009
<i>Apodemus agrarius</i>	4	Ravanica River	2007
<i>Apodemus agrarius</i>	1	Ravanica River	2011
<i>Myodes glareolus</i>	5	Ravanica River	2007
<i>Myodes glareolus</i>	3	Zajecar	2009
<i>Myodes glareolus</i>	7	Ravanica River	2011
<i>Microtus arvalis</i>	2	Ravanica River	2007
<i>Microtus subterraneus</i>	1	Zajecar	2009
<i>Glis glis</i>	2	Ravanica River	2007
<i>Glis glis</i>	2	Zajecar	2009
<i>Glis glis</i>	1	Ravanica River	2011
<i>Mus musculus</i>	2	Zajecar	2009

Table 4. List of animals sampled for genetic detection of hantaviral RNA, with their serostatus, as defined previously

Rodent species	Total	Number (%) serologically pre-screened	Number (%) tested using molecular methods only
<i>A. flavicollis</i>	70	31 (44.28)	39 (55.72)
<i>A. agrarius</i>	5	4 (80)	1 (20)
<i>A. sylvaticus</i>	10	2 (20)	8 (80)
<i>G. glis</i>	5	2 (40)	3 (60)
<i>M. arvalis</i>	2	2 (100)	0 (0)
<i>M. glareolus</i>	15	5 (33.33)	10 (66.67)
<i>M. musculus</i>	2	0 (0)	2 (100)
<i>M. subterraneus</i>	1	0 (0)	1 (100)
Total	110	46 (41.82)	64 (58.18)

4.2. HANTAVIRUS DETECTION AND IDENTIFICATION

In total, encompassing all the tested rodent species, 6/110 (5.5%) genetically tested samples in the study were found positive for hantavirus RNA, including different host and virus species. Positive samples were found in the species *A. flavicollis*, *A. agrarius*, *G. glis* and *M. arvalis*. The list of positive samples according to species is given in **Table 5**. Of note, all the positive samples were within the serologically prescreened and positive group. Initial identification using BLAST at NCBI (<http://blast.ncbi.nlm.nih.gov/Blast.cgi>), of the partial L segment sequences obtained from three *A. flavicollis*, one *A. agrarius* and one *G. glis* revealed DOBV. The sequence recovered from *M. arvalis* was identified as TULV, with the same approach.

Table 5. List of rodents positive for the presence of hantavirus RNA, correlated to previously defined serostatus

Rodent species	DOBV positive samples		TULV positive samples	
	total	seropositive	total	seropositive
<i>A. flavicollis</i>	3/70 (4.3%)	3/31 (9.7%)	0	0
<i>A. agrarius</i>	1/5 (20%)	1/4 (25%)	0	0
<i>G. glis</i>	1/5 (20%)	1/2 (50%)	0	0
<i>M. arvalis</i>		0	1/2 (50%)	1/2 (50%)
Total	5/80 (6.3%)	5/37 (13.5%)	1/2 (50%)	1/2 (50%)

Among the L segment positive samples, partial S segment was recovered from five samples (S segment was not recovered from one sample of *A. flavicollis*), while partial M segment was recovered from three *A. flavicollis* samples only. A total of 14 hantavirus sequences were obtained within the current study. Accession numbers of the newly obtained Serbian hantavirus sequences, deposited in the NCBI database, are listed in **Table 6**.

Table 6. Accession numbers of Serbian hantavirus sequences of the current study.

Virus species	Genome segment	Host species	Identification number	Accession number
DOBV	L	<i>Apodemus flavicollis</i>	LT-RS1	KF425495
DOBV	L	<i>Apodemus flavicollis</i>	LT-RS2	KF425496
DOBV	L	<i>Apodemus flavicollis</i>	LT-RS3	KF425497
DOBV	L	<i>Apodemus agrarius</i>	DOBV_RAV71	KF177177
DOBV	L	<i>Glis glis</i>	DOBV_RAV69	KF177176
DOBV	M	<i>Apodemus flavicollis</i>	MT-RS1	NA
DOBV	M	<i>Apodemus flavicollis</i>	MT-RS2	NA
DOBV	M	<i>Apodemus flavicollis</i>	MT-RS3	NA
DOBV	S	<i>Apodemus flavicollis</i>	ST-RS1	KF425493
DOBV	S	<i>Apodemus flavicollis</i>	ST-RS3	KF425494
DOBV	S	<i>Apodemus agrarius</i>	DOBV_RAV71S	KJ437510
DOBV	S	<i>Glis glis</i>	DOBV_RAV69S	KJ437511
TULV	L	<i>Microtus arvalis</i>	TULV_RAV31	KF177178
TULV	S	<i>Microtus arvalis</i>	TULV_RAV31S	KF557547

Further phylogenetic analyses of M and S segments were performed using state of the art phylogenetic methods together with corresponding sequences retrieved from NCBI database. The accession numbers of all sequences (newly detected and those retrieved from NCBI database) are listed in **Table AII, Appendix**. The best-fit models of nucleotide substitution chosen for each alignment of sequences are listed in **Table 7**.

Table 7. Best-fit models of nucleotide substitution calculated based on jModelTest 0.1.1

Virus species	Segment	Number of sequences	Length of alignment	Best-fit models of nucleotide substitution*
DOBV	L	9	312	TIM2+G+I
DOBV	S	67	501	TPM1uf +G+I
DOBV	L	9	318	TIM2 + I
DOBV	S	36	789	TrN + G
DOBV	S	68	528	TPM2uf+I+G
DOBV	L	37	260	TrN+I+G
DOBV	S	180	494	TVM+I+G
DOBV	S	180	494	TVM+I+G
DOBV	S	36	789	Trn+G
DOBV	M	16	434	TrN+G
TULV	L	21	322	TPM2u + G
TULV	S	66	570	TIM2 + G + I
TULV	S	137	543	GTR +G+I

*Detailed description is given at the end of the text in the list of abbreviations

4.3. COMPARATIVE PHYLOGENETIC ANALYSIS OF PARTIAL L, M AND S SEGMENT SEQUENCES OF DOBV

In order to characterize genetic diversity of viral strains isolated from Serbia and assess their phylogenetic relationships, Serbian sequences were compared to all corresponding DOBV L, M and S sequences reported in NCBI database until December 2016. Serbian sequences included in the study were isolated from natural reservoirs and humans from 2007-2011. However, M segment dataset was made only from Serbian sequences isolated from natural reservoirs together with sequences retrieved from NCBI. The overall number of different DOBV strains originating from Serbia, reported in the NCBI database until the date of the study was 24

(Table AII, Appendix). Geographic distribution of all Serbian strains was mostly in central and southern parts of Serbia (Figure 11).



Figure 11. All NCBI deposited DOBV sequences from Serbia until the date of the study, by geographic location. Sequences obtained within this study are shown in green. Sequence names are derived from NCBI accession number and year of collection. Human/rodent source material is depicted by the relevant symbol.

4.3.1. Phylogenetic analysis of partial DOBV L segment sequences

Detailed phylogenetic analysis was done based on 37 partial L segment sequences (position 3023 to 3282 nt according to reference strain NC005235). The alignment consisted of 22 Serbian sequences together with respective 15 L segment sequences existing in the GenBank database. Of 22 sequences originating from Serbia, 17 were taken from human cases and five were taken from rodents (three from *A. flavicollis*, one from *A. agrarius* and one from *G. glis*). All Serbian sequences recovered from rodents were obtained in the current study. Studied nucleotide alignment corresponded to 86 aa (position 995-1081aa) of the L protein.

Overall nucleotide divergence among the studied DOBV sequences was 10.81% (SD±0.06), while the mean nucleotide divergence between Serbian strains was 14.09% (SD±0.06). Based on molecular analysis of the L segment sequences, 126 variable sites were detected, of which 29 sites were with changes in aa chain. When the Serbian sequences were compared to the corresponding nt and aa reference strain, it was found that they possess 56 variable sites and 7 nonsynonymous changes in the aa chain.

Phylogenetic trees constructed by using the Bayesian methods implemented in the MrBayes software package, confirmed the results obtained by BLAST analysis. Namely, three sequences obtained from *A. flavicollis*, one sequence from *A. agrarius* and one sequence from *G. glis* clustered together with DOBV strains. Moreover, based on this phylogeny, strains from Serbia clustered in a distinctive branch of Dobrava genotype with strains from Greece, Slovenia and Turkey with posterior probability of 1 (**Figure 12**). Within Dobrava genotype cluster, three Serbian strains isolated from *A. flavicollis* (originating from Tara Mountain in western Serbia) were closely related to human isolates also originating from western Serbia. Furthermore, sequences isolated from *A. agrarius* and *G. glis* (trapped in central Serbia) were tightly clustered together with human strains from central Serbia. SEOV and HTNV reference strains were used as outgroups.

Phylogenetic analysis of hantaviral molecular evolution in different rodent species

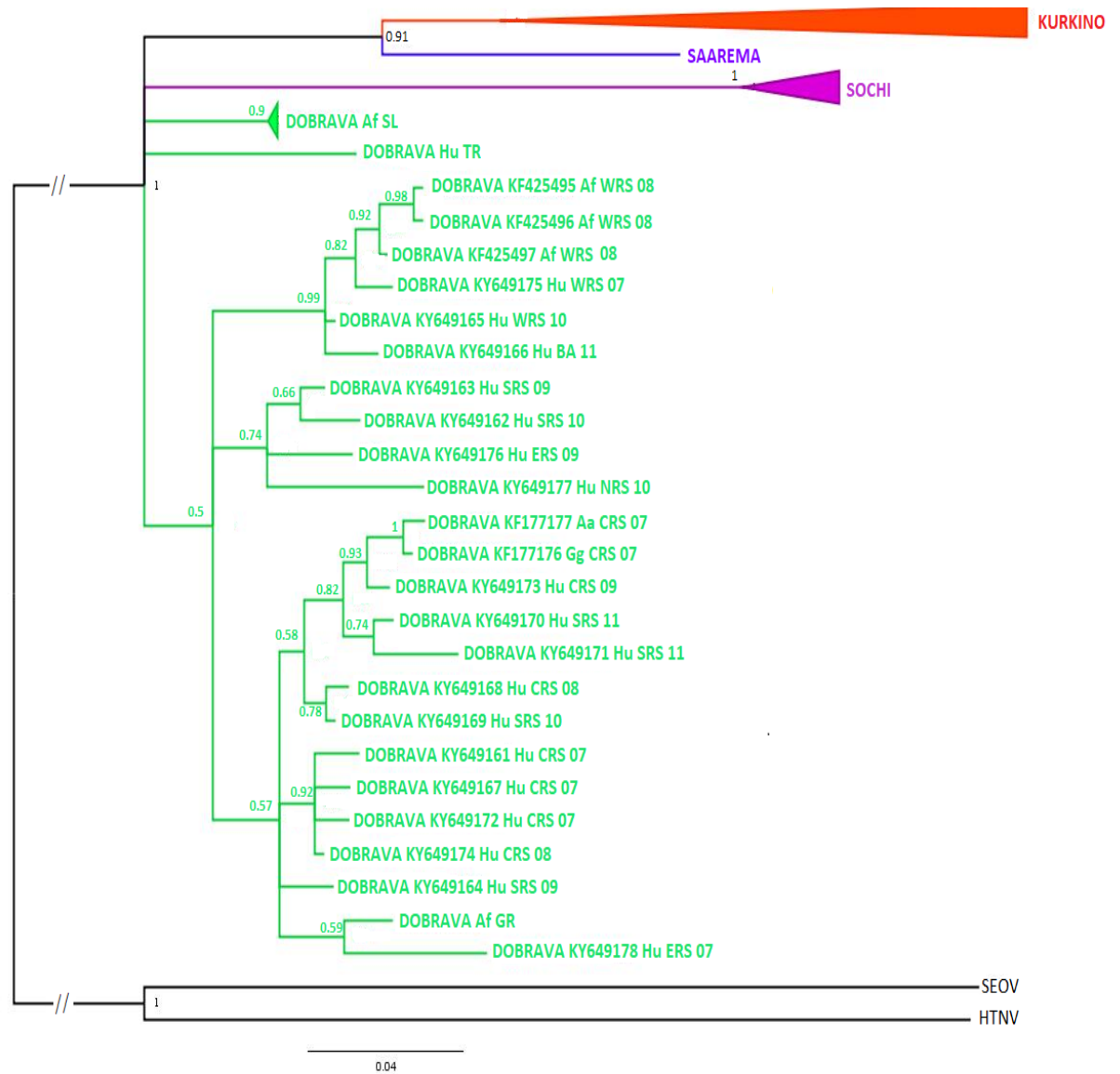


Figure 12. Phylogenetic tree based on 37 L segment DOBV sequences inferred using the Bayesian methods. Numbers on branches indicate posterior node probabilities. Scale bar represents number of nucleotide substitutions per site. DOBV genotypes Saaremaa, Dobrava, Kurkino and Sochi are shown in blue, green, red and purple, respectively. Sequences are indicated by GeneBank Accession Number, abbreviated host name (*A. flavicollis* – Af, *A. agrarius* – Aa, *A. ponticus* – Ap and Human - Hu) and name of the country.

4.3.2. Phylogenetic analysis of partial DOBV M segment sequences

The alignment for partial M segment consists of 16 sequences, including three newly detected sequences from *A. flavicollis*. The length of alignment is 434 nt. Corresponding GPC protein sequences comprise 144 aa (positions 573-717). Prior to phylogenetic analyses, all sequences included in the study were analysed for recombination and no putative recombinant regions could be detected.

Overall nucleotide divergence, calculated based on 16 DOBV M sequences, was 15.07% (SD±0.07). The average distance among Serbian sequences was 0.47% (SD±0.04). Molecular analysis of all sequences included in the study revealed 152 variable sites of which 16 were nonsynonymous mutations. However, molecular analysis of Serbian M segment sequences revealed 32 variable sites within the studied region and one aa change in all three Serbian strains compared to the corresponding nt and aa reference strain.

General topology of phylogenetic tree showed 4 clusters corresponding to previously defined DOBV genotypes: Dobrava, Kurkino, Sochi and Saaremaa (**Figure 13**). In the phylogenetic tree constructed for M segment sequences of DOBV, based on Bayesian methods, all three newly detected Serbian strains clustered within the Dobrava genotype with posterior node probability of 1.

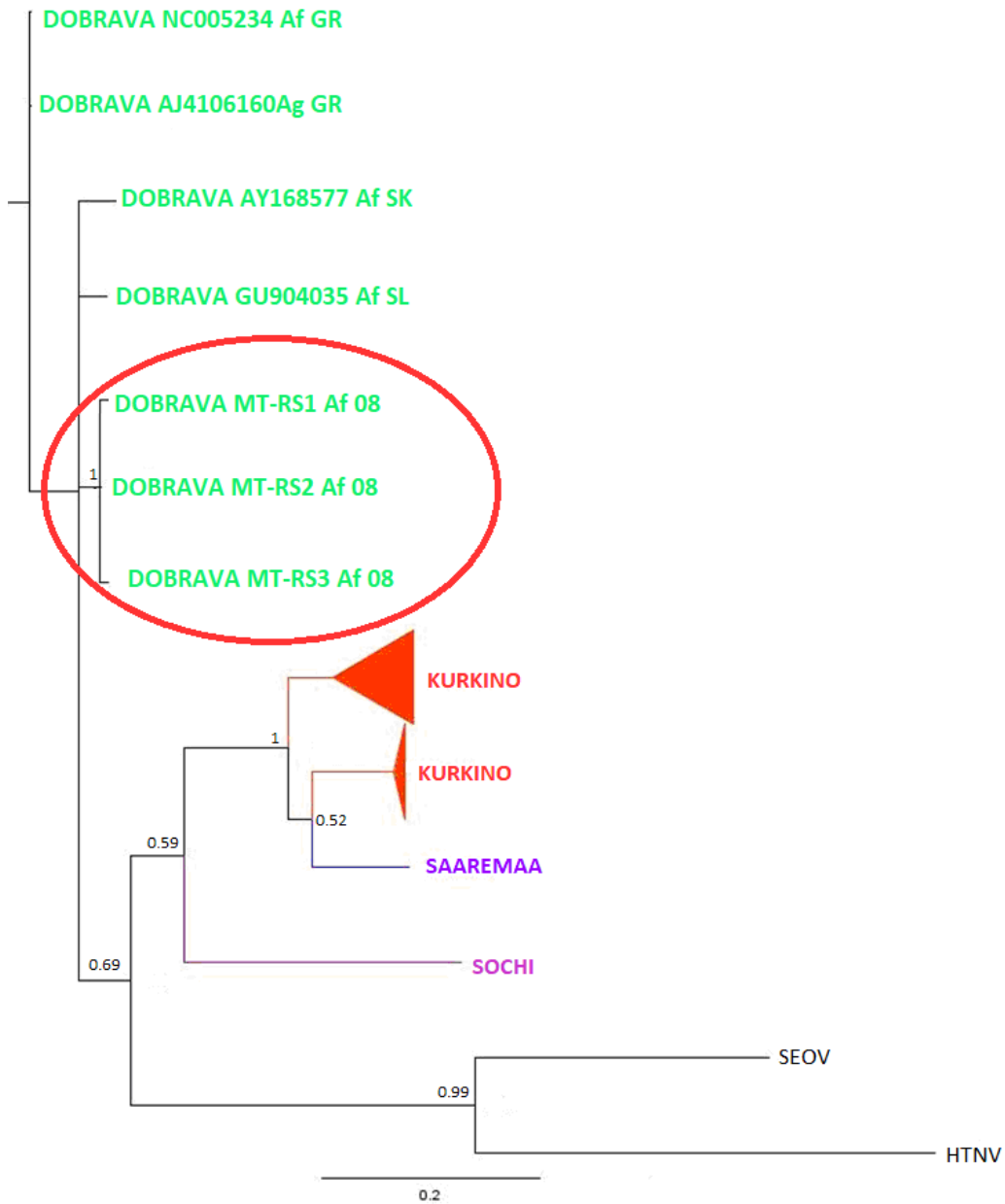


Figure 13. Phylogenetic tree based on 16 M segment sequences of DOBV, inferred using the Bayesian methods. Numbers on branches indicate posterior node probabilities. Scale bar represents number of nucleotide substitutions per site. DOBV genotypes Saaremaa, Dobrava, Kurkino and Sochi are shown in blue, green, red and purple, respectively. Sequences indicated by GeneBank Accession Number, abbreviated host name (*A. flavicollis* – Af, *A. agrarius* – Aa, *A. ponticus* – Ap and *Human* - Hu) and country.

4.3.3. Phylogenetic analysis of partial DOBV S segment sequences

Detailed phylogenetic analysis of partial S segment sequences of DOBV was done based on 180 partial S segment sequences (position 364855 nt). Within studied region, 16 sequences were from Serbia: four detected in animals (*A. flavicollis*, *A. agrarius* and *G. glis*) and 12 detected previously from human HFERS cases. Corresponding N protein sequences comprise 164 aa (position 122-285 nt). Putative recombination signal was not detected in the studied alignment.

Pair-wise comparisons of all S segment nucleotide sequences showed divergence of 7.95% (SD±0.06), with average distance between all Serbian strains samples of 2.21% (SD±0.09). Diversity among sequences from human cases from Serbia was higher compared to those from rodents (2.30%, SD±0.01 vs. 1.83%, SD±0.01). Molecular analysis of all S segment sequences revealed 189 variable sites within the examined region. However, 22 mutations were nonsynonymous (changes in aa) when the studied sequences were compared to the corresponding nt and aa reference strain. Moreover, molecular analysis of Serbian strains compared to reference strain revealed 55 variable sites of which three were nonsynonymous.

Prior to further phylogenetic analysis, alignment was examined by means of likelihood mapping. Majority (89.4%) of the random quartets in the examined alignment were equally distributed in the three corners of the triangle (**Figure 14**) approaching the threshold of 90%.

General topology of phylogenetic tree showed 4 clusters corresponding to the previously defined DOBV genotypes: Dobrava, Kurkino, Sochi and Saaremaa (**Figure 15**). All DOBV Serbian strains clustered within the Dobrava genotype. Fourteen Serbian sequences formed two discrete branches. Two sequences clustered with Greek, Bulgarian and Albanian strains, and three sequences formed separate branches. Almost all clades in the phylogenetic tree had high posterior probability, which exceeded 0.5. SEOV and HTNV reference strains were used as outgroups.

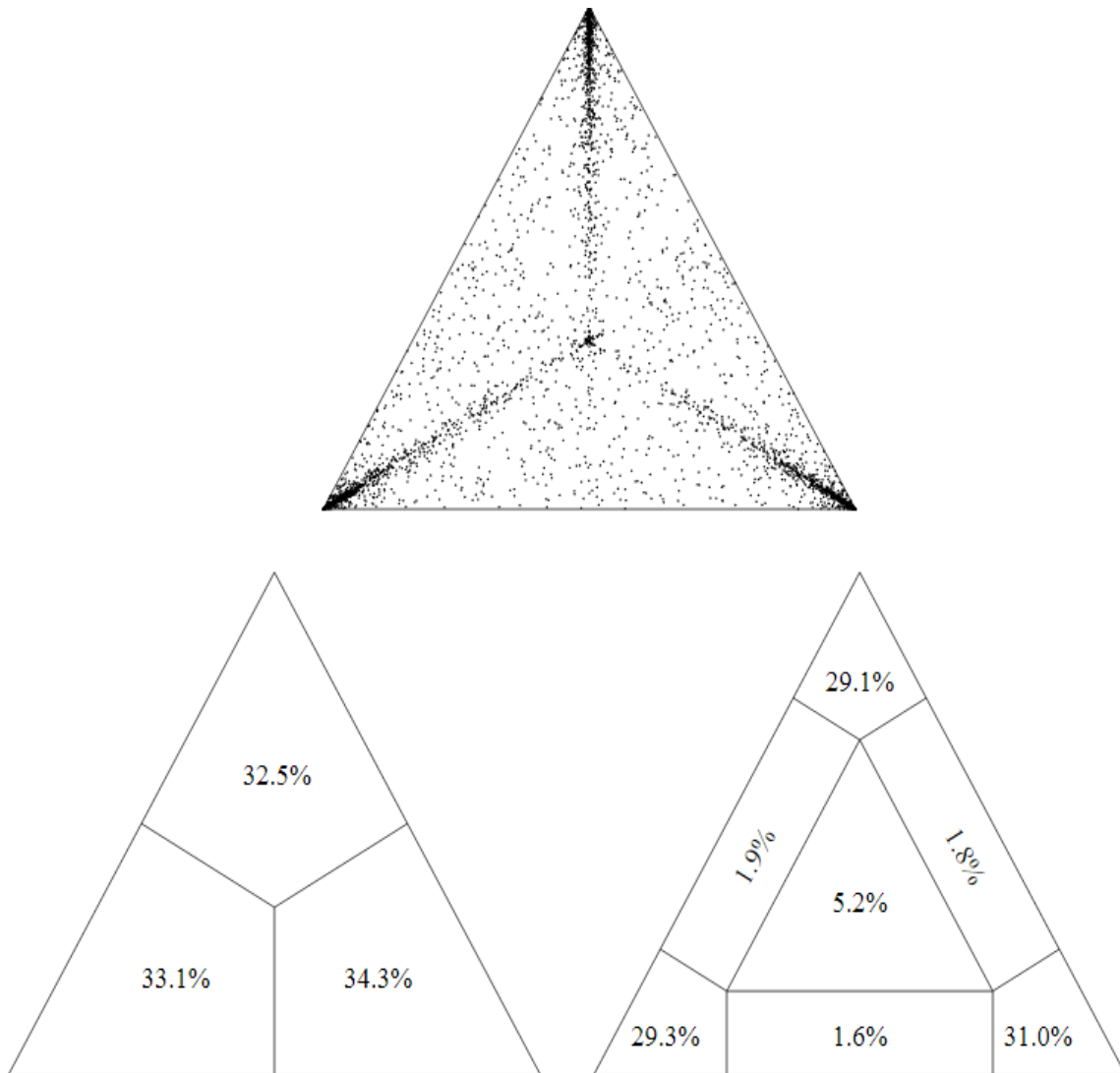


Figure 14. Likelihood mapping analysis using quartet grouping of 180 partial S segment sequences of DOBV. Number of quartets in the corners represents fully resolved phylogeny, whereas number of quartets in the center represents phylogenetic noise.

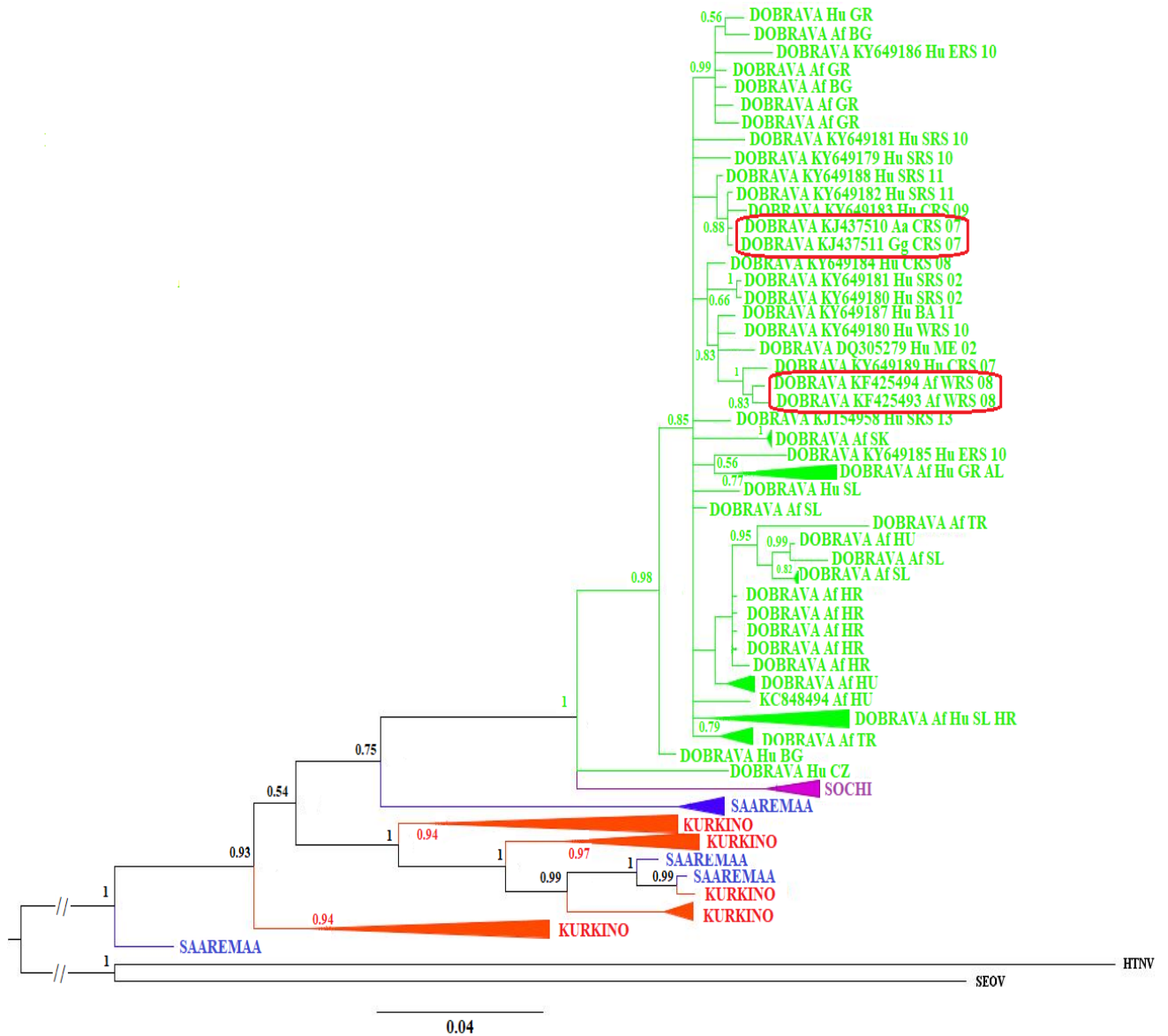


Figure 15. Phylogenetic tree based on 180 S segment sequences of DOBV, inferred using Bayesian methods. Numbers on branches indicate posterior node probabilities. Scale bar represents number of nucleotide substitutions per site. DOBV genotypes Saaremaa, Dobrava, Kurkino and Sochi are shown in blue, green, red and purple, respectively. Sequences indicated by GeneBank Accession Number, abbreviated host name (*A. flavicollis* – Af, *A. agrarius* – Aa, *A. ponticus* – Ap and *Human* - Hu) and country.

Moreover, temporal structure of the studied alignment was also examined using root-to-tip regression analyses. Since the obtained correlation coefficient was negative, implying that the existing dataset of DOBV S segment sequences is not sufficiently informative for further phylogenetic analysis, the estimation of demographic growth, substitution rate and phylogeographic distribution of DOBV was not done (**Figure 16**).

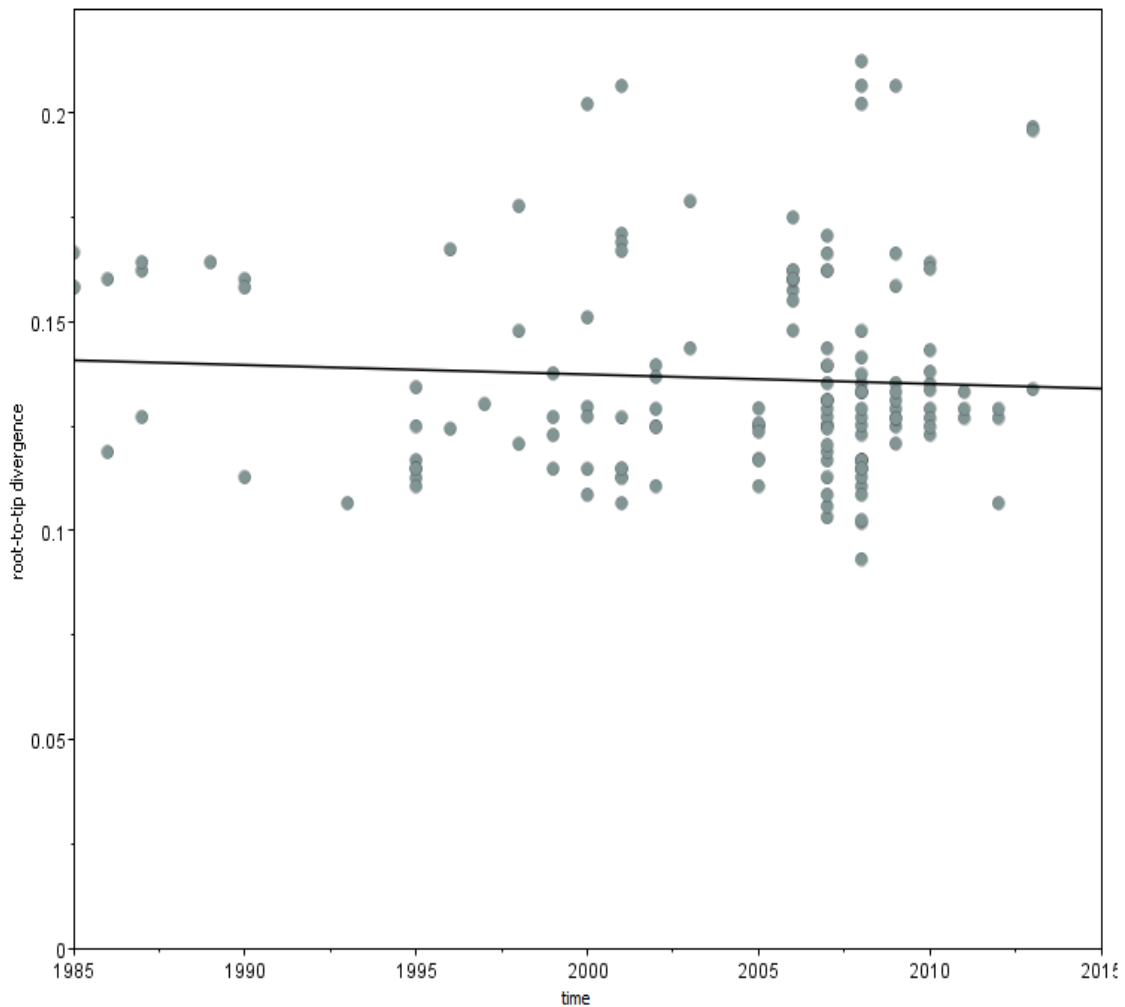


Figure 16. Root-to-tip regression analyses. Plot of the root-to-tip genetic distance against sampling time is shown for phylogeny estimated from alignment of 180 S segment sequences of TULV.

To examine the nature of codon selection on the aligned DOBV S segment sequences, we performed per-site SLAC, based on the NJ tree. The initial DOBV S segment alignment consisted of 180 sequences. However, selection analysis was done based on 151 sequences and the rest of 29 genetically identical sequences were excluded. The examined number of sites in DOBV alignment was 164. At the protein level, there were 22 amino acid variable sites. The overall value of the dN/dS ratio based on SLAC analysis was $dN/dS = 0.0225$, $\log L = -4653.26$ for $p < 0.1$ (**Figure 17**). Number of calculated codon sites under negative selection was 118.

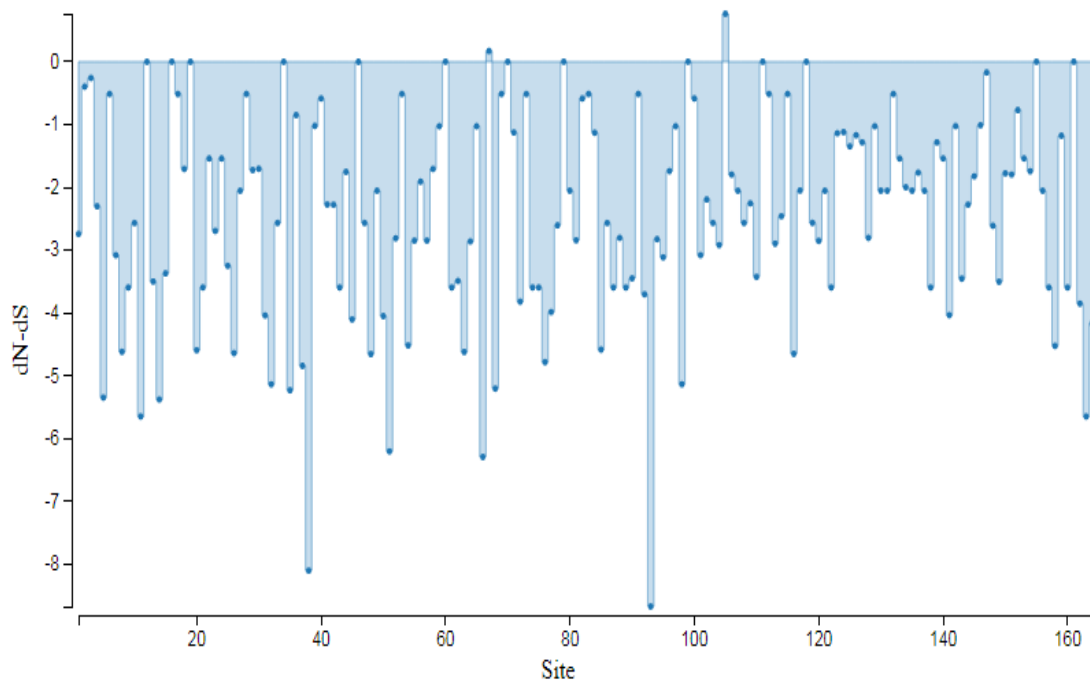


Figure 17. Selective pressure on examined portion of DOBV nucleocapsid protein based on SLAC analysis.

4.4. DETAILED PHYLOGENETIC ANALYSIS OF DOBV IN THE NEWLY FOUND NATURAL HOST

As stated under 4.2., DOBV L and S segment sequences were recovered from *G. glis* and *A. agrarius*. The animals were captured within the rodent trapping performed in autumn 2007, during several consecutive nights, using overnight strategically placed baited wooden

live traps. The trapping site was in central Serbia (**Figure 18**), in the region of the Ravanica River ($44^{\circ} 00' 17.89''$ N, $21^{\circ} 35' 26.00''$ E).



Figure 18. Map of Serbia showing the location (Ravanica, approximately 150 km south of Belgrade) where the DOBV-positive *G. glis* was trapped. . The location is indicated by a solid blue triangle.

The obtained partial L and S segment sequences were phylogenetically characterized. Detailed L segment based phylogenetic analysis showed divergence of 1.3% between two newly detected DOBV sequences from Serbia, whereas the nucleotide divergence between newly detected S segment sequences from Serbia was 0.9%. Deduced amino acid sequences of two newly detected strains were mutually identical in both genetic segments tested.

In the phylogenetic trees constructed for L and S segment datasets (**Figure 12 and Figure 15**), newly detected sequences were closely related to other strains originating from Serbia with high bootstrap support. In general, analyzed strains in both phylogenetic trees were placed in distinct highly supported clusters, matching the harbouring hosts within each DOBV genotype. Although new sequences were recovered from *G. glis* and *A. agrarius*, they clustered together with DOBV sequences obtained from *A. flavicollis* and human cases (within Dobrava genotype). The species *G. glis*, or any other species of the *Gliridae* rodent family, has not been previously associated with hantaviral infection.

4.5. PHYLOGENETIC ANALYSIS OF DOBV FROM NEWLY DESCRIBED FOCUS IN THE BALKANS

A part of the study in this doctoral research was performed on samples collected in the region of Tara Mountain (43°53048"N, 19°32023"E), where a total of 50 *A. flavicollis* were trapped on several occasions during the 3-year study period (2008–2010) (**Table 3, Figure 19**). Three of 50 rodent samples were DOBV-positive (the samples were marked as RS1 to RS3). Partial L segment sequences were taken from all three samples, while partial S sequences were taken from two (RS1 and RS3).

The recovered L segment sequences (318 nt, position 2999–3316) encode 106 amino acids (positions 988–1087) of the RdRp. Nucleotide and amino acid divergence among the newly detected sequences from Serbia was 1.1% and 1.3%, respectively.

The obtained 789-bp (position 291–1079 nt) DOBV S segment sequences (KF425493, KF425494) comprise 263 amino acids of the N protein (aa 86–348). Nucleotide divergence between RS samples was 0.8%, with amino acid divergence 0.4%.

The topology of both phylogenetic trees (L and S segments) showed that sequences recovered from *A. flavicollis* in Tara mountain were closely related to other Serbian strains with high bootstrap support (**Figures 12 and 20**). Obtained result implied geographically related clustering.



Figure 19. Map of Serbia showing the location of the new natural focus at the Tara mountain. Position of Serbia in the Balkans depicted in the lower right corner.

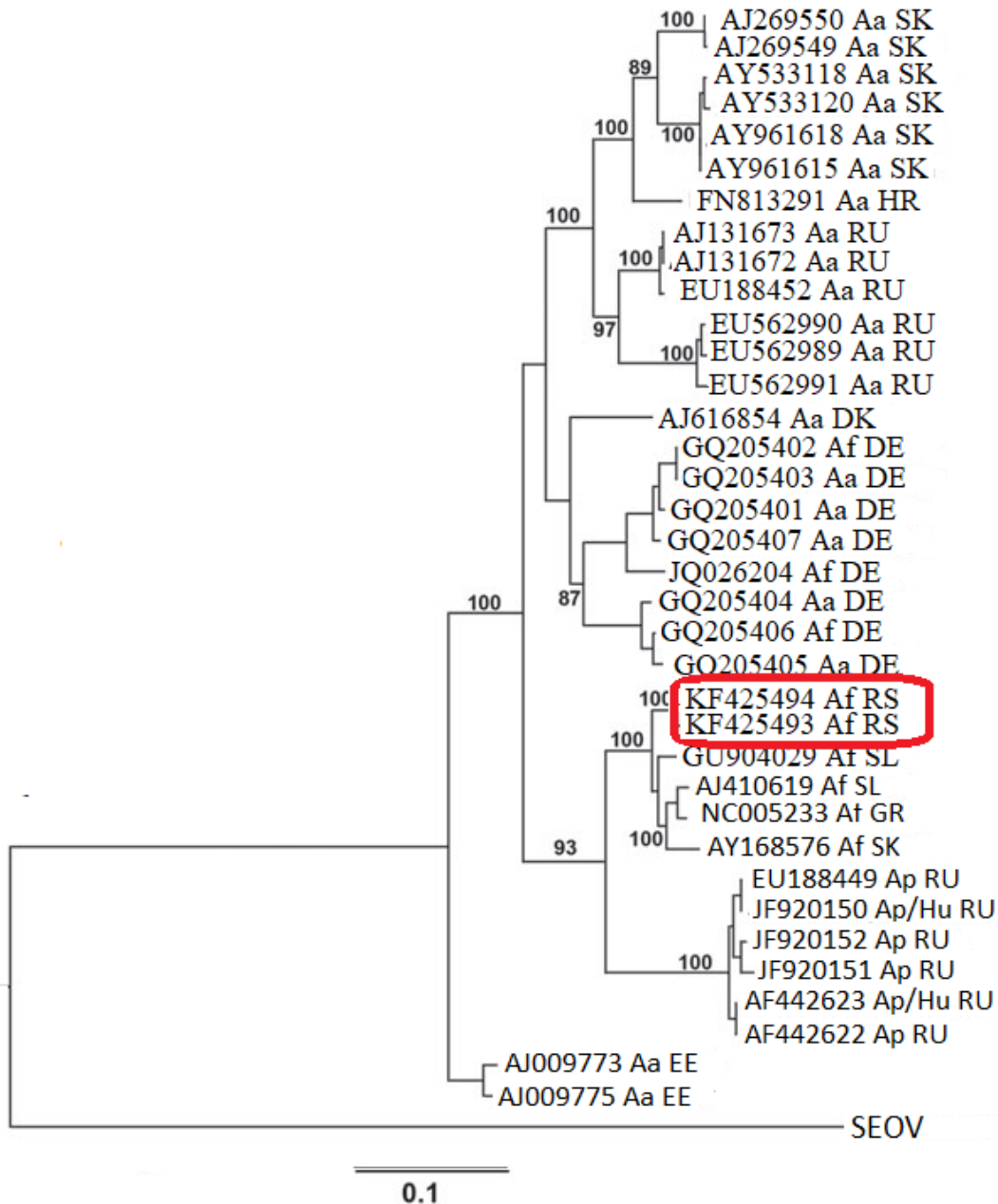


Figure 20. Phylogenetic tree of DOBV rodent isolates, based on 36 isolates of S segment sequences (789 nt, position 291–1079), generated by Mr Bayes software package. Sequences indicated by GeneBank Accession Number, host name with abbreviation (*A. flavicollis* – Af, *A. agrarius* – Aa, *A. ponticus* - Ap and Hu – isolate from human case) and country. DOBV genotypes are marked.

4.6. COMPARATIVE PHYLOGENETIC ANALYSIS OF PARTIAL L AND S SEGMENT SEQUENCES OF TULV

Eight European common voles, *M. arvalis*, were trapped in 2007 at Ravanica region (44° 00' 17.89" N, 21° 35' 26.00" E), in central Serbia, approximately 150 km south of Belgrade (**Table 3, Figure 18**). However, only two were available for genetic testing. When these two rodent samples were tested in the present study, one was found positive. The obtained partial L segment sequence was first analyzed by BLAST at NCBI (<http://blast.ncbi.nlm.nih.gov/Blast.cgi>) and the sequence was identified as TULV strain.

4.6.1. Phylogenetic analysis of the partial TULV L segment sequences

L segment sequence for the TULV strain from *M. arvalis* was 322 nucleotides long, corresponding to positions 2981-3302 nt of TULV L segment reference sequence (NC005226), partially encompassing L-protein-encoding sequence of 106 amino acids. Nucleotide divergence of 21 analyzed nucleotide sequences ranged from 0% to 22.98% (mean nt distance was 16.23%, $SD\pm 4.5$), while between the Serbian one and all other sequences included in the analysis, it ranged from 15.58% to 20.24% (mean nt distance was 17.53%, $SD\pm 1.3$). Diversity of newly detected sequence involved 57 synonymous and no non-synonymous substitutions in the examined partial L segment region, in comparison to the reference sequence (NC005226).

Reconstructed tree (**Figure 21**) comprised 21 L segment sequences originating from different countries, including Germany, Switzerland, Czech Republic, Slovenia and Serbia. Newly characterized Serbian sequence clustered separately but closely related to those isolated from Germany. The second cluster was formed by sequences originating from Slovenia and Czech Republic. The last cluster contained sequences also from Germany.

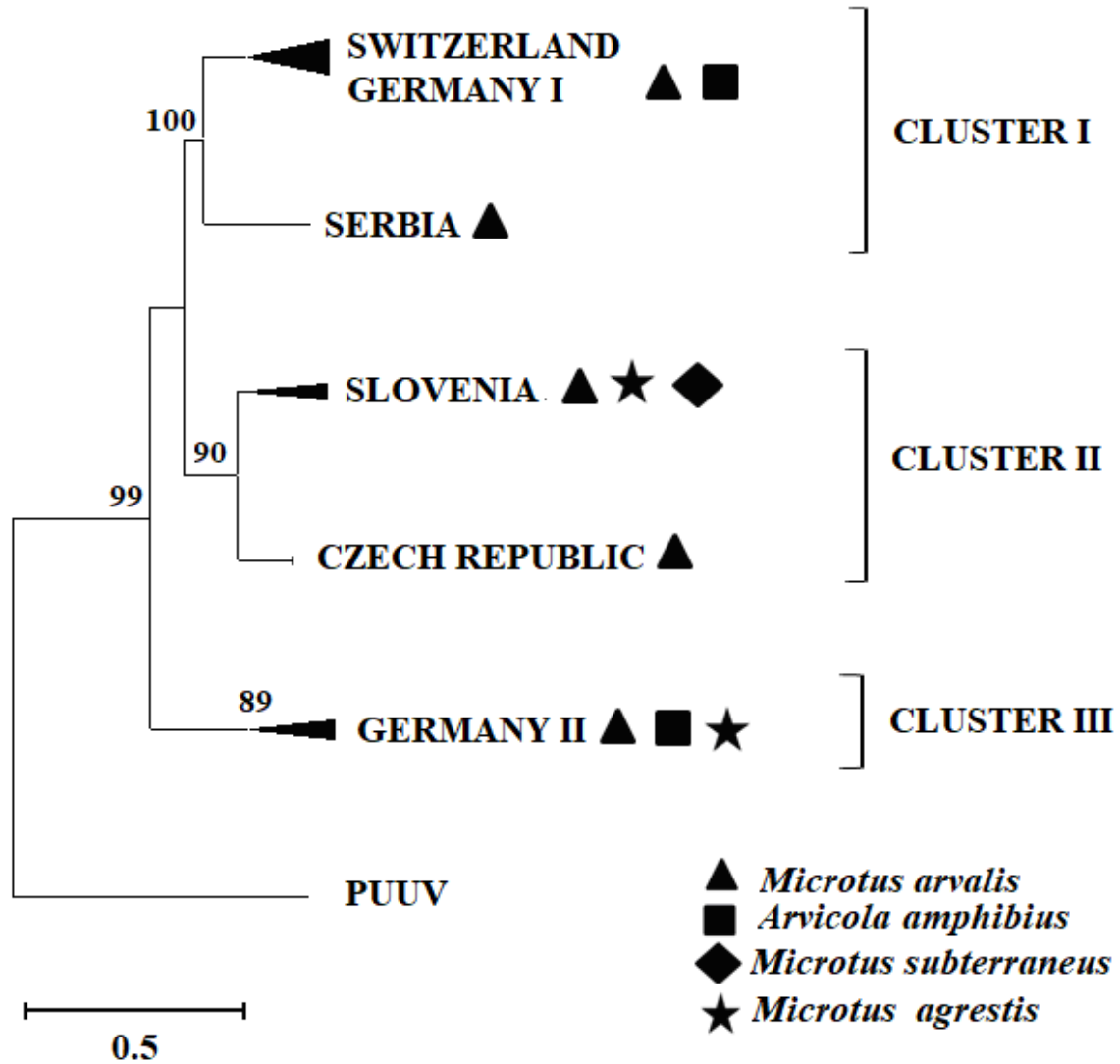


Figure 21. ML phylogenetic trees based on 21 TULV L segment sequences. For better viewing, clusters of phylogenetically closely related sequences were compressed to triangles (size proportional to the number of sequences). Both trees were rooted with PUUV as outgroup.

4.6.2. Phylogenetic analysis of the partial TULV S segment sequences

S segment phylogenetic analysis included two sequences from Serbia: TULV sequence from *M. subterraneus* (AF017659; earlier described) and the one from *M. arvalis* (described in present study), together with 64 sequences retrieved from GEnBank originating from various European and Asian countries.

The topology accuracy of the phylogenetic tree constructed for the S segment data set was inferred by using the likelihood mapping method (**Figure 22**). Obtained results of analysis support tree-like evolution. Namely, the fact that 9.3% of the dots fell in the central area and 90.7% at the corners of the triangles indicated that the alignment contained sufficient phylogenetic information.

Overall nucleotide divergence among analyzed sequences ranged from 0% to 22.67% (mean nt distance was 16.23%; $SD\pm 5.1$). Mean nucleotide distances between sequences from *M. subterraneus* strain and *M. arvalis* with all other sequences of the study were 17.78% and 18.57%, respectively. The highest diversity was observed between TULV sequences from Kazakhstan and all other analyzed sequences, with nt difference from 17.19% to 22.67% (mean nt distance was 20.35%, $SD\pm 0.9$). Nucleotide divergence between two sequences from Serbia was 13.16%, while the derived amino acids were identical. Furthermore, both sequences from Serbia were closely related to sequences originating from eastern Slovakia (Y13979 and Y13980) with nucleotide difference of 11.93% and 10.88% respectively, for sequences from *M. subterraneus* and 7.54% and 8.77% for *M. arvalis*. Comparing sequences from Serbia with the TULV reference strain (NC005227), nucleotide diversity involved seven nonsynonymous substitutions in the examined alignment. The overall frequency of detected amino acid changes was 3.68% in the studied genetic region.

Phylogenetic tree based on 66 TULV S segment sequences of 567 nt (358-924 nt) showed the existence of different clusters matching to territory of sequences origin (**Figure 23**). Sequences from Serbia were closely related to those from eastern Slovakia (Y13980 and Y13979), forming a clear separate cluster. Sequences from western Slovakia were placed together with sequences from Czech Republic. In addition to the aforementioned clusters, it was possible to distinguish 4 clusters matching to the geographic region of the country.

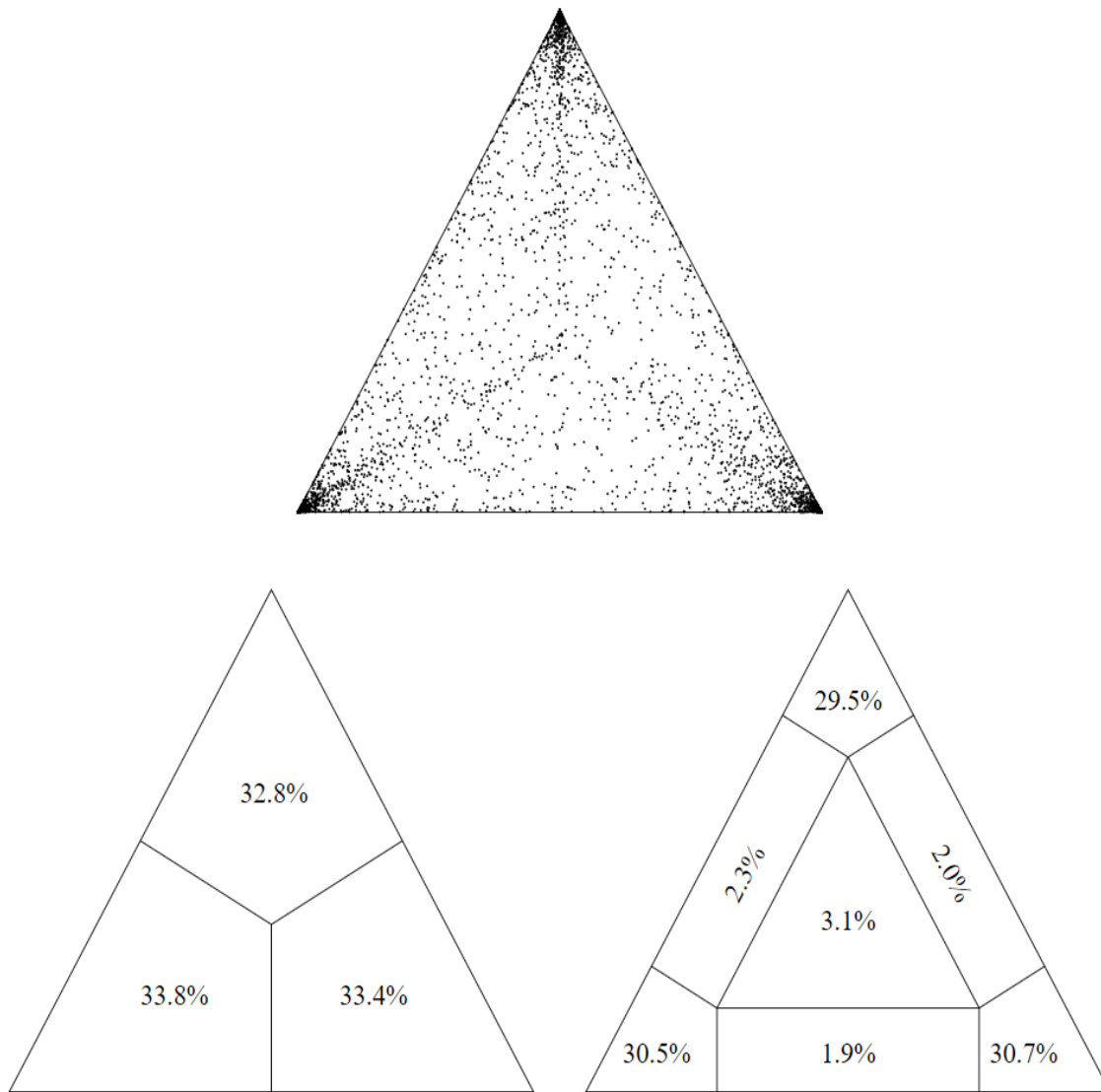


Figure 22. Likelihood mapping analysis using a quartet grouping of 66 S segment sequences of TULV. Number of quartets in the corners represents fully resolved phylogeny, whereas number of quartets in the center represents phylogenetic noise.

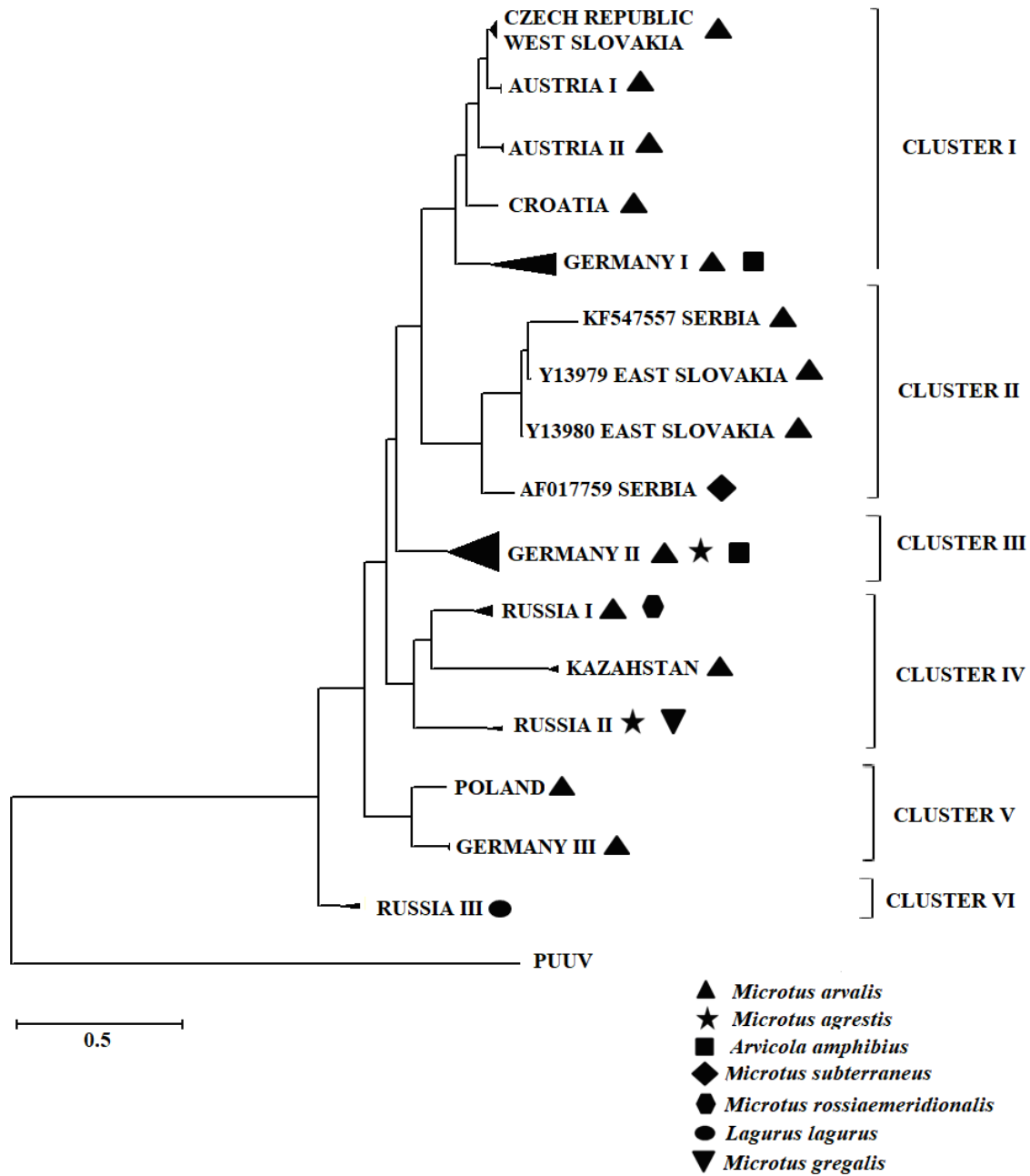


Figure 23. ML phylogenetic trees based S segment of 66 examined TULV sequences. For better viewing, clusters of phylogenetically closely related sequences were compressed to triangles (size proportional to the number of sequences). Both trees were rooted with PUUV as outgroup.

To examine the nature of codon selection on the aligned TULV S segment sequences, we performed per-site SLAC, under based on the NJ tree.

The analyzed TULV S segment alignment consisted of 137 sequences. The examined number of sites in the TULV alignment was 181. At the protein level, there were 51 amino acid variable sites. The overall value of the dN/dS ratio based on SLAC analysis was $dN/dS = 0.0197$, $\log L = -10470.52$ for $p < 0.1$ (**Figure 24**). Number of calculated codon sites under negative selection was 170.

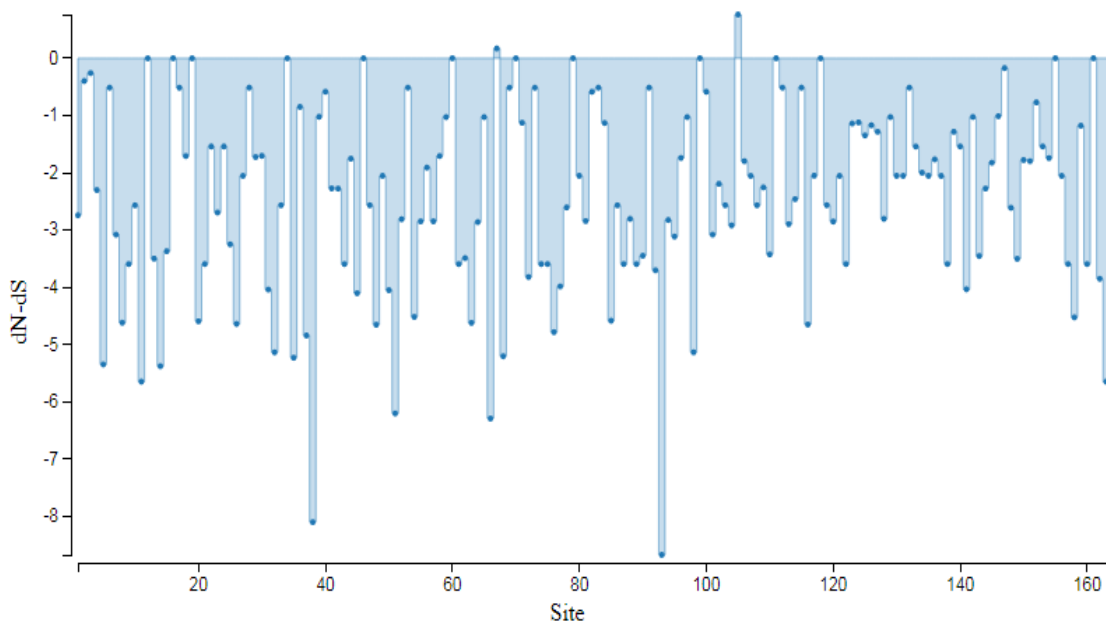


Figure 24. Selective pressure on examined portion of TULV nucleocapsid protein based on SLAC analysis.

4.7. RECOMBINATION ANALYSIS OF TULV STRAINS

Since the TULV sequences from eastern Slovakia (Y13980 and Y13979) had already been described as recombinants, and two Serbian strains were closely related with these sequences, we analyzed the potential presence of recombination in Serbian strains (**Figure 25**).



Figure 25. Locations of the trapping sites of TULV sequences in Serbia, and geographical position of Serbia in Europe, depicting also the trapping site of the Kosice strain from Slovakia.

The studied alignment consisted of 22 nearly full length TULV S segment sequences, of 928 nt in length. In order to investigate the presence of phylogenetic noise, the alignment was investigated by means of likelihood mapping. The fact that 2% of the dots fell in the central area and 98% at the corners of the triangles indicates that the alignment contained sufficient phylogenetic information (**Figure 26**).

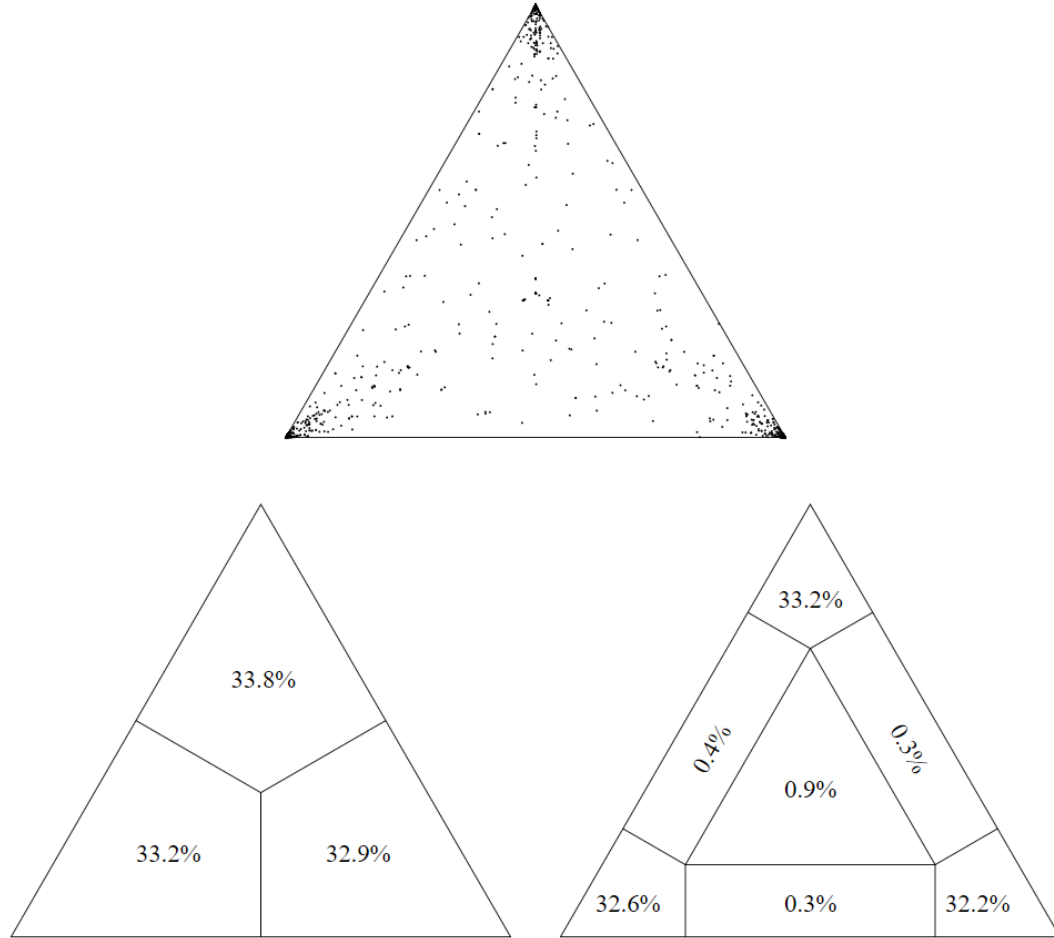


Figure 26. Likelihood mapping analysis using a quartet grouping of 22 TULV S segment sequences alignment. Number of quartets in the corners represents fully resolved phylogeny, whereas number of quartets in the center represents phylogenetic noise.

Bootscan recombination analysis by Simplot of 928 nt (400-1324) S segment sequences revealed the existence of two recombination peaks exceeding the cut-off of 70% bootstrap in both sequences from Serbia: one peak corresponding to S segment regions from positions around 600-750 that clustered together with TULV sequences from Czech Republic and West Slovakia, while the other clearly resolved peak, was located between positions 750 and 950, and clustered with TULV sequences from Russia (**Figure 27**). Reconstructed phylogenetic subtrees were clearly in correlation with corresponding peaks proposed by bootscan analysis (**Figure 28**). According to these results sequences from Serbia may be considered as recombinant forms containing sequences originated from Russia and Czech Republic. Notably, positive recombination signal was not picked up by RDP4 in either Serbian or Slovakian strains.

Analysis of variable positions in the N protein revealed uniform pattern of 10 amino acids specific to studied recombinant strains (AF017659, Y13979, Y13980 and newly detected sequence), of which six amino acid sites were comprised within signature differences identified by VESPA analysis. Based on these observations it is possible to distinguish regions along the N protein of the examined strains, corresponding alternately to strains from Russia and Czech Republic. The list of detected mutations together with aa positions in the N protein is summarized in **Table 8**.



Figure 27. Bootscan analysis of 928 nt long S segment alignment of TULV, as analyzed in Simplot (Window: 160 bp, Step: 20 bp, GapStrip: On, Reps: 100, Kimura (2-parameter), T/t: 2.0, Neighbor-Joining); The peak values exceeding 70% were considered to be significant.

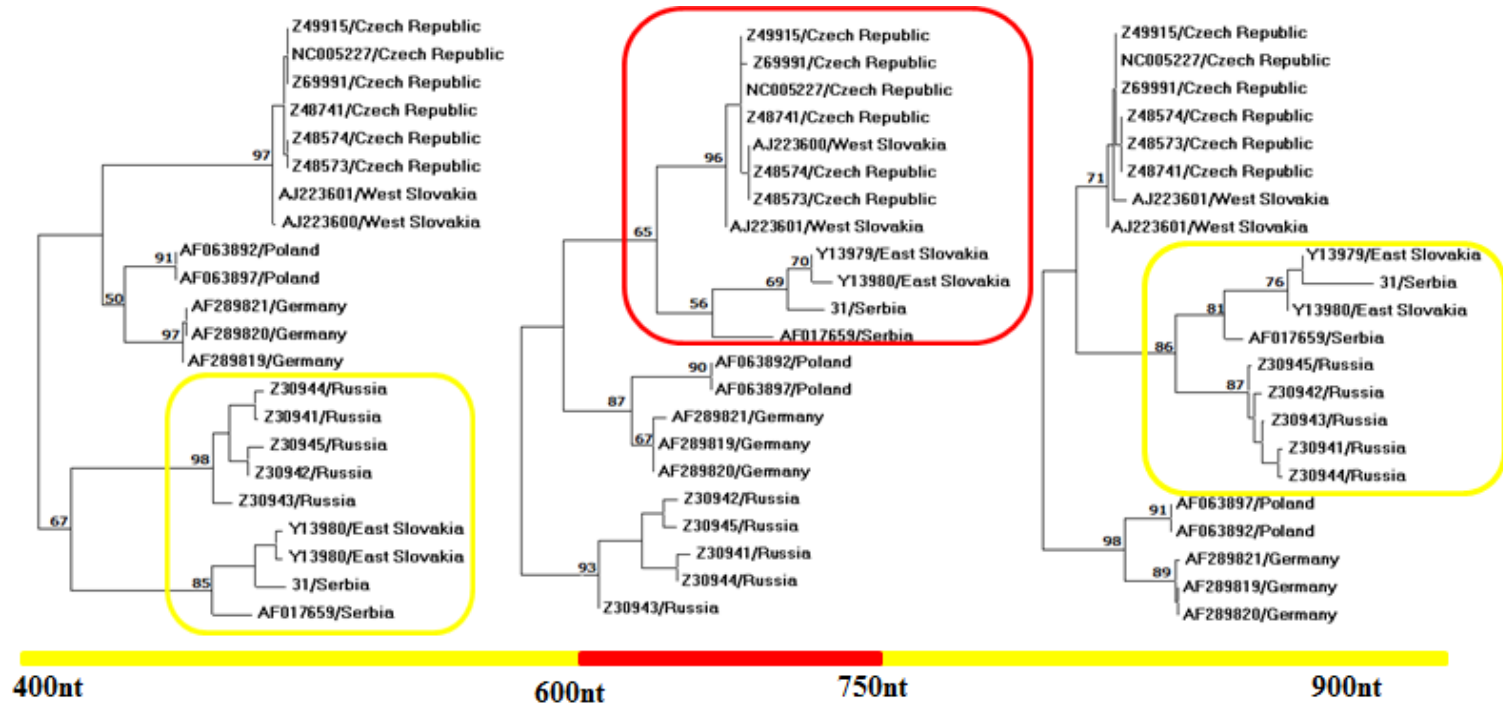


Figure 28. Reconstructed phylogenetic subtrees including positions according to bootscan analysis: S segment positions 400–600 nt (circled in yellow), 600–750 nt (circled in red) and 750–950 nt (circled in yellow), as indicated on the bar, showing alternate clustering of Serbian sequences according to positions analyzed; TULV sequences used in the analysis are listed in the text.

Table 8. Amino acid sequence variation of N protein in Serbian and Slovakian TULV strains. Numbers denote the position of aa in the N protein. Boxes shaded in gray represent aa positions within signature pattern specific to examined recombinant sequences, as obtained by VESPA.

Position of aa	127	134	165	251	252	254	258	268	312	387
Czech Republic/NC005227	T	I	Y	S	G	S	D	L	R	T
Czech Republic/Z48741	T	I	Y	S	G	S	D	L	R	T
Czech Republic/Z48573	T	I	Y	S	G	S	D	L	R	T
Czech Republic/Z49915	T	I	Y	S	G	S	D	L	R	T
Czech Republic/Z48574	T	I	Y	S	G	S	D	L	R	T
Czech Republic/Z69991	T	I	Y	S	G	S	D	L	R	T
West Slovakia/AJ223600	T	I	Y	S	G	S	D	L	R	T
West Slovakia/AJ223601	T	I	Y	S	G	S	D	L	R	T
Serbia/31	I	V	F	G	A	G	D	L	A	T
Serbia/AF017659	I	V	F	G	A	G	D	L	A	T
East Slovakia/Y13979	I	V	F	G	A	G	D	L	A	T
East Slovakia/Y13980	I	V	F	G	A	G	D	L	A	T
Russia/Z30941	I	V	F	G	S	G	E	I	A	M
Russia/Z30942	I	V	F	G	S	G	E	I	A	M
Russia/Z30943	I	V	F	G	A	G	E	I	A	M
Russia/Z30944	I	V	F	G	S	G	E	I	A	M
Russia/Z30945	I	V	F	G	S	G	E	I	A	M

4.8. BAYESIAN PHYLOGENETIC ANALYSIS OF TULV PHYLODYNAMICS AND PHYLOGEOGRAPHY

The phylogeny, including population dynamic, evolutionary rates and phylogeographic analysis were co-estimated in a Bayesian framework using MCMC method implemented in the BEAST package v 1.8.4. A total of 137 TULV sequences with known time and location of sampling were included in the analysis. The alignment was of 543 nt in length, corresponding to nt positions 418-960 of TULV S segment reference sequence.

Prior to phylogeographic analysis, phylogenetic noise of the dataset was investigated by means of likelihood mapping. The assessment of 10,000 randomly chosen quartets showed that only 7.8% fell in the central area of the likelihood map, and 92.2% were at the corners of the triangle, which suggested that the alignment contained sufficient phylogenetic information (**Figure 29**).

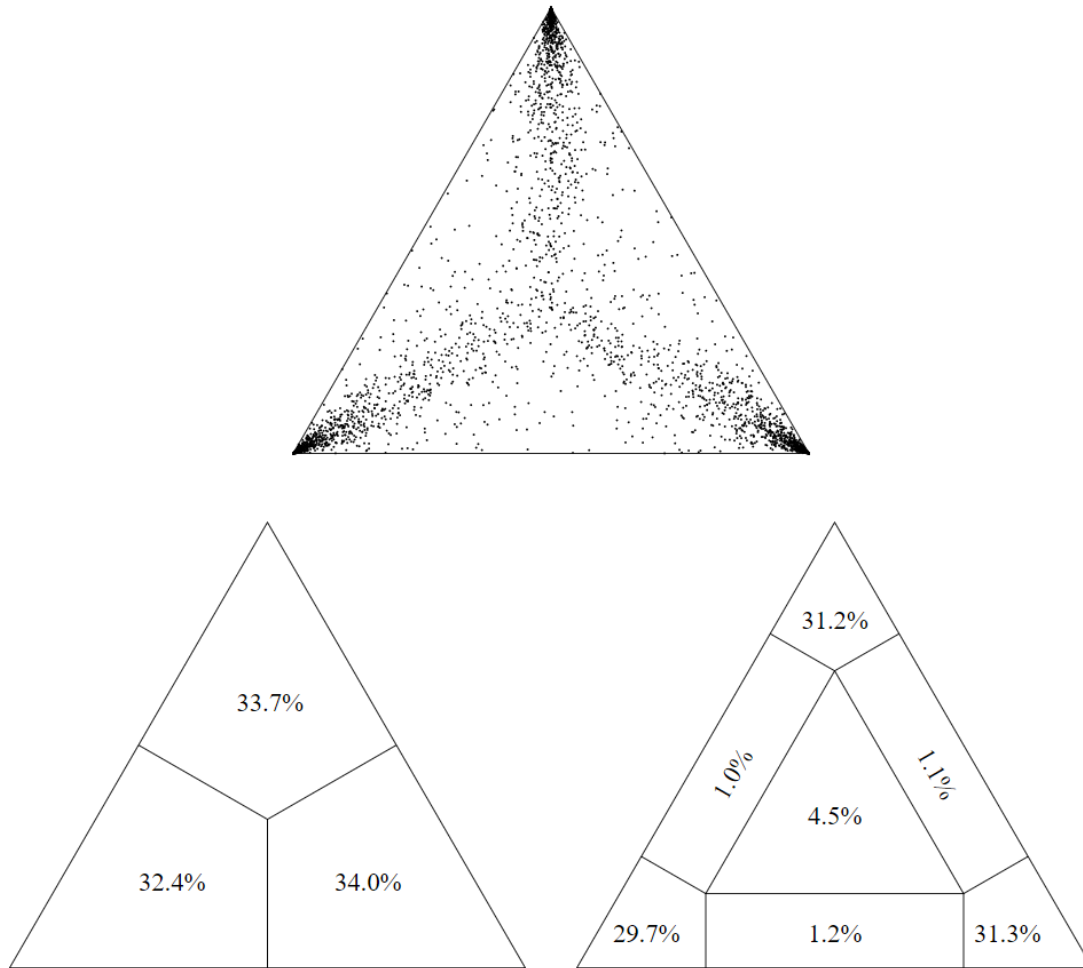


Figure 29. Likelihood mapping analysis using a quartet grouping 137 S segment sequences of TULV. Number of quartets in the corners represents fully resolved phylogeny, whereas number of quartets in the center represents phylogenetic noise

Temporal structure of sequences included in this study was also examined using root-to-tip regression analyses. Obtained correlation coefficient was 0.31 (**Figure 30**), close to the threshold of 0.4 indicating that the analyzed dataset is suitable for further phylogenetic analysis.

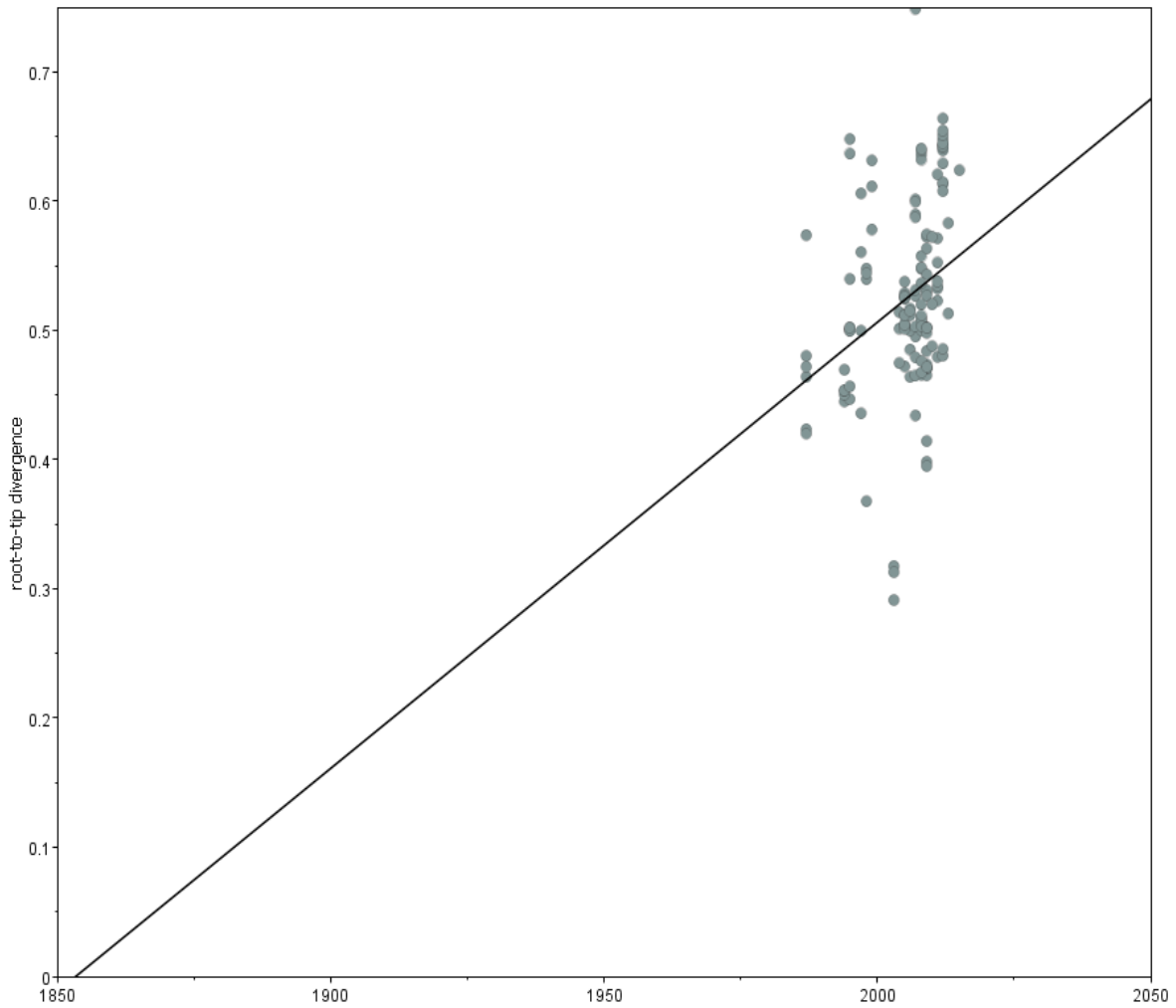


Figure 30. Root-to-tip regression analyses. Plot of the root-to-tip genetic distance against sampling time is shown for phylogeny estimated from alignment of 137 S segment sequences of TULV.

Initially, we analyzed population dynamics using Bayesian skyline plot analysis, which depicts the changes in effective population size over time (**Figure 31**). The effective population size of examined strains seems to be constant over time.

Relaxed Log normal clock together with constant population size as tree prior were found to be the best model for calculation of substitution rate. Under these conditions, the

estimated substitution rate of analyzed part of the S segment was 1.787×10^{-3} (SE of mean = 1.72×10^{-4} ; 95% HPD interval: $8.75 \times 10^{-4} - 2.55 \times 10^{-3}$) integrated in BEAST v.1.8.4.

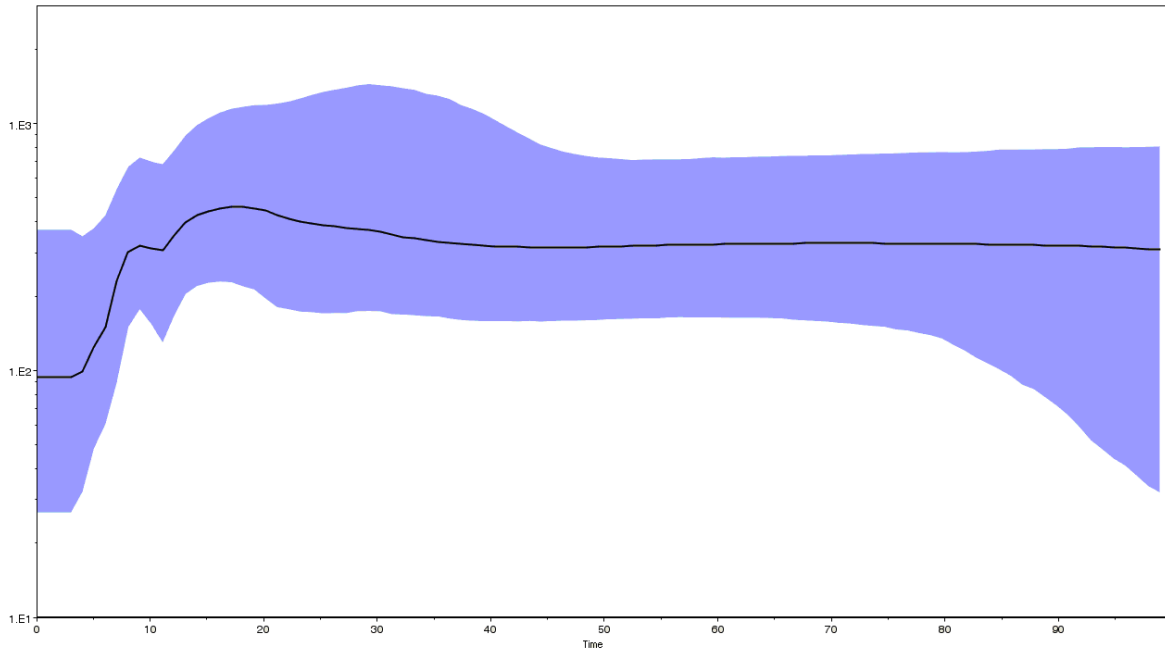


Figure 31. Bayesian skyline plots representing the estimates of the effective number of TULV S segment sequences in the studied population. The y-axis measures the effective number of infections in log₁₀ scale while the x-axis represents time in years with 0 (zero point) indicating the most recent year of sampling (2013). The line showing the median estimate of effective number of infections over time and blue colored areas limiting the 95% HPD interval.

Based on log marginal likelihood calculated using stepping stone sampling, Cauchy PRW was the best chosen model to investigate gene flow on a time-scaled genealogy by implementing geographic coordinates (latitude and longitude) for continuous space. Moreover, Log-normal molecular clock model together with the constant population demography was found to be the best fit for our dataset. ESS values for each parameter was higher than 100.

The most possible root of MCC tree was placed in central Asia, most probably in Kazakhstan, with posterior probability of 1 (**Figure 32**). The exact place of origin was assessed around Aqtöbe city in Kazakhstan. The root age was assessed to be around 300 years ago.

Studied TULV strains formed three well supported clades matching the geographical origin: the clade closest to the tree root consisted of sequences from Russia and Kazakhstan; the second clade contained strains originating from western and central Europe (Germany, France, and Poland); the third clade consisted of sequences from western and southeast Europe (France, Luxemburg, Germany, Austria, Czech Republik, Slovakia, Slovenia, Croatia and Serbia) were found, together with recombinant strains from Serbia and east Slovakia.

The patterns of viral spread suggested by phylogeographic analysis were plotted (**Figure 33**). The routes of viral spread included further distribution across Russia and further to Europe. Moreover, phylogeographic analysis suggested single introduction of TULV to Europe from central Asia, with the complex pattern of local viral migration throughout Europe further on. Obtained results also showed single introduction of TULV from Czech Republic to Serbia with further spread locally and to Slovakia.

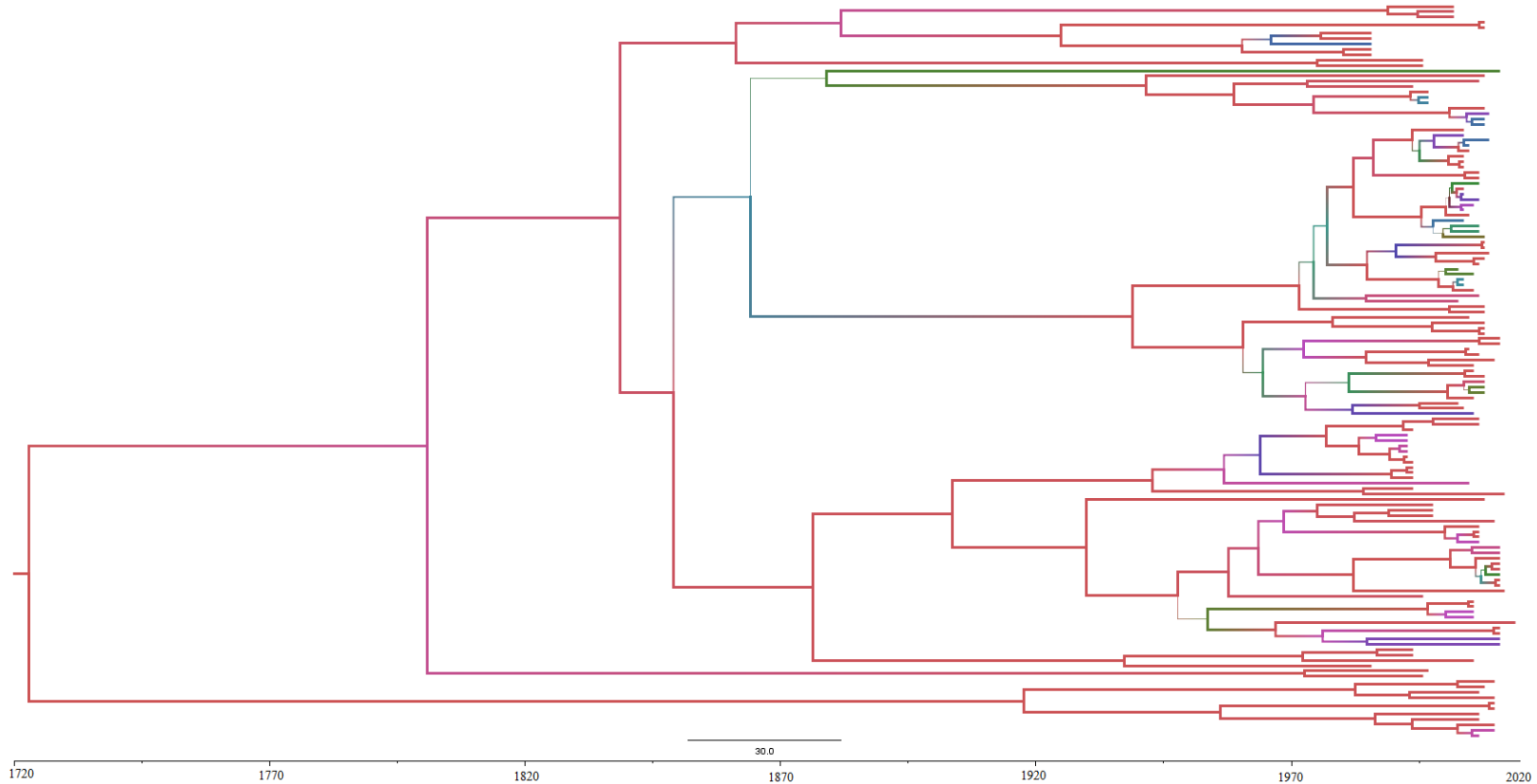


Figure 32. The maximum clade credibility (MCC) tree of TULV S partial sequences. The branches are colored on the basis of the most probable location of the nodes. The thickness of the branches reflects the posterior probabilities (values below 50 are thin) and the scale at the bottom of the tree represents the number of years before the most recent sampling time (2013)

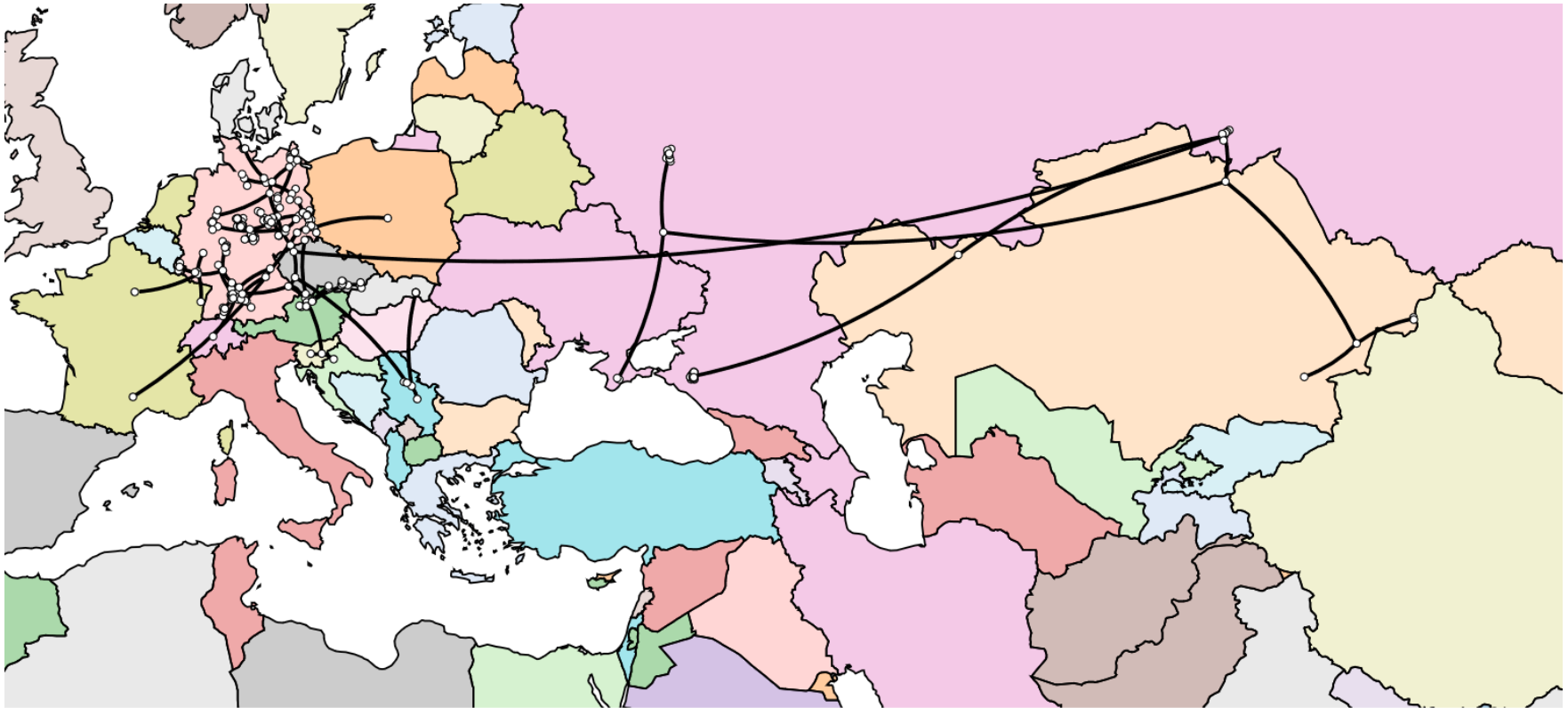


Figure 33. The patterns of TULV spread generated by Spread

5. DISCUSSION

Hantaviruses are known to be endemic in the Balkan region, where sporadic cases and/or outbreaks of HFRS have been reported repeatedly. In south Balkan countries, including Greece, Romania, Albania, Macedonia, Serbia and Montenegro, DOBV is considered to be the predominant cause of HFRS cases. However, in the north Balkan countries, like Slovenia and Croatia more PUUV infections are observed (Avsic-Zupanc et al., 2014). Hantavirus seroprevalence to either antibodies and/or antigens was found on average in 16% of *A. flavicollis*, 8.1% *A. agrarius* and 16% of *M. glareolus*, with significant differences observed between epidemic and non-epidemic years (Avsic-Zupanc et al., 2014). While during the non-epidemic years the prevalence of hantaviruses in hosts in endemic areas of HFRS in the former Yugoslavia was on average 9.2%, the prevalence of infection was on average 19.7% and 23% for the epidemic years 1986 and 1989, respectively (Avsic-Zupanc et al., 1990; Avsic-Zupanc et al., 1993; Avsic-Zupanc et al., 1994; Gligic et al., 1992; Lukac et al., 1990). Ever since the first clinical and epidemiological evidence of HFRS in Serbia dating to the middle of last century, serological evidence of hantaviral infection has been detected in both humans and animal reservoirs. The first serological results on hantaviruses in small mammals in Serbia were published in 1986, and concerned the localities Rugovo and Čačak, with 34% and 30% seroprevalence, respectively (Gligic et al., 1989). In the following decade, hantavirus antigen and/or antibodies-positive rodents have been repeatedly found in these and other foci, at similar or slightly lower rates (Gligic, 2008). Positive detection of hantaviral antigens and/or antibodies has been found in multiple rodent species (*A. flavicollis*, *A. sylvaticus*, *A. agrarius*, *A. microps*, *M. arvalis*, *M. subterraneus*, *M. musculus*, *R. norvegicus*, *My. glareolus*) and insectivores (*Sorex alpinus*, *S. araneus*, *Crocidura suaveolens*) (Gligic et al., 1988). So far, serological findings imply circulation of multiple hantaviruses in Serbia, including HFRS-causing DOBV, PUUV, but also TULV (Gligic et al., 1988; Papa, 2012). Moreover, reported frequency of serological DOBV detection in *Apodemus* rodents or small mammals in other Balkan countries ranges from 3.6% in Bosnia and Herzegovina, 6.3% in Croatia, 17% in northern Croatia and Hungary to 21.21% in Slovenia (Lundkvist et al., 1997; Avsic-Zupanc et al., 2000; Plyusnina et al., 2009, 2011; Nemeth et al., 2011). In endemic regions in Greece, 13% of *A. flavicollis* are infected by DOBV (genogroup Dobrava) (Papa et al., 2001).

However, until the study presented in this doctoral thesis, hantaviral genetic analyses from either human or rodent populations in Serbia were very scarce. Only one study reported three DOBV sequences for M and two sequences for S segment obtained from three patients during an epidemic in Serbia and Montenegro (Papa et al., 2006). Regarding the genetic data obtained from small mammals, PUU-like virus and TULV RNA were detected in *M. musculus* *M. subterraneus*, respectively (Diglisic et al., 1994; Song et al., 2002). Nevertheless, detailed molecular characterization of hantaviruses circulating in Serbia has not been performed yet, leaving the natural hosts and geographical distribution of hantaviruses in its reservoir host in Serbia largely unknown. As such, this study provides the first effort to gain insight into the molecular epidemiology of hantaviruses in wild rodents in Serbia. The present study of 110 rodent samples encompassed molecular investigation and genetic characterization of hantaviruses recovered from different rodent reservoirs of three subfamilies (*Murinae*, *Arvicolinae* and *Glirinae*). This thesis focuses on the evolutionary analysis of hantaviral sequence data using multiple phylogenetic methods. These methods were employed to examine complex biological processes, such as evolutionary dynamics, natural selection, recombination and migration of hantaviruses. However, the present study was not designed to evaluate the seroprevalence of hantavirus antigens/antibodies in natural reservoirs. Since the pool of animals and samples that gave rise to the study population was collected within research unrelated to hantaviruses, the resulting rodent population was too diverse and could not be considered representative for sero- and epidemiological surveys. Hence, the obtained proportions of positive animals may only be taken as informative. Nevertheless, although the percentage of positive samples found in this study (6.3% in total, among species that tested positive, 5.5% overall, including all the viruses and hosts) may seem low, in particular for the endemic region, the overall percentage of hantavirus RNA detection in similar studies that used molecular approach varies widely. Similar to our finding of 4.3% molecular positivity of the total of tested *A. flavicollis* (9.7% among seropositive animals) and 2% , in the study designed to examine hantavirus infection in host population in south Bulgaria, the prevalence of hantavirus RNA among studied animals was 7.7% in *A. flavicollis* and 1.43 % in *A. agrarius* (Chassovnikarova et al., 2013). Moreover, in Bulgaria 691 rodents were captured in three different HFRS-endemic regions during 2011-2012 and DOBV RNA was recovered from

six *Apodemus* mice: five of species *A. flavicollis* and one *A. agrarius* (Christova et al., 2015) In the Kırklareli province, located in Turkish Thrace (neighbouring Bulgaria), DOBV RNA was detected in eight of 73 rodents (Polat et al., 2018). In the study designed to test the presence of hantaviruse in Poland, five of 60 tested small mammals (belong to four different species; *A. agrarius*, *M. agrestis*, *My. glareolus*, *S. araneus*) were found to be hantavirus RNA positive (Wójcik-Fatla et al., 2013). In the study which tested the occurrence of SEOV in the wild rat population in the Netherlands, two out of 16 animals were found to be positive using molecular methods (Verner-Carlsson et al., 2015).

The possible explanation for seemingly low prevalence of hantavirus RNA among the tested animals is that viremia is very brief (7-10 days) before the host develops detectable antibody, following by simultaneous presence of both anti hantaviral antibody and hantaviral RNA in blood of rodents in the period of 3 months and then consequent clearance of virus from the blood (Kuenzi et al., 2005). Simultaneously, hantavirus is established in certain cells and can be transmitted via urine, feces, and saliva. During the period of chronic infection hantaviral RNA may be alternately detected. Viral RNA is probably consistently present in the blood of chronically infected animals, however, under the limits of PCR detectability (Kuenzi et al., 2005). Finally, when focusing on the molecular positivity rate among the seropositive animals, the obtained results might reflect some discrepancy of low detectable hantaviral RNA among seropositive animals. However, the prevalence of hantavirus RNA positive samples among seropositive animals varied widely among different studies (Avsic-Zupanc et al., 2000; Chandy et al., 2013).

DOBV positive animals were captured in western (three *A. flavicollis*) and central (one *A. agrarius* and one *G. glis*) Serbia. *M. arvalis* was also captured in central Serbia. In general, DOBV is known to be mostly associated with different *Apodemus* species, including *A. flavicollis*, *A. agrarius*, and *A. ponticus* (Papa et al., 2016). Since DOBV genotypes Dobrava and Sochi have the potential to cause severe form of HFRS in humans, with high mortality rate, knowledge of the distribution and infection rates of their natural hosts, *A. flavicollis* and *A. ponticus*, respectively, is very important and helpful for the Public Health.

Rodent species of the *Apodemus* genus are the most widespread compared to all other groups of small mammals. These small mammals inhabit Palearctic zone (Corbet & Ovenden, 1980; Orlov et al. 1996). Currently, around 20 different species have been described, of which roughly half inhabit Europe and North Africa and species of the other half inhabit Asia (Musser & Carleton, 1993; Wilson & Reeder, 2005).

A. flavicollis inhabits wide range from southern England and Wels to the west, to Belarus and Ukraine to the east and from southern Finland and Sweden to the north to Spain and Greece to the south (Bugarski-Stanojevic, 2010). This species inhabits the entire Apennine and the Balkan Peninsula. *A. flavicollis* is granivorous rodent species and therefore it can be found in deciduous forests with high seed production, mostly accompanied by *A. sylvaticus* (Balaz and Ambros, 2012). Moreover, this small terrestrial mammal species utilizes nest boxes as hiding place, shelter and food storage. *A. flavicollis* is characterized by great mobility, but it is strictly depended on the forest environment. The assumed mean home range size for *A. flavicollis* was 625 m² for males and 551 m² for females (Vukicevic-Radic et al., 2006). In the present study three *A. flavicollis* captured in west Serbia found to be DOBV positive.

A. agrarius has the largest range of distribution of all *Apodemus* species, including parts of Europe and Asia. In Europe, it inhabits areal from Baltic region to the north to Turkey to the south, including Balkan Peninsula, Greece and Bulgaria. Eastward, it ranges to Caucasus, including parts of Kyrgyzstan and Kazakhstan, the western part of the Baikal region, north-western China and Mongolia. Moreover, *A. agrarius* inhabits the region of Amur River, the Far East of Russia, Korea, and even some Japanese islands (Bugarski-Stanojevic, 2010). This rodent species is commonly found in grassy fields, cultivated areas, and woodlands. *A. agrarius* is also granivorous, with seed and fruits of trees being their predominant food resource. Mean home range size assumed for this species was 716 m² for and 585 m² for females (Vukicevic-Radic et al., 2006). In our study, *A. agrarius* is confirmed to be a DOBV, host, with one positive animal trapped in central Serbia.

The distribution range of *G. glis* is mostly in concordance with deciduous forest zone in the western Palearctic (Krystufek, 2010). This small mammal is widespread in western, central, and southeastern Europe except Denmark, France and the majority of the Iberian

Peninsula. They frequently inhabit deciduous and mixed woodland with high amount of mast seeders. The most preferable habitats are the edges of forest with sparse trees but dense herb and structured forests with high trees and dense understory. In general, the key trees in the deciduous and mixed forests are mast seeders, belonging to genus *Quercus* and *Fagus*. Since the seed is the preferable food of these mammals, the yearly fluctuation in its produce noticeably affects the main physiological event in *G. glis*, hibernation. Moreover, the oscillation in seed production is followed by skipping reproduction cycle. Adult forms of edible dormouse have small home-range sizes (< 1-7 ha), with males having larger home ranges than females with high site fidelity suggesting that dispersal occurs during the juvenile/yearling stage (Marteau and Sara, 2015). DOBV RNA was found in one *G. glis* captured in central Serbia.

Regarding phylogenetic analysis based on molecular approaches, it provides highly reliable insight in evolutionary relations among virus strains (Hofmann et al., 2014). All three hantavirus genome segments can be used for genotyping and for studying the virus phylogeny. However, sometimes the results obtained for all three segments are incongruent, due to possible recombination and reassortment events. The number of reported sequences within certain segment of hantaviruses (especially for M and L segment sequences) may also influence the obtained results.

Phylogenies for partial DOBV L, M and S segment alignments obtained using different phylogenetic methods within the current study were highly consistent. Obtained results provided insight into the phylogenetic relatedness of newly detected sequences from Serbia and sequences retrieved from NCBI.

Phylogenetic analysis of DOBV L segment sequences placed all Serbian strains (the newly detected strains and those retrieved from the database), within the Dobrava genotype. In the phylogenetic tree, the newly detected sequences isolated from *A. agrarius* and *G. glis*, were placed together with Serbian sequences isolated from *A. flavicollis* and human HFRS cases. The positioning of the newly detected Serbian sequences, isolated from *A. agrarius* and *G. glis*, on the phylogenetic tree could possibly reflect local host switching of DOBV between *A. flavicollis* and *A. agrarius*. However, the number of available sequences for L segment is rather limited (37, including 22 sequences originating from Serbia) to allow broader conclusions.

Moreover, the possibility of host switching is supported by the fact that these two *Apodemus* species are known to share the same habitat. In this aspect, detailed phylogenetic analysis was done based on the S segment of DOBV.

The analyzed DOBV L segment protein coding sequence included the complete motif B and almost complete inter-motif (between motifs A and B) of the L protein (pos. 988–1087 aa). Motifs B, E and pre-motif A found in all RNA-dependent RNA polymerases are responsible for positioning of the template and primer relative to the active site (Nemirov et al., 2003). In all aligned DOBV L protein sequences in our study, motif B (pos. 1044–1065 aa) was fully conserved and the A-to-B inter-motif was highly conserved with rare amino acid changes, suggesting their importance in enzyme function (Kukkonen et al., 2005).

Phylogeny of the M segment mirrored the classification of DOBV into four genotypes, in spite of the relatively short length of the studied region (434 nt compared to the 3601 nt of the complete length of DOBV M segment) and limited number of sequences included. Notably, only 13 M segment sequences spanning the studied region were found in the database. Serbian strains were placed within Dobrava genotype and showed local-geographic clustering. Studied M segment region (pos. 573-717 aa) encompasses the glycoprotein precursor cleavage sites placed at the position 647, thus it included small coding parts of both Gn and Gc proteins (Guardado-Calvo and Rey, 2017). This functional constrain influences the variability of the analyzed M segment region that was found to be highly conserved with only 16 variable sites within the studied aa region.

Phylogeny of DOBV S segment was assessed based on 180 DOBV S segment sequences. The studied dataset contained animal and human isolates. Phylogenetic analyses indicated local geographical clustering of all Serbian sequences, regardless of either the host or year of collection. Serbian strains were placed in several different clusters within Dobrava genotype, conforming to location of isolation (central or western Serbia). A similar topology of the phylogenetic tree was described in previous studies, with the exception of SAAV whose exact position depends on the length of studied S segment sequences (Klempa et al., 2005; Papa et al., 2006; Papa 2012; Schlegel et al., 2009).

The N protein of hantaviruses is of approximately 430 (429 to 433) aa residues and has a molecular weight of approximately 50 kDa (Kaukinen et al., 2005). Within each hantavirus species, the primary structure of N protein is highly conserved. The pattern of N

protein is characterized by three conserved domains separated by two more variable regions spanning aa residues from approximate positions 50 to 80 and from 230 to 310. The amino-terminal part of N protein forms the main human IgG epitope (pos. 1–118 aa) (Kaukinen et al., 2005). The central conserved domain (pos. 175–217 aa) contains a large cluster of 15 lysines/arginines residues located between positions 136 and 213. Particularly, all 15 positive charges are completely conserved in all known hantaviruses. This cluster overlaps with the RNA-binding domain. The region of the S segment under study codes for the partial conserved amino-terminal N protein, forming genome RNA binding domain (pos. 122–285 aa), important for RNP assembly (Kaukinen et al., 2005).

Obtained results, based on phylogenies of all three DOBV segments, imply DOBV as one of main hantavirus circulating in Serbia. Genetic detection of DOBV in *A. agrarius* and *A. flavicollis* is in line with a fact that these rodents are the most common *Apodemus* species on the territory of Serbia. These results are in congruence with previous serological and molecular studies of hantaviruses on the territory of Serbia (Gligic et al., 1988; Papa, 2012).

Specimens of DOBV positive *A. agrarius* and *G. glis* were trapped in 2007 in the region of Ravanica River at altitudes ranging between 580 m and 716 m, along hilly and wooded terrain of mixed deciduous forest (beech, oak, oak, hazel, hornbeam) with wild pear and apple trees on the fringes. Detailed S segment based phylogenetic analysis suggested local geographically specific clustering. However, clustering pattern also reflected the main host species harboring DOBV (*A. flavicollis* and *A. agrarius*): newly acquired DOBV strains from Serbia isolated from *A. agrarius* and *G. glis* clustered together with other DOBV sequences associated with the rodent *A. flavicollis* within Dobrava genotype.

Based on the clustering in the S segment phylogenetic tree, both newly described sequences (isolated from *A. agrarius* and *G. glis*) were found to be very similar to DOBV strains isolated from patients who originated from central and southern Serbia, implying local circulation of DOBV strains between different hosts. Furthermore, one of two DOBV sequences was retrieved from *G. glis*. Previously, this species, or any other species of the Gliridae rodent family, has not been associated with DOBV infection. This finding implies an uncommon DOBV spillover event; further studies are underway to explore the scope and nature of DOBV infection in Gliridae rodent species in Serbia.

A. flavicollis is considered the main rodent reservoir of DOBV-Dobrava genotype in the Balkan region (Papa, 2012). Considering phylogenetic results, it may also be regarded as the putative source of spillover infection for the other species (*A. agrarius* and *G. glis*).

In general, spillover may play very important role in evolution and emergence of hantaviruses. It represents a fundamental precondition for genetic reassortment and recombination of viruses. The process of spillover is also prerequisite for virus host switching between different species. After the occurrence of spillover, it takes some time for the virus to establish replication and transmission cycle within the new host. Under these conditions, virus switch from one to another host species may be considered. However, recent findings indicate that host switch might be less rare event than previously believed (Schlegel et al., 2009, Schmidt-Chanasit et al., 2010; Schlegel et al., 2012). Recent results of phylogenetic analysis of DOBV Kurkino genotype strains originating from Germany, confirmed the evidence of multiple spillovers with several strains isolated from *A. flavicollis* clustering together with sequences isolated from *A. agrarius* (Schlegel et al., 2009).

Moreover, spillover of TULV was described between different host genera, such as *Microtus* and *Arvicola*, sharing the last common ancestor more than three million years ago (Schlegel et al., 2012). A comparative phylogenetic analysis showed the presence of spillover in TULV strains isolated from sympatrically occurring *M. arvalis* and *M. agrestis* hosts (Schmidt-Chanasit et al., 2010).

For a long time rodents were considered the original mammalian hosts of primordial hantaviruses (Zhang, 2014). Recently, this concept has been strongly challenged in favor of host switching and local host-specific adaptation. The fact that the first ever hantavirus was TPMV isolated in 1971 from the Asian house shrew (*Suncus murinus*) has long been neglected. In addition, in 2007 the second hantavirus was isolated also from shrew *Crocidura theresae*, sampled from Guinea. However, only recent studies showed that phylogeny of hantaviruses and their hosts need to be reassessed, indicating that importance of their evolutionary history is far more complex than previously thought. New data also point that insectivores and bats play important role in hantavirus evolution. The fact that the hantaviruses from both the Chiroptera and Soricomorpha form paraphyletic groups powerfully suggests that ancestral hantaviruses cross between mammalian orders (Zhang, 2014).

Furthermore, the significance of virus–host switching lies in the emergence of pathogenic viruses, presumably through acquisition of genes associated with virulence and tissue targeting. As outcome of the above mentioned, it is clear that cross-species hantavirus transmission, as well as geographic dispersal of Chiroptera, Soricomorpha and Rodentia, have also contributed to the high biodiversity and near global distribution of those hantaviruses known today. However, since the sequence database of hantaviruses is limited yet, it is beforehand to make final conclusions regarding the significance of co-divergence and host switching in the similarities between the phylogeny of hantaviruses and their mammalian reservoir hosts (Yanagihara et al., 2014). Namely, the phylogenetic relationship among hantaviruses and their hosts can be explained by periodic episodes of co-divergence through deep evolutionary time.

DOBV (Dobrava genotype) is the causative agent of the most severe form of HFRS in Europe, with case-fatality up to 12%-18% (Gligic et al., 2008). Considering that *Apodemus* rodents are the main natural reservoir of DOBV, detailed epidemiological investigation of DOBV infection in these small mammals is a pre-conditional first step in organizing measures to prevent spread to humans. In our research, three samples of *A. flavicollis*, captured on Tara Mountain were hantavirus positive. All animals were trapped on the touristic complex of Tara Mountain. Up to now, western Serbia, where mountain Tara is located, has not been investigated for the presence of hantaviruses in the animal reservoirs. As such, this study represents the first effort to study the possible circulation of hantaviruses in this part of Serbia. Regarding human infection, the majority of reported serologically documented DOBV human infections so far in Serbia occurred in the south of the country, represented by the Vranje trapping site in this study (Papa et al., 2006). Two of the locations in our work were Kosutnjak and Avala, in the municipality of Belgrade, where the first human DOBV case was detected (Gligic et al., 1992). During the period of animal collection, 40 cases of human hantavirus infection were immunologically detected in Serbia (unpublished data from National Reference Laboratory for ARBO viruses and HF viruses). Unfortunately, epidemiological data regarding the exact or most probable place of infection are very scarce or completely missing. Detection of hantavirus genome in *A. flavicollis* animals and identification of a new endemic focus in western Serbia indicate the need for

permanent monitoring. Testing should include both endemic and non-endemic areas, especially areas with frequent human visits.

DOBV L segment sequences were obtained from three *A. flavicollis* captured on Tara Mountain (RS1 to RS3), whereas S RNA segment sequences were obtained from two of them (RS1 and RS3). Absence of amplification for the S segment in the RS2 isolate suggests better detection sensitivity by degenerate primers for the L segment (Klempa et al., 2006).

It is important to emphasize that newly acquired sequences from Tara Mountain clustered together with Serbian human isolates included within S segment phylogenetic tree regardless of the date of collection. A similar trend, concerning high phylogenetic similarity regardless of temporal distance, has also been shown in Greek and Slovenian sequences from humans and animals. This phenomenon points to unidirectional transmission of infection, from mice to man. In accordance with that, the short residence time of the virus in human tissue could be insufficient to induce fixation of virus genome changes in different hosts (Schilling et al., 2007).

TULV is widespread across Eurasia, including France, Germany, the Netherlands, Austria, Slovenia, Croatia, Hungary, Poland and Russia, where numerous mammal species have been shown to be its reservoirs, including *M. arvalis*, *M. subterraneus*, *M. rossiaemeridionalis*, *M. agrestis*, *M. gregalis*, *A. amphibius* and *Lagurus lagurus* (Schlegel et al., 2012; Schmidt-Chanasit et al., 2010). Serbia was the first country in the Balkans where TULV was detected (Song et al., 2002). Molecular analysis of the TULV L segment of the new Serbian strain showed no evidence of aa divergence, compared to the reference sequence (NC005226). Examined L segment region mostly encompassed conserved region, including motif B. This motif, responsible for the positioning of template and primer relative to the active site, is one of six L protein conserved motifs (premotif A and motifs A, B, C, D, E) in all hantaviruses (Nemirov et al., 2003).

Phylogenetic analysis of both L and S segment sequences included in the study is suggestive of geographically related clustering, as previously shown for majority of hantaviruses (Avsic-Zupanc et al., 2000; Plyusnin et al., 1996). In addition, obtained molecular data do not suggest host related clustering, with the presence of particular natural reservoirs in different branches of phylogenetic tree. Phylogenetic tree based on partial S segment alignment showed that both strains from Serbia clustered together with those from East Slovakia

(Y13980 and Y13979), that have already been shown to be recombinants (Kosice strain) (Sibold et al., 1999). Herein, we reported the evidence of putative recombination events in two TULV sequences from Serbia. The analyzed sequences of both Serbian strains covered most of the S segment coding region, including partial central domain and near complete C-terminal domain of the nucleocapsid protein. Using Simplot, the first recombination breakpoint was detected in the conserved region of the central domain (around position 600), while the other two breakpoints (around the positions 750 and 950) were observed in the variable region of the C-terminal domain. Two of these breakpoint positions (600 and 950) corresponded to those described in PUUV sequences (AJ314598, AJ314599) (Sironen et al., 2001). However, the observed TULV recombination pattern in our study could not be detected using the RDP4. Of note, reanalysis by RDP4 of the mentioned PUUV recombinants did not reveal the reported recombination breakpoints either (data not shown), illustrating the lack of sensitivity of this approach for mosaic like recombination pattern. Similar recombination breakpoints have also been described in transfection-mediated TULV recombinants (Plyusnin et al., 2002).

Separate phylogenetic analysis of putative recombination regions has been proposed as gold-standard for detection of recombination (Han and Worobey, 2011). Thus, phylogenetic analysis of subalignments based on bootscan analysis, confirmed the positions of recombinant peaks. The putative recombination breakpoints found in Serbian TULV sequences are of very similar pattern to those in Kosice lineage from Slovakia. Likewise, both sets of recombinant sequences contain the same pattern of nonsynonymous nucleotide substitutions in both conserved and variable part of nucleocapsid protein (Table 1).

The two Serbian TULV sequences were retrieved from different host reservoirs and on different locations. Namely, the first sequence was retrieved from *M. subterraneus* captured in Cacak region, western Serbia (Song et al., 2002), while the newly detected sequence was obtained from *M. arvalis* trapped in central Serbia, some 100 km eastward. No major geographical obstacles exist between the two trapping sites (e.g. rivers, mountains...), which could facilitate local migration of host rodents and spread of the recombinant virus. Spillover spread of hantavirus infection among voles living in sympatry has been described (Schlegel et al., 2012; Schmidt-Chanasit et al., 2010). The two TULV host species have been

shown to occur sympatrically on the territory of Serbia (Gligic et al. 2008). Furthermore, Serbian TULV sequences were isolated in different time points, 20 years apart (1987 and 2007). The time span of 20 years between the detection of the two sequences might be the reason for the high nucleotide diversity (13.16%) between the two Serbian sequences of reflecting the accumulation of nucleotide point mutations. In contrast, to the nucleotide diversity between sequences from Slovakia, both obtained in 1995 was much less (2.47%).

In general, *M. arvalis* occupies the whole Europe, from the Ukraine and central Russia to Atlantic coast of France (Heckel et al., 2005). This common vole inhabits subterraneous borrows in the open habitats like fields and meadows (Schweizer et al., 2007). The dispersal capacity of voles is very restricted, with several hundred meters or few kilometers within one day (Schweizer et al., 2007). The consequence of this limited movement of voles is reduction in the opportunity of TULV dissemination on long distance. On the other hand, voles tend to build subterraneous burrows in their natural habitats which serve as shelters for colonies of voles during the winter (Heckel et al., 2005). This type of complex social behavior may increase the possibility of direct TULV transmission among these small rodents (Deter et al., 2008). In addition, indirect transmission of TULV through contaminated excretes and environment also influences the spread of TULV.

Recombination is one of the molecular mechanisms responsible for genetic diversity and it has been described in various families of RNA viruses (Worobey and Holmes, 1990). The most likely mechanism proposed for this process is copy-choice model, primarily described for poliovirus (Copper et al., 1974). This process requires jumping of RdRp from one to another RNA molecule during RNA replication. During this process polymerase remains bound with nascent nucleic acid chain allowing formation of genetically distinct viral strains (Simon-Loriere and Holmes, 2011). However, it was documented to occur with very low frequency in negative stranded RNA viruses (Chare et al., 2003). Actually, the best evidence of recombination among negative stranded RNA viruses is seen in hantaviruses (Han and Worobey, 2011). Genome structure and life cycle of viruses may play important role in occurrence of recombination.

Secondary structure in genome organization of segmented RNA viruses may influence the rate of recombination, facilitating the transition of RNA polymerase. Hairpin-like secondary structure has been described between nt 332 and nt 368 of TULV S segment,

and its link has been identified to potential recombination hot spots (Plyusnina and Plyusnin, 2005). This structure might be involved in initiating transition in positioning of the RNA polymerase. The regions of recombination breakpoints described in both Serbian sequences are found immediately downstream this secondary structure position.

Persistent infection is an important factor influencing the rate of recombination, facilitating coinfection of infected cell with two different virus lineages (Sibold et al., 1999; Simon-Loriere and Holmes, 2011). Hantaviruses establish persistent infection within their natural hosts, so they have higher probability of recombination compared to other negative sense RNA viruses causing acute infection. Besides, the existence of different hantavirus strains on the same geographical territory is essential for recombination to occur (Sibold et al., 1999).

The first evidence of homologous recombination within the hantaviral S genomic segment was discovered in TULV lineage Kosice, originating from East Slovakia, where mosaic-like structure of the S segment was seen, consistent with several recombination events (Sibold et al., 1999). The existence of recombinant TULV lineages within S segment was also confirmed in experimental conditions, where the existence of recombination hot-spots is correlated to features of the S segment secondary structure (Plyusnin et al., 2002). The same evolutionary mechanism was observed in PUUV, with recombination breakpoints detected around the positions 440/630 and 940/1130, as well as in HTNV (Sironen et al., 2001; Chare et al., 2003). Additionally, the possible event of recombination is reported between different DOBV strains in *A. agrarius* and *A. flavicollis* in nature (Klempa et al., 2003b).

The occurrence of recombinant TULV forms with similar recombination pattern in different parts of Europe raise the question of two possible scenarios: one being direct dispersion of recombinant TULV lineage between Slovakia and Serbia, and the other being independent occurrence of TULV recombination events in different European regions. Geographical distance between the two trapping sites (Kosice and Ravanica) of over 700 km, including obstacles (e.g. rivers, mountains), would pose a major barrier in direct spread, whereas the possibility of repeated, independent occurrence of such similar recombination breakpoints has, so far, been taught to be extremely low (Han and Worobey, 2011).

The function of the portion of 164 aa of DOBV N protein (122-285 aa) analyzed in our study is responsible for RNP assembly and this part of N protein includes 15

highly conserved lysines/arginines residues. The type of detected aa changes and evidence of negative selection ($p < 0.1$) in action on this region both imply a high tendency for protein structure conservation. Protein function plays an important role in selection pressure, restraining fixation of new mutations. Consequently, examined part of DOBV S segment has lower nucleotide divergence compared to the examined L segment region (7.17% versus 10.81%, respectively), conversely to the results obtained in comparison of their whole-nucleotide sequences (Nemirov et al., 2003; Papa, 2012).

Regarding the analysis of TULV N protein, it included 189 aa (positions 120-308 aa). This studied region includes the conserved RNA-binding domain, but it also partly covers the variable domain (aa positions 230-308). Obtained results showed the evidence of negative selection ($p < 0.1$), in both conserved and variable studied nucleocapsid region. The possible role of purifying selection in this case might be to act against deleterious variants in protein-coding gene by selective pressure over time.

The results of substitution rate of TULV strains isolated in different parts of the world over time spanning 28 years (1987-2015) revealed that the rate of accumulation of nucleotide changes is 1.787×10^{-3} substitutions/site/year. The substitution rate of molecular evolution obtained in a previous study, which ranged from 1.99×10^{-2} to 8.87×10^{-3} substitutions/site/year, is in concordance with our results (Ramsden et al., 2008). This high substitution rate in TULV is the consequence of many factors regarding the viral life cycle, such as mutation rate, generation time, transmission and natural selection (Duffy et al., 2008). Hantaviruses possess RdRp for replication, which lacks the proofreading and repair mechanisms and operates with an error rate of ~ 1 mutation/replication/genome (Drake 1999). Previously calculated mutation rate for hantaviruses (1×10^{-3} to 3×10^{-3}) is in concordance with the obtained substitution rate in our study (order of 10^{-3} substitutions/site/year) (Ramsden et al., 2008)

Time span, which is here 28 years, is an important factor for estimation of long-term evolutionary rates of viruses. Sampling over longer time period may more accurately denote the real substitution rate. In contrast, if the analyzed time span is not sufficient, the number of nucleotide substitutions may include deleterious mutations that would later be removed by purifying selection.

Evolution and diversification of hantaviruses have been largely influenced by migration pattern of viruses and their hosts. In general, the pattern of hantavirus divergence is in congruence with distribution of their hosts. Certain groups of both rodent-borne and shrew-borne hantaviruses are geographically restricted to either New World or Old World hantaviruses, while other hantaviruses are globally distributed. Nevertheless, mechanisms and timing of virus diversification have not been fully resolved yet. For example, host switching may play important role in virus divergence. Sympatrical occurrence of different rodent species may facilitate the process of host switching and, therefore, influences the hantavirus diversification.

Geographic distribution of hantaviruses has been explored in multiple studies so far (Bennett et al., 2014, Torres-Perez et al., 2011, Souza et al., 2014). Obtained results of some studies placed the putative root of potential hantavirus origin in Asia, with further local and global viral spread, e.g. independent spreaded to Americas, as colorfully depicted in **Figure 9** (Bennett et al., 2014). *Arvicolinae* associated hantaviruses probably emerged in China. Initially, these hantaviruses had probably been adapted to the *Myodes* genus and gave rise to viral spread towards North Europe and further evolution of viruses such as PUUV. By the same time *Arvicolinae* associated hantaviruses were adapted to the *Microtus* genus and spread towards central Asia (e.g. Kazakhstan), Europe and North America. TULV, as the member of *Microtus* genus-associated hantaviruses, might be an ancestral hantavirus species in Europe and Asia.

TULV is widely distributed since its main host reservoir (*M. arvalis*) occupies whole Europe (Heckel et al., 2005). As also confirmed within this study, based on detailed phylogenetic analysis of both L and S segment sequences, TULV is characterized by geographically related clustering, as previously shown for majority of hantaviruses (Avsic-Zupanc et al., 2000; Plyusnin et al., 1996). Furthermore, host related clustering is not present within TULV sequences, since different natural reservoirs can be observed in different branches of phylogenetic tree. These facts underlined the importance of analyzing the migration pathways of TULV strains in order to reconstruct the possible origin and dispersion pathways of the different viral strains. Herein, phylogeographical approach based on Bayesian methods was used which simultaneously identifies the possible pattern of virus migration and the root of virus origin.

Phylogeographical study was based on 137 TULV S segment strains isolated from 69 locations within Europe and central Asia with large time span of isolation of 28 years (1987-2015). The TULV dataset comprised four recombinant strains: two from east Slovakia (Sibold et al., 1999), where the host animals (*M. arvalis*) were trapped in 1995 in Kosice region, and two from Serbia (one from *M. subterraneus* captured in 1987 in Cacak region (west Serbia) and the other from *M. arvalis* captured in 2007 in Ravanica region (central Serbia) (Song et al., 2002). In view of the the same pattern of recombination and time span of animal trapping of 20 years, we speculated that TULV of this genetic shape has become a stable part of virus population, allowing their inclusion into the analysis.

Phylogeographic analysis performed using Cauchy RRW model together with Log-normal molecular clock and constant population size as tree prior, revealed that potential root and origin of spread of all known TULV clades was placed in central Asia, most probably in Kazakhstan. According to our findings, the common ancestor, placed in the root of TULV origin, probably existed around 300 years ago. This result is in accordance with some previously published data (Saxenhofer et al., 2017). However, it is very likely that this finding does not depict accurately the time of TULV origin with the age of origin being highly underestimated. The possible cause might be the lack of sensitivity of existing Bayesian methods, since the extinct basal viral lineages in the data set could not be in the analysis. It has already been speculated that application of molecular clock analyses calibrated by contemporary sequences proved to be accurate in inferring short-term evolution, whereas errors could arise at larger time scales, especially for highly variable viruses, due to the large number of accumulated mutations and consequent effect of saturation (Worobey et al., 2010, Saxenhofer et al., 2017).

In our reconstruction, initial TULV spread started locally, throughout Russia and Kazakhstan and then the virus was introduced into central Europe (Czech Republic) by a single pathway. The possible reason underlying this dispersal pattern might simply be the distance between central Asia and central Europe. Namely, voles as the most important hosts of TULV, have very limited dispersal areal with only few hundred meters a day (Schweizer et al., 2007). TULV further spread locally throughout Europe and central Asia. Soon after TULV was introduced into Czech Republic, it entered Serbia once as recombinant strain and further spread in two directions: locally and also to Slovakia. This is in consistence with the

fact that Serbian strains were the result of recombination among TULV sequences originating from Czech Republic and Russia. Moreover, these results imply that the recombination event had happened previously, probably on the territory of Czech Republic, upon single introduction of TULV into Czech Republic from Russia. Nevertheless, phylogeny based on TULV S segment showed that TULV strains originating from Czech Republic were closely related to sequences from Austria, implying that TULV might have alternatively been introduced to Czech Republic from Austria and recombined with sequences from Russia further on.

In this doctoral thesis we explored molecular data of DOBV and TULV by means of phylogenetic analysis, including different methods (Neighbor-Joining, maximum likelihood and Bayesian statistics). Obtained results revealed some new data regarding the ecology and evolution of hantaviruses. Detection of potentially new hantavirus host species provides better insight within pull of host sources of hantavirus infection. Moreover, detection of recombination and detailed phylogenetic analysis of recombination pattern, as molecular mechanism of evolution of hantavirusnog genome, may improve knowledge regarding the evolution of hantavirues. Results obtained by investigation of spatial and temporal transmission patterns derived from time-calibrated phylogeny of hantavirus sequences may facilitate understanding of the process of disease emergence and spread.

Hantaviruses belong to the increasing group of emerging zoonotic pathogens. Since many countries worldwide have been affected by hantaviruses, the understanding and recognition of this problem has been improved over the past few decades. Among others, extensive research of hantavirus natural reservoirs and development of more sensitive diagnostic tools can act strongly against this global health problem. However, factors like climate change and landscape alternation still affect the geographic distribution, abundance and the dynamic of the carrier rodent species, and therefore change the epidemiology of hantaviruses. Consequently, comprehensive research on hantavirus ecology, evolution, pathogenesis, and diagnostics are still needed.

6. CONCLUSIONS

According to the defined objectives and based on the obtained results the following conclusions have been reached:

- During the five-year study period (2007-2011) two hantaviruses, Dobrava-Belgarde virus (DOBV) and Tula virus (TULV), were genetically characterized in four different rodent species: *A. flavicollis*, *A. agrarius*, *G. glis* and *M. arvalis*.
- *Glis glis* species was found as the novel host and putative natural reservoir of DOBV, since this species, or any other species of the *Gliridae* rodent family, has not been previously associated with hantaviral infection. Phylogenetic analyses of the obtained sequences did not exclude the potential DOBV spillover infection from *A. flavicollis*.
- Molecular screening of *A. flavicollis* from mountain Tara in western Serbia detected the presence of DOBV in tested animals, revealing this locality as a novel DOBV focus in the Balkans.
- Phylogenetic analyses of all three RNA segments (L, M and S) revealed that all Serbian DOBV strains from the novel focus belong to the DOBV-Dobrava genotype.
- Molecular screening of different rodent species in central Serbia detected TULV in *M. arvalis*. Phylogenetic analysis of both L and S segment sequences of the newly detected TULV strain was suggestive of geographically related clustering, as previously shown for the majority of hantaviruses.
- Exploratory recombination analysis, supported by phylogenetic and aa pattern analysis, revealed the presence of recombination in the S segment of the Serbian TULV, resulting in mosaic-like structure, similar to the one of Kosice strain originating from east Slovakia.

- Population dynamics of TULV was found to be relatively constant in size with high estimated substitution rate of 1.787×10^{-3} substitutions/site/year.
- Phylogeographic analysis encompassing all relevant TULV S segment sequences present in the NCBI database at the time of the analysis placed the potential root and origin of TULV spread in central Asia, most probably in Kazakhstan.
- Phylogeographic analysis implied single introduction of TULV to Europe from central Asia, with the complex pattern of local viral migration, including single introduction to Serbia with further spread locally and also to Slovakia.

7. REFERENCES

Amroun A, Priet S, de Lamballerie X, Quérat G. Bunyaviridae RdRps: structure, motifs, and RNA synthesis machinery. *Crit Rev Microbiol*. 2017; 18:1-26.

Antoniadis A, Pырpasopoulos M, Sion M, Daniel S, Peters CJ. Two cases of hemorrhagic fever with renal syndrome in northern Greece. *J Infect Dis*. 1984; 149(6):1011-1013.

Antoniјević B, Gligić A. Hemoragična groznica sa bubrežnim sindromom. Prikaz prvog virusološki potvrđenog slučaja u nas. *Vojno sanitetski pregled*. 1982; 39:205-208.

Arai S, Bennett SN, Sumibcay L, Cook JA, Song J-W, Hope A, Parmenter C, Nerurkar VR, Yates TL, Yanagihara R. Phylogenetically distinct hantaviruses in the masked shrew (*Sorex cinereus*) and dusky shrew (*Sorex monitcolus*) in the United States. *Am J Trop Med Hyg*. 2008; 78:348-351.

Arai S, Nguyen ST, Boldgiv B, Fukui D, Araki K, Dang CN, Ohdachi SD, Nguyen NX, Pham TD, Boldbaatar B, Satoh H, Yoshikawa Y, Morikawa S, Tanaka-Taya K, Yanagihara R, Oishi K. Novel bat-borne hantavirus, Vietnam *Emerg Infect Dis*. 2013; 19(7):1159-1161.

Armien B, Pascale JM, Muñoz C, Mariñas J, Núñez H, Herrera M, Trujillo J, Sánchez D, Mendoza Y, Hjelle B, Koster F. Hantavirus fever without pulmonary syndrome in Panama. *Am J Trop Med Hyg*. 2013; 89(3):489-94.

Armien B, Ortiz PL, Gonzalez P, Cumbreira A, Rivero A, AvilaM, Armien AG, Koster F, Glass G. Spatial-Temporal Distribution of Hantavirus Rodent-Borne Infection by *Oligoryzomys fulvescens* in the Agua Buena Region-Panama. *PLoS Negl Trop Dis*. 2016; 19:10(2):e0004460.

Avsic-Zupanc T, Nemirov K, Petrovec M, Trilar T, Poljak M, Vaheri A, Plyusnin A. Genetic analysis of wild-type Dobrava hantavirus in Slovenia: co-existence of two distinct genetic lineages within the same natural focus. *J Gen Virol*. 2000; 81:1747-1755.

Avsic-Zupanc T, SY Xiao, R Stojanovic, A Gligic, G van der Groen, JW LeDuc. Characterization of Dobrava virus: a hantavirus from Slovenia. Yugoslavia. *J Med Virol.* 1992; 38:132-137.

Avsic-Zupanc T, Saksida A, Korva M. Hantavirus infections. *Clin Microbiol Infect.* 2015; S1198-743X(15)00536-4.

Avsic-Zupanc T, Korva M, Markotić A. HFRS and hantaviruses in the Balkans/South-East Europe. *Virus Res.* 2014; 17:27-33.

Avsic-Zupanc T, Likar M, Novakovic S, Cizman B, Kraigher A, van der Groen G. Evidence of the presence of two hantaviruses in Slovenia. *Arch Virol.* 1990; 115:87–94.

Avsic-Zupanc T, Trilar T, Poljak M, Likar M. Biologija uzročnika hemoragične groznice s bubrežnim sindromom. *Praxis Veterinaria.* 1993; 41:37–43.

Avsic-Zupanc T, Poljak M, Furlan P, Kaps R, Xiao SY, Leduc JW. Isolation of a strain of a Hantaan virus from a fatal case of hemorrhagic fever with renal syndrome in Slovenia. *Am J Trop Med Hyg.* 1994; 51:393–400.

Balaz I, Ambros, M. population analysis and spatial activity of rodents in flooded forest conditions. *Ekológia (Bratislava).* 2012; 31:249–263.

Battisti AJ, Chu YK, Chipman PR, Kaufmann B, Jonsson CB, Rossmann MG. Structural studies of Hantaan virus. *J Virol.* 2011; 85:835-841.

Bennett SN, Gu SH, Kang HJ, Arai S, Yanagihara R. Reconstructing the evolutionary origins and phylogeography of hantaviruses. *Trends Microbiol.* 2014; 22(8):473-82.

Bernshtein AD(1), Apekina NS, Mikhailova TV, Myasnikov YA, Khlyap LA, Korotkov YS, Gavrilovskaya IN. Dynamics of Puumala hantavirus infection in naturally infected bank voles (*Clethrionomys glareolus*). *Arch Virol.* 1999; 144:2415-28.

Bi Z, Formenty PB, Roth CE. Hantavirus infection: a review and global update. *J Infect Dev Ctries.* 2008; 1;2(1):3-23.

Bogdanovic R, Gligic A, Nikolic V, Ognjanovic M. Belgrade and Hantaan hantaviruses—the causative agents of haemorrhagic fever with renal syndrome in children in Serbia. *Srp Arh Celok Lek.* 1995; 123:12-17.

Bowen MD, Gelbmann W, Ksiazek TG, Nichol ST, Nowotny N. Puumala virus and two genetic variants of Tula virus are present in Austrian rodents. *J Med Virol.* 1997; 53:174-181.

Bugarski-Stanojevic V. Molekularna filogenija vrsta roda *Apodemus* (Mammalia, Rodentia) sa područja Srbije. 2010

Calderon G, Pini N, Bolpe J, Levis S, Mills J, Segura E, et al. Hantavirus reservoir hosts associated with peridomestic habitats in Argentina. *Emerg Infect Dis.* 1999; 5:792e7.

Carey DE, Reuben R, Panicker KN, Shope RE, Myers RM. Thottapalayam virus: a presumptive arbovirus isolated from a shrew in India. *Indian J Med Res.* 1971; 59:1758-1760.

Chandy SRG, Ulrich M, Schlegel R, Petraityte K, Sasnauskas DJ, Prakash V, Balraj P. Hantavirus infection among wild small mammals in Vellore, South India. *Zoonoses Public Hlth.* 2013; 60:336–340.

Chassovnikarova T, Atanassov N, Christova I, Dimitrov H, Mitkovska V, Trifonova I, et al. Hantavirus Infections in Host Populations of Yellow-Necked and Field Mice (Rodentia: Muridae) in South Bulgaria. *Acta zool bulg.* 2013; 65:397-402.

Christova I, Plyusnina A, Gladnishka T, Kalvatchev N, Trifonova I, Dimitrov H, et al. Detection of Dobrava Hantavirus RNA in *Apodemus* mice in Bulgaria. *J Med Virol.* 2015; 87:263-8.

Chumakov M, Shindarov L, Gavrilovskaya I, Vasilenko S, Gorbachkova E, Katzarov G. Seroepidemiology of haemorrhagic fever with renal syn-drome in Bulgaria. *Acta Virol.* 1988; 32(3):261-266.

Clement J, McKenna P, Avsic-Zupanc T, Skinner CR. Rat-transmitted han-tavirus disease in Sarajevo. *Lancet* 1994; 344:(8915):131.

Clement J, Vercauteren J, Verstraeten WW, Ducoffre G, Barrios JM, Vandamme AM, Maes P, Van Ranst M. Relating increasing hantavirus incidences to the changing climate: the mast connection. *Int J Health Geogr.* 2009; 16;8:1.

Chare ER, Gould EA, Holmes EC. Phylogenetic analysis reveals a low rate of homologous recombination in negative-sense RNA viruses. *J Gen Virol.* 2003; 84:2691-2703.

Childs JE, Ksiazek TG, Spiropoulou CF, Krebs JW, Morzunov S, Maupin GO, Gage KL, Rollin PE, Sarisky J, Enscoe RE, Frey JK, Peters CJ, Nichol ST. Serologic and genetic identification of *peromyscus maniculatus* as the primary rodent reservoir for a new hantavirus in the southwestern united states. *J Infect Dis.* 1994; 169:1271-1280.

Childs JE, Glass GE, Korch GW, LeDuc JW. Effects of hantaviral infection on survival, growth and fertility in wild rat (*Rattus norvegicus*) populations of Baltimore, Maryland. *J Wildl Dis.* 1989; 25:469e76.

Chomczynski, P. and Sacchi, N. Single-step method of RNA isolation by acid guanidinium thiocyanate-phenol-chloroform extraction. *Anal Biochem.* 1987; 162:156-159.

Chu YK, Owen RD, Jonsson CB. Phylogenetic exploration of hantaviruses in Paraguay reveals reassortment and host switching in South America. *Virology*. 2011; 12;8:399.

Copper PD, Steiner-Pryor A, Scotti PD, DeLong D. On the nature of poliovirus genetic recombinants. *J Gen Virol*. 1974; 23:41-49.

Dearing MD, Disney L. Ecology of hantavirus in a changing world. *Ann N Y Acad Sci*. 2010; 1195:99-112.

Deter J, Chaval Y, Galan M, Gauffre B, Morand S, Henttonen H, Laakkonen J, Voutilainen L, Charbonnel N, Cosson JF. Kinship, dispersal and hantavirus transmission in bank and common voles. *Arch Virol*. 2008; 153:435–444.

Diglisic G, Xiao SY, Gligic A, Obradovic M, Stojanovic R, Velimirovic D, et al. Isolation of a Puumala-like virus from *Mus musculus* captured in Yugoslavia and its association with severe hemorrhagic fever with renal syndrome. *J Infect Dis*. 1994; 169:204–207.

Douglass RJ, Calisher CH, Wagoner KD, Mills JN. Sin Nombre virus infection of deer mice in Montana: characteristics of newly infected mice, incidence, and temporal pattern of infection. *J Wildlife Dis*. 2007; 43:12e22.

Douron E, Moriniere B, Matheron S, Girard PM, Gonzalez JP, Hirsch F, et al. HFRS after a wild rodent bite in the Haute-Savoie and risk of exposure to Hantaan-like virus in a Paris laboratory. *Lancet*. 1984; 1:676e7.

Drake JW. 1999. The distribution of rates of spontaneous mutation over viruses, prokaryotes, and eukaryotes. *Ann N Y Acad Sci*. 870:100–107.

Drummond, AJ, Rambaut, A. BEAST: Bayesian evolutionary analysis by sampling trees. *BMC Evol Biol*. 2007; 7:214.

Duffy S, Shackelton L A , Holmes EC. Rates of evolutionary change in viruses: patterns and determinants. *Nat Rev Genet.* 2008; 9:267–276.

Eboriadou M, Kalevrosoglou I, Varlamis G, Mitsiakos G, Papa A, Antoniadis A, et al. Hantavirus nephropathy in a child. *Nephrol Dial Transplant.* 1999; 14:1040–1041.

Elliott RM, Bouloy M, Calisher C H, Goldbach R, Moyer J T, Nichol S T, et al. Bunyaviridae. In *Virus Taxonomy: The Classification and Nomenclature of Viruses. The Seventh Report of the International Committee on Taxonomy of Viruses.* edn, Edited by M. H. V. Van Regenmortel, C. M. Fauquet, D. H. L. Bishop, E. B. Carsten, M. K. Estes, S. M. Lemon, J. Maniloff, M. A. Mayo, D. J. McGeoch, C. R. Pringle & R. B. Wickner. 2000; San Diego: Academic Press.

Eltari, E, Nuti, M, Hasko, I, Gina, A. Haemorrhagic fever with renal syndrome in a case in northern Albania. *Lancet.* 1987; 2:1211.

Faria NR, Suchard MA, Rambaut A, Lemey P. Toward a quantitative understanding of viral phylogeography. *Curr Opin Virol.* 2011; 1(5):423-9.

Ferres M, Vial P, Marco C, Yanez L, Godoy P, Castillo C, et al. Prospective evaluation of household contacts of persons with hantavirus cardiopulmonary syndrome in Chile. *J Infect Dis* 2007; 195:1563–71.

Flint SJ, Enquist LW, Racaniello VR, Skalka AM *Principles of Virology*, Washington, DC, ASM Press. 2009.

Gavrilovskaya IN, Shepley M, Shaw R, Ginsberg MH, Mackow, ER. beta3 Integrins mediate the cellular entry of Hantaviruses that cause respiratory failure. *Proc Natl Acad Sci USA.* 1998; 95:7074–7079.

Gavrilovskaya IN, Brown E J, Ginsberg M Mackow, ER. Cellular entry of hantaviruses which cause hemorrhagic fever with renal syndrome is mediated by beta3 integrins. *J Virol.* 1999; 73:3951-9.

Gledovic ZB, Jeknic AS, Grgurevic AD, Rakocevic BB, Bozovic BR, Mugosa BV. Hemorrhagic fever with renal syndrome in Montenegro. *Jpn J Infect Dis.* 2008; 61(5):386–387.

Gligic A, Obradovic M, Stojanovic R, Hlaca D, Antonijevic B, Arnautovic A, et al. Hemorrhagic fever with renal syndrome in Yugoslavia: detection of hantaviral antigen and antibody in wild rodents and serological diagnosis of human disease. *Scand J Infect Dis.* 1988; 20:261–266.

Gligic A, M Frusic, M Obradovic R. Stojanovic D. Hlaca, CJ Jr Gibbs, et al. Hemorrhagic fever with renal syndrome in Yugoslavia: antigenic characterization of hantaviruses isolated from *Apodemus flavicollis* and *Clethrionomys glareolus*. *Am J Trop Med Hyg.* 1989b; 41:109–115.

Gligic A, Obradovic M, Stojanovic S, Ujosevic N, Ovccaric A, Frusic M, et al. Epidemic hemorrhagic fever with renal syndrome in Yugoslavia, 1986a. *Am J Trop Med Hyg.* 1989; 41:102-108.

Gligic A, Dimkovic N, Xiao SY, Buckle GJ, Jovanovic D, Velimirovic D, et al. Belgrade virus: a new hantavirus causing severe hemorrhagic fever with renal syndrome in Yugoslavia. *J Infect Dis.* 1992; 166:113–120.

Gligic, A. 2008: Etiology of hemorrhagic fever with renal syndrome, viruses and their reservoirs. In: Kovacevic, Z., D. Jovanovic, A. Gligic, and V. Skataric, (eds), Hemorrhagic Fever with Renal Syndrome. pp. 17–34. Medicinski fakultet, Kragujevac.

Gligic A, Stojanovic R, Obradovic M, Hlaca D, Dimkovic N, Diglisic G, et al. Hemorrhagic fever with renal syndrome in Yugoslavia: epidemiologic and epizootologic features of a nationwide outbreak in 1989. *Eur J Epidemiol.* 1992b; 8(6):816–825.

Gonzalez JP, McCormick JB, Baudon D, Gautun JP, Meunier DY, Dournon E, Georges AJ. Serological evidence for Hantaan-related virus in Africa. *Lancet.* 1984; 3:1036-1037.

Guardado-Calvo P, Rey FA. The Envelope Proteins of the Bunyavirales. *Adv Virus Res.* 2017; 98:83-118.

Guindon S, Dufayard JF, Lefort V, Anisimova M, Hordijk W, Gascuel O. "New Algorithms and Methods to Estimate Maximum-Likelihood Phylogenies: Assessing the Performance of PhyML 3.0." *Systematic Biology.* 2010; 59(3):307-321.

Guo WP, Lin XD, Wang W, Tian JH, Cong ML, Zhang HL, et al. Phylogeny and origins of hantaviruses harbored by bats, insectivores, and rodents. *PLoS Pathog.* 2013; 9(2):e1003159.

Han GZ, Worobey, M. Homologous recombination in negative sense RNA viruses. *Viruses.* 2011; 3:1358–1373.

Hardestam J, Simon M, Hedlund KO, Vaheri A, Klingström J, Lundkvist A. Ex vivo stability of the rodent-borne Hantaan virus in comparison to that of arthropod-borne members of the Bunyaviridae family. *Appl Environ Microbiol.* 2007; 73:2547–2551.

Hardestam J, Karlsson M, Falk KI, Olsson G, Klingstrom J, Lundkvist A. Puumala hantavirus excretion kinetics in bank voles (*Myodes glareolus*). *Emerg Infect Dis.* 2008; 14:1209-1215.

Heckel G, Burri R, Fink S, Desmet JF, Excoffier L. Genetic structure and colonization processes in European populations of the common vole, *Microtus arvalis*. *Evolution.* 2005; 59:2231–2242.

Heneberg D, Morelj M, Heneberg N, Mikes M, Dordevic Z. Hemorrhagic fever in Yugoslavia and detection of its natural foci. *Hig Cas Hig Mikrobiol Epidemiol Sanit Teh.* 1964; 16:28–37.

Heyman P, Klingstrom J, De Jaegere, F, Leclercq G, Rozenfeld F, Escutenaire S, et al. Tula hantavirus in Belgium. *Epidemiol Infect.* 2002; 128:251-256.

Heyman P, Vaheri A, Lundkvist A, Avsic-Zupanc T. Hantavirus infections in Europe: from virus carriers to a major public-health problem. *Exp Rev Antiinfect Ther* 2009; 7:205e17.

Heyman P, Vaheri, A. Situation of hantavirus infections and haemorrhagic fever with renal syndrome in European countries as of December 2006. *EuroSurveill.* 2008; 13:28.

Heyman P, Ceianu CS, Christova I, Tordo N, Beersma M, Joao Alves, et al. A five-year perspective on the situation of haemorrhagic fever with renal syndrome and status of the hantavirus reservoirs in Europe, 2005–2010. *Euro Surveill.* 2011; 16:36.

Hjelle B, Yates T. Modeling hantavirus maintenance and transmission in rodent communities. *Curr Topics Microbiol Immunol* 2001; 256:77e90.

Hofmann J, Meier M, Enders M, Führer A, Ettinger J, Klempa B, et al. Hantavirus disease in Germany due to infection with Dobrava-Belgrade virus genotype Kurkino. *Clin Microbiol Infect.* 2014; 20(10):O648-55.

Holmes EC. Evolutionary history and phylogeography of human viruses. *Annu Rev Microbiol.* 2008; 62:307-328.

Hughes AL, Friedman R. Evolutionary diversification of protein coding genes of hantaviruses. *Mol Biol Evol.* 2000; 17:1558–1568.

Huiskonen JT, Hepojoki J, Laurinmaki P, Vaheri A, Lankinen H, Butcher SJ, et al. Electron cryotomography of Tula Hantavirus suggests a unique assembly paradigm for enveloped viruses. *J Virol.* 2010; 84, 4889–4897.

Hukic M, Valjevac A, Tulumovic D, Numanovic F, Heyman P. Pathogenicity and virulence of the present hantaviruses in Bosnia and Herzegovina: the impact on renal function. *Eur J Clin Microbiol Infect Dis.* 2011; 30(3): 381–385.

Hukic M, Nikolic J, Valjevac A, Seremet M, Tesic G, Markotic A. A sero-survey reveals Bosnia and Herzegovina as a Europe's hotspot in hantavirus seroprevalence. *Epidemiol Infect.* 2010; 138(8):1185–1193.

Jonsson CB, Figueiredo LT, Vapalahti O. A global perspective on hantavirus ecology, epidemiology, and disease. *Clin Microbiol Rev.* 2010; 23: 412-441.

Kallio ER, Klingstrom J, Gustafsson E, Manni T, Vaheri A, Henttonen H, et al. Prolonged survival of Puumala hantavirus outside the host: evidence for indirect transmission via the environment. *J Gen Virol.* 2006 ;87:2127e34.

Kang HJ, Arai S, Hope AG, Song JW, Cook JA, Yanagihara R. Genetic diversity and phylogeography of Seewis virus in the Eurasian common shrew in Finland and Hungary. *Virology.* 2009; 6:208.

Kang HJ, Arai S, Hope AG, Cook JA, Yanagihara R. Novel hantavirus in the flat-skulled shrew (*Sorex roboratus*). *Vector Borne Zoonotic Dis.* 2010; 10(6):593-597.

Kaukinen P, Vaheri a, Plyusnin A. Hantavirus nucleocapsid protein: a multifunctional molecule with both housekeeping and ambassadorial duties. *Arch Virol.* 2005; 150:1693–1713.

Kim JA, Kim WK, No JS, Lee SH, Lee SY, Kim JH, et al. Genetic Diversity and Reassortment of Hantaan Virus Tripartite RNA Genomes in Nature, the Republic of Korea. *PLoS Negl Trop Dis*. 2016; 10(6):e0004650.

Klempa B, Fichet-Calvet E, Lecompte E, Auste B, Aniskin V, Meisel H, et al. Novel hantavirus sequences in shrew, Guinea. *Emerg Infect Dis*. 2007; 13:520e2.

Klempa B, Avsic-Zupanc T, Clement J, Dzagyurova TK, Henttonen H, Heyman P, et al. Complex evolution and epidemiology of Dobrava-Belgrade hantavirus: definition of genotypes and their characteristics. *Arch Virol*. 2013;158:521–529.

Klempa B, Fichet-Calvet E, Lecompte E, Auste B, Aniskin V, Meisel H, et al. Hantavirus in African wood mouse, Guinea *Emerg Infect Dis*. 2006; 12:838-840.

Klempa B, Schmidt HA, Ulrich R, Kaluz S, Labuda M, Meisel H, Hjelle B, Krüger DH. Genetic interaction between distinct Dobrava hantavirus subtypes in *Apodemus agrarius* and *A. flavicollis* in nature. *J Virol*. 2003; 77(1):804-809.

Klempa B. Hantaviruses and climate change. *Clin Microbiol Infect*. 2009; 15(6):518-523.

Klempa B, Koivogui L, Sylla O, Koulemou K, Auste B, Kruger DH, et al. Serological evidence of human hantavirus infections in Guinea, West Africa. *J Infect Dis*. 2010; 201:1031–1034.

Klingstrom J, Heyman P, Escutenaire S, Sjölander KB, De Jaegere F, Henttonen H, et al. Rodent host specificity of European hantaviruses: evidence of Puumala virus interspecific spillover. *J Med Virol*. 2002; 68:581e8.

Korber B, Myers G. Signature pattern analysis: a method for assessing viral sequence relatedness. *AIDS Res Hum Retroviruses*. 1992; 8:1549–1560.

Koren N, Grilc E, Blasko M, Avsic T, Kraigher A. An increase in reported cases of haemorrhagic fever with renal syndrome in Slovenia in early 2008. *EuroSurveill.* 2008; 13:(17).

Kraigher A, Frelj T, Korva M, Avsic T. Increased number of cases of haemorrhagic fever with renal syndrome in Slovenia, January to April 2012. *EuroSurveill.* 2012; 17:(21).

Kruger DH, Figueiredo LT, Song JW, Klempa B. Hantaviruses--globally emerging pathogens. *J Clin Virol.* 2015; 64:128-136.

Krystufek B. *Glis glis* (Rodentia: *Gliridae*). *Mammalian species.* 2010; 42(865):195–206.

Kuenzi AJ, Douglass RJ, Bond CW, Calisher CH, Mills JN. Long-term dynamics of Sin Nombre viral RNA and antibody in deer mice in Montana. *J Wildl Dis.* 2005; 41:473-81.

Kuismanen E, Hedman K, Saraste J, Pettersson RF. Uukuniemi virus maturation: accumulation of virus particles and viral antigens in the Golgi complex. *Mol Cell Biol.* 1982; 2:1444–1458.

Kukkonen SK, Vaheri A, Plyusnin A. L protein, the RNA-dependent RNA polymerase of hantaviruses. *Arch Virol.* 2005; 150(3):533-556.

Kuzman I, Markotic A, Turcinov D, Beus I. An epidemic of hemorrhagic fever with renal syndrome in Croatia in 1995. *Lijec Vjesn.* 1997; 119(11–12):311–315.

Lahdevirta J. Nephropathia epidemica in Finland. A clinical histological and epidemiological study. *Ann Clin Res.* 1971; 3:1-54.

Lee HW, Antoniadis A. Serological evidence for Korean haemorrhagic fever in Greece. *Lancet.* 1981; 1(8224):832.

Lednicky JA. Hantaviruses. a short review. Arch Pathol Lab Med [Internet]. 2003; 127(1):30–5.

Lemey P, Rambaut A, Drummond AJ, Suchard MA. Bayesian phylogeography finds its roots. PLoS Comput Biol. 2009; 5(9):e1000520.

Lemey P, Rambaut A, Welch JJ, Suchard MA. Phylogeography takes a relaxed random walk in continuous space and time. Mol Biol Evol. 2010; 27(8):1877-1885.

Linard C, Tersago K, Leirs H, Lambin EF. Environmental conditions and Puumala virus transmission in Belgium. Int J Health Geogr. 2007; 6: 55

Lole KS, Bollinger RC, Paranjape RS, Gadkari D, Kulkarni SS, Novak NG, Ingersoll R, Sheppard HW, Ray SC. Full-length human immunodeficiency virus type 1 genomes from subtype C-infected seroconverters in India, with evidence of intersubtype recombination. J Virol. 1999; 73(1):152-160.

Lozach PY, Mancini R, Bitto D, Meier R, Oestereich L, Overby AK, Pettersson RF, Helenius A. Entry of bunyaviruses into mammalian cells. Cell Host Microbe. 2010; 7:488–499.

Lukac V, Obradovic M, Gligic A, Stojanovic R, Rakovic-Savcic L. Hemoragicna groznica sa bubreznim sindromom u SFRJ u periodu od 1951. do 1988. Vojnosanit Pregl. 1990; 47:242–248.

Lundkvist A, Hukic M, Hörling J, Gilljam M, Nichol S, Niklasson B. Puumala and Dobrava viruses cause hemorrhagic fever with renal syndrome in Bosnia-Herzegovina:

evidence of highly cross-neutralizing antibody responses in early patient sera. J Med Virol. 1997; 53(1):51-59.

Maes P, Klempa B, Clement J, Matthijssens J, Gajdusek DC, Krüger DH, et al. A proposal for new criteria for the classification of hantaviruses, based on S and M segment protein sequences. *Infect Genet Evol.* 2009; 9:813–820.

Maftei ID, Segall L, Panculescu-Gatej R, Ceianu C, Covic, A. Hantavirusinfection – hemorrhagic fever with renal syndrome: the first case series reported in Romania and review of the literature. *Int Urol Nephrol.* 2012; 44 (4):1185–1191.

Manasia M, Olinic N, Zagreanu I, Serban A. Hemorrhagic fever with renal syndrome: report of 11 observations. *Int Urol Nephrol.* 1977; 9 (2):177–184.

Manigold T, Vial P. Human hantavirus infections: epidemiology, clinical features, pathogenesis and immunology. *Swiss Med Wkly.* 2014; 20:144:w13937.

Markotic A, LeDuc JW, Hlaca D, Rabatic S, Sarcevic A, Dasic G, et al. Hantaviruses are likely threat to NATO forces in Bosnia and Herzegovina and Croatia. *Nat Med.* 1996; 2(3):269–270.

Maroli M, Vadell MV, Iglesias A, Padula PJ, Gómez Villafañe IE. Daily Movements and Microhabitat Selection of Hantavirus Reservoirs and Other Sigmodontinae Rodent Species that Inhabit a Protected Natural Area of Argentina. *Ecohealth.* 2015; 12(3):421-431.

Marteau M, Sara, M. Habitat preferences of edible dormouse, *Glis glis italicus*: implications for the management of arboreal mammals in Mediterranean forests. *Folia Zool.* 2015; 64(2):136–150.

Martin DP, Murrell B, Golden M, Khoosal A, Muhire B. RDP4: Detection and analysis of recombination patterns in virus genomes. *Virus Evolution.* 2015; 26;1(1):vev003.

Milazzo ML, Cajimat MN, Romo HE, Estrada-Franco JG, Iñiguez-Dávalos LI, Bradley RD, Fulhorst CF. Geographic distribution of hantaviruses associated with neotomine and sigmodontine rodents, Mexico. *Emerg Infect Dis.* 2012; 18(4):571-576

Mills JN. Regulation of rodent-borne viruses in the natural host: implications for human disease. *Arch Virol Suppl.* 2005; 45–57.

Minskaya ES. *Studies on the Hantavirus S Segment Gene Products.* 2003.

Mir MA, Duran WA, Hjelle BL, Ye C, Panganiban AT. Storage of cellular 5' mRNA caps in P bodies for viral cap-snatching. *Proc Natl Acad Sci U S A.* 2008; 105:19294-19299.

Musser GG, Carleton MD. Family Muridae. In: Wilson D.E. & Reeder D.M. (eds.) *Mammal Species of the World*, 2nd ed. Smithsonian Institution Press, Washington and London: 1993; 501–755.

Muyangwa M, Martynova EV, Khaiboullina SF, Morzunov SP, Rizvanov AA. Hantaviral Proteins: Structure, Functions, and Role in Hantavirus Infection. *Front Microbiol.* 2015; 27(6):1326.

Myhrman, G. Nephropathia epidemica a new infectious disease in northern Scandinavia. *Acta Med Scand.* 1956; 140(1), 52-6.

Nemeth V, Madai M, Maraczi A, Berczi B, Horvath G, Oldal M. Detection of Dobrava-Belgrade hantavirus using recombinant-nucleocapsid-based enzyme-linked immunosorbent assay and SYBR Green-based real-time reverse transcriptase-polymerase chain reaction. *Arch Virol.* 2011; 156:1655–1660.

Nemirov K, Vapalahti O, Papa A, Plyusnina A, Lundkvist A, Antoniadis A, et al. Genetic characterization of new Dobrava hantavirus isolate from Greece. *J Med Virol.* 2003; 69:408–416.

Nichol ST. Bunyaviruses. In: Knipe DM, Howley PM, eds. *Field's Virology* Vol 2, 4th ed Philadelphia, Pa Lippincott Williams Wilkins. 2001. p.1603–33.

Nuovo GJ, Simsir A, Steigfigel RT, Kuschner M. Analysis of fatal pulmonary hantaviral infection in New York by reverse transcriptase in situ polymerase chain reaction. *Am J Pathol.* 1996;148:685-92.

Nystrom K. Isolation and propagation of nephropathia epidemica virus in bank voles. *Scand J Infect Dis.* 1984; 16:225-228.

Papa A, Bino S, Papadimitriou E, Velo E, Dhimolea M, Antoniadis A. Suspected Crimean Congo haemorrhagic fever cases in Albania. *Scand J Infect Dis.* 2008; 40(11–12):978–980.

Papa A. Dobrava-Belgrade virus: Phylogeny, epidemiology, disease. *Antiviral Res.* 2012; 95:104-117.

Papa A, Christova I. Genetic detection of dobrava/belgrade virus, Bulgaria. *Emerg Infect Dis.* 2011;17(2):308–309.

Papa A, Bojovic B, Antoniadis A. Hantaviruses in Serbia and Montenegro. *Emerg Infect Dis.* 2012; 12:1015–1018.

Papa A, Antoniadis A. Hantavirus infections in Greece – an update. *Eur J Epidemiol* 2001; 17(2):189–194.

Papa A, Rogozi E, Velo E, Papadimitriou E, Bino S. Genetic detection of hantaviruses in rodents, Albania. *J Med Virol.* 2016; 88(8):1309-1313.

Parker J, Rambaut A, Pybus OG. Correlating viral phenotypes with phylogeny: accounting for phylogenetic uncertainty. *Infect Genet Evol.* 2008; 8(3):239-246.

Peco-Antic A, Popovic-Rolovic M, Popovic D, Gligic A, Jovanovic O. Hemorrhagic fever with renal syndrome in children. *Srp Arh Celok Lek.* 1991; 119(1-2):58-61.

Plyusnin A, Vapalahti O, Vaheri A. Hantaviruses: genome structure, expression and evolution. *J Gen Virol.* 1996; 77:2677–2687.

Plyusnin A, Kukkonen SKJ, Plyusnina A, Vapalahti O, Vaheri A. Transfection-mediated generation of functionally competent Tula hantavirus with recombinant S RNA segment. *EMBO J.* 2002; 21:1497–1503.

Plyusnin A, Vapalahti O, Lankinen H, Lehvaslaiho H, Apekina N, Myasnikov Y, et al. Tula virus: a newly detected hantavirus carried by European common voles. *J Virol.* 1994; 68:7833-7839.

Plyusnin A, Cheng Y, Vapalahti O, Pejcoch M, Unar J, Jelinkova Z, et al. Genetic variation in Tula hantaviruses: sequence analysis of the S and M segments of strains from Central Europe. *Virus Res.* 1995; 39:237-250.

Plyusnina A, Ferenczi E, Rácz GR, Nemirov K, Lundkvist A, Vaheri A, Vapalahti O et al. Co-circulation of three pathogenic hantaviruses: Puumala, Dobrava, and Saaremaa in Hungary. *J Med Virol* 2009; 81:2045–2052.

Poch O, Sauvaget I, Delarue M, Tordo N. Identification of four conserved motifs among the RNA-dependent polymerase encoding elements. *EMBO J.* 1989; 8:3867–3874.

Polat C, Sironen T, Plyusnina A, Karatas A, Sozen M, Matur F, et al. Dobrava hantavirus variants found in *Apodemus flavicollis* mice in Kirklareli Province, Turkey. *J Med Virol.* 2018; doi: 10.1002/jmv.25036. [Epub ahead of print].

Polenakovic M, Grcevska L, Gerasimovska-Tanevska V, Oncevski A, Dzikova S, Cakalaroski K, et al. Hantaan virus infection with acute renal failure. *Artif Organs.* 1995; 19(8):808–813.

Pond SL, Frost SD. Datamonkey: rapid detection of selective pressure on individual sites of codon alignments. *Bioinformatics*, 2005; 21:2531–2533.

Posada D. JModelTest: phylogenetic model averaging. *Mol Biol Evol*. 2008; 25:1253–1256.

Powel GM. Clinical manifestations of epidemic fever. *J Amer Med Ass*. 1953; 1261-1264.

Pringle CR. The Bunyaviridae and their genetics-an overview. In D. Kolakofsky (Ed.), *Bunyviridae* (pp. 1-25.). Berlin: Springer-Verlag. *Curr Top Microbiol Immunol*. 1991;169:1-25.

Radosevic Z, Mohacek I. The problem of nephropathia epidemica Myhrman–Zetterholm in relation to acute interstitial nephritis. *Acta Med Scand*. 1954; 149(3):221–228.

Rambaut A, Lam TT, Max Carvalho L, Pybus OG. Exploring the temporal structure of heterochronous sequences using TempEst (formerly Path-O-Gen). *Virus Evol*. 2016; 9;2(1):vew007.

Ramsden C, Holmes EC, Charleston MA. Hantavirus evolution in relation to its rodent and insectivore hosts: no evidence for codivergence. *Mol Biol Evol*. 2009; 26(1):143-53.

Ramsden C, Melo FL, Figueiredo LM, Holmes EC, Zanotto PM; VGDN Consortium. High rates of molecular evolution in hantaviruses. *Mol Biol Evol*. 2008; 25(7):1488-92.

Reynes JM, Carli D, Boukezia N, Debruyne M, Herti S. Tula hantavirus infection in a hospitalised patient, France, June 2015. *Euro Surveill*. 2015; 20(50).

Ronquist F, Huelsenbeck JP. MrBayes 3: Bayesian phylogenetic inference under mixed models. *Bioinformatics*. 2003; 19(12):1572-1574.

Ryou J, Lee HI, Yoo YJ, Noh YT, Yun SM, Kim SY, et al. Prevalence of hantavirus infection in wild rodents from five provinces in Korea, 2007. *Wildl Dis.* 2011; 47(2):427-432.

Salanueva IJ, Novoa RR, Cabezas P, Lopez-Iglesias C, Carrascosa JL, Elliott RM, Risco C. Polymorphism and structural maturation of bunyamwera virus in Golgi and post-Golgi compartments. *J Virol.* 2003; 77:1368–1381.

Sambrook J, Fritsch EF, Maniatis T. *Molecular Cloning. A laboratory Manual*, 2nd Edition, Cold Spring Harbor Laboratory Press. 1989.

Saxenhofer M, Weber de Melo V, Ulrich RG, Heckel G. Revised time scales of RNA virus evolution based on spatial information. *Proc Biol Sci.* 2017; 16:284(1860). pii: 20170857.

Scharninghausen JJ, Meyer H, Pfeffer M, Davis DS, Honeycutt RL. Genetic evidence of Dobrava virus in *Apodemus agrarius* in Hungary. *Emerg Infect Dis.* 1999; 5:468-470.

Schilling S, Emmerich P, Klempa B, Auste B, Schnaith E, Schmitz H, et al. Hantavirus disease outbreak in Germany: limitations of routine serological diagnostics and clustering of virus sequences of human and rodent origin. *J Clin Microbiol.* 2007; 45:3008–3014.

Schlegel M, Kindler E, Essbauer SS, Wolf R, Thiel J, Groschup MH, et al. Tula virus infections in the Eurasian water vole in Central Europe. *Vector Borne Zoonotic Dis.* 2012; 12:503-513.

Schlegel M, Radosa L, Rosenfeld UM, Schmidt S, Triebenbacher C, Löhr PW, et al. Broad geographical distribution and high genetic diversity of shrewborne Seewis hantavirus in Central Europe. *Virus Genes.* 2012; 45:48e55.

Schlegel M, Klempa B, Auste B, Bemann M, Schmidt-Chanasit J, Büchner T, et al. Dobrava-Belgrade virus spillover infections, Germany. *Emerg Infect Dis.* 2009; 15: 2017-2020.

Schmaljohn CS, Hasty SE, Dalrymple JM, LeDuc JW, Lee HW, von Bonsdorff CH, et al. Antigenic and genetic properties of viruses linked to hemorrhagic fever with renal syndrome. *Science*. 1987; 227:1041-1044.

Schmidt-Chanasit J, Essbauer S, Petraityte R, Yoshimatsu K, Tackmann K, Conraths, FJ, et al. Extensive host sharing of central European Tula virus. *J Virol*. 2010; 84:459–474.

Schonrich G, Rang A, Lutteke N, Raftery MJ, Charbonnel N, Ulrich RG. Hantavirus-induced immunity in rodent reservoirs and humans. *Immunol Rev*. 2008; 225:63–189.

Schweizer M, Excoffier L, Heckel G. Fine-scale genetic structure and dispersal in the common vole (*Microtus arvalis*). *Mol Ecol*. 2007; 16:2463-2473.

Sibold C, Ulrich R, Labuda M, Lundkvist A, Martens H, Schütt M, et al. Dobrava hantavirus causes hemorrhagic fever with renal syndrome in central Europe and is carried by two different *Apodemus* mice species. *J Med Vir*. 2001; 63: 158–167.

Sibold C, Sparr S, Schulz A, Labuda M, Kozuch O, Lysy J, et al. Genetic characterization of a new hantavirus detected in *Microtus arvalis* from Slovakia. *Virus Genes*. 1995; 10:277-281.

Sibold C, Meisel H, Krüger DH, Labuda M, Lysy J, Kozuch O, et al. Recombination in Tula hantavirus evolution: analysis of genetic lineages from Slovakia. *J Virol*. 1999; 73: 667-675.

Simic M. Successful application of peritoneal dialysis in a case of renal insufficiency. *Vojnosanit Pregl*. 1952; 9(9–10):285–290.

Simon M, Johansson C, Lundkvist A, Mirazimi A. Microtubule-dependent and microtubule-independent steps in Crimean-Congo hemorrhagic fever virus replication cycle. *Virology*. 2009; 385:313–322.

Simon-Loriere E, Holmes EC. Why do RNA viruses recombine? *Nat Rev Microbiol*. 2011; 9:617–626.

Sironen T, Vaheri A, Plyusnin A. Molecular evolution of Puumala hantavirus. *J Virol.* 2001; 75:11803–11810.

Smadel JE. Epidemic Hemorrhagic Fever. *Am J Public Health Nations Health.* 1953; 43:1327-1330.

Song JW, Gligic A, Yanagihara R. Identification of Tula hantavirus in *Pitymys subterraneus* captured in the Cacak region of Serbia-Yugoslavia. *Int J Infect Dis.* 2002; 6:31-36.

Song JW, Baek LJ, Schmaljohn CS, Yanagihara R. Thottapalayam virus, a prototype shrewborne hantavirus. *Emerg Infect Dis.* 2007; 13:980–985.

Souza WM, Bello G, Amarilla AA, Alfonso HL, Aquino VH, Figueiredo LT. Phylogeography and evolutionary history of rodent-borne hantaviruses *Infect Genet Evol.* 2014;21:198-204.

Strimmer K, von Haeseler A. Likelihood-mapping: A simple method to visualize phylogenetic content of a sequence alignment. *Proc Natl Acad Sci USA.* 1997; 94:6815-6819.

Sumibcay L, Kadjo B, Gu SH, Kang HJ, Lim BK, Cook JA, et al. Divergent lineage of a novel hantavirus in the banana pipistrelle (*Neoromicia nanus*) in Côte d'Ivoire. *Virol J.* 2012; 9:e34.

Swofford DL (2003) PAUP*: phylogenetic analysis using parsimony (*and other methods), version 4 beta. Sinauer Associates, Sunderland, MA.

Taller A, Xiao S, Godec M, Gligic A, Avsic-Zupanc T, Goldfarb LG, et al. Belgrade virus, a cause of hemorrhagic fever with renal syndrome in the Balkans, is closely related to Dobrava virus of field mice. *J Infect Dis.* 1993; 168:750–753.

Tamura K, Peterson D, Peterson N, Stecher G, Nei M, Kumar S. MEGA5: molecular evolutionary genetics analysis using maximum likelihood, evolutionary distance, and maximum parsimony methods. *Mol Biol Evol.* 2011; 28(10):2731-2739.

Torres-Pérez F, Palma RE, Hjelle B, Holmes EC, Cook JA. Spatial but not temporal co-divergence of a virus and its mammalian host. *Mol Ecol.* 2011; 20(19):4109-22.

Traub R, Wisseman C L. Korean hemorrhagic fever. *J Infect Dis.* 1978; 138:267-272.

Vaheri A, Strandin T, Hepojoki J, Sironen T, Henttonen H, Mäkelä S, et al. Uncovering the mysteries of hantavirus infections. *Nat Rev Microbiol.* 2013; 11(8):539–50.

Vaheri A, Strandin T, Hepojoki J, Sironen T, Henttonen H, Makela S, et al. Uncovering the mysteries of hantavirus infections. *Nat Rev Microbiol.* 2013; 11:539–550.

Vapalahti, O., Mustonen, J., Lundkvist, A., Henttonen, H., Plyusnin, A., Vaheri, A., 2003. Hantavirus infections in Europe. *Lancet Infect. Dis.* 3, 653-661.

Vapalahti O, Kallio-Kokko H, Narvanen A, Julkunen I, Lundkvist A, Plyusnin A, et al. Human B-cell epitopes of Puumala virus nucleocapsid protein, the major antigen in early serological response. *J Med Virol.* 1995; 46:293–303.

Verbev P, Gabev E. Haemorrhagic nephroso-nephritis in Bulgaria. *J. Hyg.Epidemiol. Microbiol. Immunol.* 1963; 7:136–144.

Verner-Carlsson J, Löhmus M, Sundström K, Strand TM, Verkerk M, Reusken C, et al. First evidence of Seoul hantavirus in the wild rat population in the Netherlands. *Infect Ecol Epidemiol.* 2015; 6:5:27215.

Vesenjak-Hirjan J, Hrabar A, Vince-Ribaric V, Borcic B, Brudnjak Z. An outbreak of hemorrhagic fever with a renal syndrome in the Plitvice Lakes area (preliminary report). *Folia Parasitol.* 1971; 18(3):275–279.

Virus Taxonomy, ICTV (10th) report.

(https://talk.ictvonline.org/ictvreports/ictv_online_report/)

Vukicevic-Radic O, Matić R, Kataranovski D, Stamenković S. Spatial organization and home range of *apodemus flavicollis* and *a. agrarius* on Mountain Avala, Serbia. *Acta Zoologica Academiae Scientiarum Hungaricae.* 2006; 52:81–96.

Watson DC, Sargianou M, Papa A, Chra P, Starakis I, Panos G. Epidemiology of Hantavirus infections in humans: a comprehensive, global overview. *Crit Rev Microbiol.* 2014; 40(3):261-272.

Weiss S, Witkowski PT, Auste B, Nowak K, Weber N et al. Hantavirus in bat, Sierra Leone. *Emerg Infect Dis.* 2012; 18:159–161.

Wells RM, Sosa Estani S, Yadon ZE, Enria D, Padula P, Pini N, et al. An unusual hantavirus outbreak in southern Argentina: person-to-person transmission. *Emerg Infect Dis.* 1997;3:171–174.

Wilson DE, Reeder DM. *Mammal species of the world: A taxonomic and geographic reference*, third ed. Baltimore: John Hopkins University Press. 2005.

Witkowski PT, Klempa B, Ithete NL, Auste B, Mfunze JK, Hoveka J, et al. Hantaviruses in Africa. *Virus Res.* 2014;187:34–42.

Wójcik-Fatla A, Zając V, Knap JP, Sroka J, Cisak E, Sawczyn A, et al. A small-scale survey of hantavirus in mammals from eastern Poland. *Ann Agric Environ Med.* 2013; 20:283-6.

Worobey M, Holmes EC. Evolutionary aspects of recombination in RNA viruses. *J Gen Virol.* 1999; 80:2535–2543.

Worobey M, Telfer P, Souquiere S, Hunter M, Coleman CA, Metzger MJ, et al. Island biogeography reveals the deep history of SIV. *Science.* 2010; 329:1487.

Yanagihara R, Gu SH, Arai S, Kang HJ, Song JW. Hantaviruses: rediscovery and new beginnings. *Virus Res.* 2014; 187:6-14

Yanagihara R, Svedmyr A, Amyx HL, Lee P, Goldgaber D, Gajdusek DC, et al. Prospect hill virus: Serologic evidence for infection in mammologists. *N Engl J Med.* 1984; 310:1325-1326.

Yanagihara R, Amyx L Gajdusek DC. Experimental infection with Puumala virus, the etiologic agent of nephropathia epidemica, in bank voles (*Clethrionomys glareolus*). *J Virol.* 1985; 55:34-8.

Yanagihara R, Goldgaber D, Gajdusek DC. Propagation of nephropathia epidemica virus in Mongolian gerbils. *J Virol.* 1985; 53:973e5.

Yashina LN, Abramov SA, Gutorov VV, Dupal TA, Krivopalov AV, Panov VV, et al. Seewis virus: phylogeography of a shrew-borne hantavirus in Siberia, Russia. *Vector Borne and Zoonotic Dis.* 2010; 10:585e91.

Zelená H, Mrázek J, Kuhn T. Tula hantavirus infection in immunocompromised host, Czech Republic. *Emerg Infect Dis.* 2013; 19(11):1873-1875.

Zhang YZ. Discovery of hantaviruses in bats and insectivores and the evolution of the genus Hantavirus. *Virus Res.* 2014; 187:15-21.

Zhang YZ, Zou Y, Fu ZF, Plyusnin A. Hantavirus infections in humans and animals, China. *Emerg Infect Dis.* 2010; 16(8):1195-203.

Zou Y, Hu J, Wang ZX, Wang DM, Yu C, Zhou JZ, et al. Genetic characterization of hantaviruses isolated from Guizhou, China: evidence for spillover and reassortment in nature. *J Med Virol.* 2008;80:1033e41.

LIST OF ABBREVIATIONS AND ACRONYMS

aa	Amino Acid
agRNAs	anti-genomic RNAs
AIC	Akaike information criteria
AI	association index
ANDV	Andes virus
ARQV	Araraquara virus
BIC	Bayesian information criteria
BLAST	Basic Local Alignment Search Tool
BD	Brownian diffusion
BEAST	Bayesian Evolutionary Analysis by Sampling Trees
CPE	cytopathic effect
CTMC	continous-time Markov chain
DT	decision theory method
dS	Synonymous substitutions
dN	non-synonymous substitutions
D3	Data Driven Document
dLRT	dynamical likelihood ratio tests
DNA	Deoxyribonucleic Acid
DOBV	Dobrava Belgrade virus
FDA	Food and drug administration agency
FEL	fixed-effects likelihood
FASTA	text-based format for representing nucleotide sequences
GTR +G+I	gamma-distributed rate heterogeneity and a proportion of invariant sites
GPC	glycoprotein precursor
gRNAs	genomic RNAs
hLRT	Hierarchical likelihood ratio tests
HTNV	Hantaan virus
HFRS	hemorrhagic fever with renal syndrome

HPS	hantavirus pulmonary syndrome
ICTV	International Committee on Taxonomy of Viruses
JSON	java script object
KHG	Korean hemorrhagic fever
MC	maximum exclusive single-state clade size
MLE	marginal likelihoods
MP	Maximum Parsimony
MCMC	Markov chain Monte Carlo
MCC	maximum clade credibility
mRNAs	messenger RNAs
ML	Maximum Likelihood
NVAV	Nova virus
NCBI	National Center for Biotechnology Information
NEXUS	text-based format for representing nucleotide sequences
NE	Nephropathia Epidemica
NJ	Neighbor- Joining
NCR	non-coding sequence
NAO	North Atlantic Oscillation
ORFs	open reading frame
PS	path sampling
PS	parsimony score
PSTs	posterior sets of trees
PUUV	Puumala virus
PHV	Prospect Hil virus
ORFs	open reading frame
PHYLIP	text-based format for representing nucleotide sequences
RNA	Ribonucleic Acid
RdRp	RNA-dependent RNA polymerase
RDP	Recombination Detection Program
RT-PCR	reverse transcriptase polymerase chain reaction
REL	random effects likelihood

RDP4	Recombination Detection Program version 4
RRWs	relaxed random walks
Spread3	Spatial Phylogenetic Reconstruction of Evolutionary Dynamics
SLAC	single likelihood ancestor counting
SAAV	Saaremaa virus
SEOV	Seoul virus
SANGV	Sangassou virus
SNV	Sin Nombre virus
SS	stepping stone sampling
TIM2 + I	transitional model 2 of nucleotide substitution and a proportion of invariant sites
TIM2+G+I	transitional model with gamma-distributed rate heterogeneity and a proportion of invariant sites
TPM1uf +G+I	threeparameter model with gamma-distributed rate heterogeneity and a proportion of invariant sites
TrN + G	Tamura-Nei model with gamma-distributed rate heterogeneity
TPM2u + G	3-parameter model 2 and gamma distributed rate heterogeneity
TrN93	Tamura-Nei model
TAE	Tris-acetate-EDTA
TPMV	Thottapalayam virus
TMRCA	the most recent common ancestor
TULV	Tula virus
VESPA	viral epidemiology signature pattern analysis
vRdRp	viral RNA-dependent RNA polymerase

APPENDIX

Table AI. List of trapped rodents together with sampling location and year of trapping.

Host species	Number of animals	Location	Year
<i>Apodemus flavicollis</i>	50	Ravanica River	2007
<i>Apodemus agrarius</i>	14	Ravanica River	2007
<i>Apodemus sylvaticus</i>	8	Ravanica River	2007
<i>Myodes glareolus</i>	17	Ravanica River	2007
<i>Microtus arvalis</i>	8	Ravanica River	2007
<i>Glis glis</i>	4	Ravanica River	2007
<i>Apodemus flavicollis</i>	33	Tara Mountain	2008
<i>Apodemus flavicollis</i>	14	Kosutnjak	2008
<i>Apodemus flavicollis</i>	11	Lisine	2008
<i>Apodemus flavicollis</i>	16	Tara Mountain	2009
<i>Apodemus flavicollis</i>	8	Kosutnjak	2009
<i>Apodemus flavicollis</i>	15	Avala Mountain	2009
<i>Apodemus flavicollis</i>	17	Cer Mountain	2009
<i>Apodemus flavicollis</i>	3	Lisine	2009
<i>Apodemus flavicollis</i>	32	Zajecar	2009
<i>Apodemus sylvaticus</i>	8	Zajecar	2009
<i>Myodes glareolus</i>	3	Zajecar	2009
<i>Microtus subterraneus</i>	1	Zajecar	2009
<i>Glis glis</i>	2	Zajecar	2009
<i>Mus musculus</i>	2	Zajecar	2009
<i>Apodemus flavicollis</i>	1	Tara Mountain	2010
<i>Apodemus flavicollis</i>	35	Kosutnjak	2010
<i>Apodemus flavicollis</i>	17	Avala Mountain	2010
<i>Apodemus flavicollis</i>	3	Cer Mountain	2010
<i>Apodemus flavicollis</i>	12	Vranje	2010
<i>Apodemus flavicollis</i>	7	Ravanica River	2011
<i>Apodemus agrarius</i>	1	Ravanica River	2011
<i>Myodes glareolus</i>	7	Ravanica River	2011
<i>Glis glis</i>	1	Ravanica River	2011

Table AII. Accession numbers of all sequences, including newly detected and those retrieved from NCBI database included in the study

DOBV	L segment	NC005235	Af	GR	99
DOBV	L segment	JQ026206	Af	DE	08
DOBV	L segment	KF536033	Hu	DE	10
DOBV	L segment	KJ425422	Aa	DE	02
DOBV	L segment	KF536031	Hu	DE	08
DOBV	L segment	JF920148	Ap/Hu	RU	09
DOBV	L segment	KM192208	Ap	RU	08
DOBV	L segment	KP878309	Ap	RU	13
DOBV	L segment	KM192209	Ap	RU	08
DOBV	L segment	GU904042	Af	SL	09
DOBV	L segment	KT885041	Af	SL	15
DOBV	L segment	GU904039	Aa	SK	09
DOBV	L segment	AJ410618	Aa	EE	00
DOBV	L segment	KF039740	Hu	TR	10
DOBV	L segment	KF177177	Aa	RS	07
DOBV	L segment	KF177176	Gg	RS	07
DOBV	L segment	KF425495	Af	RS	08
DOBV	L segment	KF425496	Af	RS	08
DOBV	L segment	KF425497	Af	RS	08
DOBV	L segment	KY649161	Hu	CRS	07
DOBV	L segment	KY649167	Hu	CRS	07
DOBV	L segment	KY649175	Hu	WRS	07
DOBV	L segment	KY649172	Hu	CRS	07
DOBV	L segment	KY649168	Hu	CRS	08
DOBV	L segment	KY649174	Hu	CRS	08
DOBV	L segment	KY649163	Hu	SRS	09
DOBV	L segment	KY649164	Hu	SRS	09
DOBV	L segment	KY649173	Hu	CRS	09
DOBV	L segment	KY649176	Hu	ERS	09
DOBV	L segment	KY649165	Hu	WRS	10
DOBV	L segment	KY649162	Hu	SRS	10
DOBV	L segment	KY649169	Hu	SRS	10
DOBV	L segment	KY649177	Hu	NRS	10
DOBV	L segment	KY649178	Hu	ERS	10
DOBV	L segment	KY649170	Hu	SRS	11
DOBV	L segment	KY649171	Hu	SRS	11
DOBV	L segment	KY649166	Hu	BA	11

DOBV	M segment	NC005234	Af	GR	99
DOBV	M segment	AJ410616	Af	GR	99
DOBV	M segment	AY168577	Af	SK	98
DOBV	M segment	GU904035	Af	SI	09
DOBV	M segment	MT-RS1	Af	RS	08
DOBV	M segment	MT-RS2	Aa	RS	08
DOBV	M segment	MT-RS3	Af	RS	08
DOBV	M segment	AY961616	Aa	SK	99
DOBV	M segment	AY168578	Aa	SK	97
DOBV	M segment	AJ009774	Aa	ES	00
DOBV	M segment	GQ205413	Af	DE	08
DOBV	M segment	GQ205412	Aa	DE	08
DOBV	M segment	GQ205410	Af	DE	07
DOBV	M segment	GQ205409	Aa	DE	07
DOBV	M segment	GQ205411	Af	DE	07
DOBV	M segment	JF920149	Hu	RU	09

DOBV	S segment	NC005233	Af	GR	99
DOBV	S segment	KT315637	Af	TR	09
DOBV	S segment	KT315635	Af	TR	09
DOBV	S segment	KT315636	Af	TR	09
DOBV	S segment	KT315640	Af	TR	09
DOBV	S segment	KT315639	Af	TR	09
DOBV	S segment	KT315638	Af	TR	09
DOBV	S segment	KT315642	Af	TR	09
DOBV	S segment	KT885043	Af	SI	15
DOBV	S segment	KC848494	Af	HU	07
DOBV	S segment	KC848495	Af	HU	07
DOBV	S segment	KC848497	Af	HU	07
DOBV	S segment	KC848496	Af	HU	07
DOBV	S segment	KC848498	Af	HU	07
DOBV	S segment	KC848499	Aa	HU	06
DOBV	S segment	KC848500	Aa	HU	06
DOBV	S segment	KC848501	Aa	HU	06
DOBV	S segment	FN813292	Af	HR	03
DOBV	S segment	FN813291	Aa	HR	03
DOBV	S segment	KC676600	Af	HR	08
DOBV	S segment	KC676599	Af	HR	08
DOBV	S segment	KC676593	Af	HR	08
DOBV	S segment	KC676591	Af	HR	08
DOBV	S segment	KC676590	Af	HR	08
DOBV	S segment	KC676589	Af	HR	08
DOBV	S segment	KC676605	As	HR	07
DOBV	S segment	KC676604	Af	HR	07
DOBV	S segment	KC676602	Af	HR	07

DOBV	S segment	KC676598	Af	HR	08
DOBV	S segment	KC676595	Af	HR	08
DOBV	S segment	KC676596	Af	HR	08
DOBV	S segment	KC676597	Af	HR	08
DOBV	S segment	KC676594	Af	HR	08
DOBV	S segment	KC676607	As	HR	07
DOBV	S segment	KF776810	Af	SI	08
DOBV	S segment	KF776809	Af	SI	07
DOBV	S segment	KF776798	Af	SI	07
DOBV	S segment	KF776806	Af	SI	07
DOBV	S segment	KF776829	Af	SI	00
DOBV	S segment	KF776821	Af	SI	08
DOBV	S segment	KF776820	Af	SI	01
DOBV	S segment	KF776812	Af	SI	00
DOBV	S segment	KF776827	Af	SI	02
DOBV	S segment	KF776824	Af	SI	99
DOBV	S segment	KF776818	Af	SI	02
DOBV	S segment	KF776816	Af	SI	01
DOBV	S segment	KF776815	Af	SI	01
DOBV	S segment	KF776808	Af	SI	95
DOBV	S segment	KF776803	Af	SI	02
DOBV	S segment	KF776799	Af	SI	02
DOBV	S segment	KF776828	Af	SI	95
DOBV	S segment	KF776823	Af	SI	95
DOBV	S segment	KF776819	Af	SI	01
DOBV	S segment	KF776817	Af	SI	01
DOBV	S segment	KF776813	Af	SI	95
DOBV	S segment	KF776811	Af	SI	95
DOBV	S segment	KF776814	Af	SI	01
DOBV	S segment	KF776804	Af	SI	99
DOBV	S segment	KF776807	Af	SI	07
DOBV	S segment	KF776805	Af	SI	95
DOBV	S segment	KF776851	Hu	SI	08
DOBV	S segment	KF776795	Hu	SI	12
DOBV	S segment	KF776797	Hu	SI	08
DOBV	S segment	KF776848	Hu	SI	10
DOBV	S segment	KF776845	Hu	SI	08
DOBV	S segment	KF776844	Hu	SI	08
DOBV	S segment	KF776835	Hu	SI	05
DOBV	S segment	KF776832	Hu	SI	00
DOBV	S segment	KF776830	Hu	SI	05
DOBV	S segment	KF776850	Hu	SI	09
DOBV	S segment	KF776838	Hu	SI	07
DOBV	S segment	KF776833	Hu	SI	00
DOBV	S segment	KF776793	Hu	SI	12

DOBV	S segment	KF776837	Hu	SI	07
DOBV	S segment	KF776843	Hu	SI	08
DOBV	S segment	KF776796	Hu	SI	12
DOBV	S segment	KF776794	Hu	SI	12
DOBV	S segment	KF776840	Hu	SI	08
DOBV	S segment	KF776836	Hu	SI	05
DOBV	S segment	KF776831	Hu	SI	01
DOBV	S segment	KF776826	Hu	SI	00
DOBV	S segment	KF776841	Hu	SI	08
DOBV	S segment	KF776839	Hu	SI	08
DOBV	S segment	KF776849	Hu	SI	08
DOBV	S segment	KF776846	Hu	SI	10
DOBV	S segment	KF776842	Hu	SI	08
DOBV	S segment	KT971007	Af	AL	06
DOBV	S segment	KT971006	Af	AL	06
DOBV	S segment	KT971010	Af	AL	06
DOBV	S segment	KT971005	Af	AL	06
DOBV	S segment	KT971009	Af	AL	06
DOBV	S segment	KT971008	Af	AL	06
DOBV	S segment	KT971014	Af	AL	07
DOBV	S segment	KT971013	Af	AL	07
DOBV	S segment	KT971011	Af	AL	07
DOBV	S segment	KT971012	Af	AL	07
DOBV	S segment	KF039739	Hu	TR	10
DOBV	S segment	KP878313	Hu	RU	13
DOBV	S segment	KP878312	Ap	RU	13
DOBV	S segment	JQ026204	Af	DE	08
DOBV	S segment	JF920151	Ap	RU	08
DOBV	S segment	JF920152	Ap	RU	08
DOBV	S segment	JF920150	Hu	RU	09
DOBV	S segment	GU904029	Af	SI	09
DOBV	S segment	EU562989	Aa	RU	05
DOBV	S segment	EU562991	Aa	RU	05
DOBV	S segment	EU562990	Aa	RU	05
DOBV	S segment	AF442622	Ap	RU	00
DOBV	S segment	AF442623	Hu	RU	00
DOBV	S segment	GQ205407	Aa	DE	08
DOBV	S segment	GQ205408	Af	DE	08
DOBV	S segment	GQ205405	Aa	DE	05
DOBV	S segment	GQ205401	Aa	DE	07
DOBV	S segment	GQ205403	Aa	DE	07
DOBV	S segment	GQ205406	Af	DE	05
DOBV	S segment	GQ205404	Aa	DE	07
DOBV	S segment	GQ205402	Af	DE	07
DOBV	S segment	EU188449	Ap	RU	01

DOBV	S segment	EU188452	Aa	RU	02
DOBV	S segment	AJ410619	Af	GR	99
DOBV	S segment	AJ131672	Aa	RU	98
DOBV	S segment	AJ131673	Aa	RU	98
DOBV	S segment	AJ616854	Aa	DK	00
DOBV	S segment	AY168576	Af	SK	98
DOBV	S segment	AJ269549	Aa	SK	98
DOBV	S segment	AJ269550	Aa	SK	98
DOBV	S segment	AJ269554	Af	SK	XX
DOBV	S segment	AY533120	Aa	SK	01
DOBV	S segment	AY961615	Aa	SK	01
DOBV	S segment	AY533118	Aa	SK	01
DOBV	S segment	AY961618	Aa	SK	01
DOBV	S segment	AJ009775	Aa	EE	97
DOBV	S segment	AJ009773	Aa	EE	96
DOBV	S segment	JQ344114	Aa	DE	09
DOBV	S segment	JF499666	Hu	HR	95
DOBV	S segment	HQ174469	Hu	BG	10
DOBV	S segment	HQ174470	Hu	BG	10
DOBV	S segment	HQ174468	Hu	BG	09
DOBV	S segment	FJ986109	Hu	CZ	08
DOBV	S segment	GQ205398	Aa	RU	02
DOBV	S segment	GQ205396	Hu	RU	07
DOBV	S segment	GQ205394	Hu	RU	07
DOBV	S segment	GQ205397	Hu	RU	07
DOBV	S segment	GQ205395	Hu	RU	07
DOBV	S segment	GQ205393	Hu	RU	07
DOBV	S segment	AF060024	Hu	GR	96
DOBV	S segment	AF060022	Hu	GR	87
DOBV	S segment	AF060020	Hu	GR	87
DOBV	S segment	AF060018	Hu	GR	87
DOBV	S segment	AF060016	Hu	GR	85
DOBV	S segment	AF060014	Hu	GR	86
DOBV	S segment	AF060023	Hu	GR	86
DOBV	S segment	AF060021	Hu	GR	89
DOBV	S segment	AF060019	Hu	GR	90
DOBV	S segment	AF060017	Hu	GR	85
DOBV	S segment	AF060015	Hu	GR	85
DOBV	S segment	AF039525	Hu	GR	90
DOBV	S segment	FN377828	Aa	HU	00
DOBV	S segment	FN377826	Af	HU	00
DOBV	S segment	AJ251996	Af	SI	90
DOBV	S segment	AJ251997	Af	SI	93
DOBV	S segment	KJ154958	Hu	SRS	13
DOBV	S segment	KF425493	Af	WRS	08

DOBV	S segment	KF425494	Af	WRS	08
DOBV	S segment	KJ437510	Aa	CRS	07
DOBV	S segment	KJ437511	Gg	CRS	07
DOBV	S segment	DQ305280	Hu	SRS	02
DOBV	S segment	DQ305281	Hu	SRS	02
DOBV	S segment	DQ305279	Hu	ME	02
DOBV	S segment	KY649189	Hu	CRS	07
DOBV	S segment	KY649184	Hu	CRS	08
DOBV	S segment	KY649183	Hu	CRS	09
DOBV	S segment	KY649181	Hu	SRS	10
DOBV	S segment	KY649180	Hu	WRS	10
DOBV	S segment	KY649179	Hu	SRS	10
DOBV	S segment	KY649185	Hu	NRS	10
DOBV	S segment	KY649186	Hu	ERS	10
DOBV	S segment	KY649187	Hu	BA	11
DOBV	S segment	KY649188	Hu	SRS	11
DOBV	S segment	KY649182	Hu	SRS	11

TULV	L segment	NC005226	Ma	CZ	95
TULV	L segment	HQ728465	Ma	DE	08
TULV	L segment	HQ728463	Ma	DE	08
TULV	L segment	HQ728461	Ma	DE	08
TULV	L segment	HQ728459	Aa	DE	99
TULV	L segment	HQ728457	Aa	DE	99
TULV	L segment	HQ728455	Aa	SW	09
TULV	L segment	HQ728453	Aa	DE	08
TULV	L segment	HQ728466	Ma	DE	08
TULV	L segment	HQ728464	Ma	DE	08
TULV	L segment	HQ728462	Ma	DE	08
TULV	L segment	HQ728460	Mag	DE	09
TULV	L segment	HQ728458	Aa	DE	99
TULV	L segment	HQ728456	Aa	DE	08
TULV	L segment	HQ728454	Aa	DE	09
TULV	L segment	FJ495102	Ms	SI	97
TULV	L segment	FJ495100	Mag	SI	02
TULV	L segment	FJ495101	Ma	SI	99
TULV	L segment	FJ495099	Ma	SI	01
TULV	L segment	AJ005637	Ma	CZ	95
TULV	L segment	KF177178	Ma	RS	07

TULV	S segment	Z69991	CZE	MOR	95
TULV	S segment	Z48741	CZE	MOR	94
TULV	S segment	Z48573	CZE	MOR	94
TULV	S segment	Z30945	RUS	TUL	87
TULV	S segment	Z30944	RUS	TUL	87

TULV	S segment	Z30943	RUS	TUL	87
TULV	S segment	Z30942	RUS	TUL	87
TULV	S segment	Z30941	RUS	TUL	87
TULV	S segment	Y13980	SVK	KOS	95
TULV	S segment	Y13979	SVK	KOS	95
TULV	S segment	U95305	AUT	KOR	95
TULV	S segment	U95304	AUT	WEL	95
TULV	S segment	U95303	AUT	WEL	95
TULV	S segment	U95302	AUT	WEL	95
TULV	S segment	NC005227	CZE	MOR	94
TULV	S segment	KU139605	FRA	MIL	12
TULV	S segment	KU139604	FRA	ELS	12
TULV	S segment	KU139603	LUX	LUX	12
TULV	S segment	KU139602	LUX	LUX	12
TULV	S segment	KU139601	DEU	KOB	12
TULV	S segment	KU139598	DEU	THE	06
TULV	S segment	KU139597	DEU	SOE	09
TULV	S segment	KU139596	DEU	RUE	09
TULV	S segment	KU139595	DEU	RUE	09
TULV	S segment	KU139594	DEU	GRI	11
TULV	S segment	KU139593	DEU	MUE	07
TULV	S segment	KU139592	DEU	MUE	07
TULV	S segment	KU139591	DEU	MUE	07
TULV	S segment	KU139590	DEU	MUE	07
TULV	S segment	KU139589	DEU	LAU	13
TULV	S segment	KU139587	DEU	KIR	12
TULV	S segment	KU139586	DEU	KIR	12
TULV	S segment	KU139585	DEU	KIR	12
TULV	S segment	KU139584	DEU	KIR	12
TULV	S segment	KU139583	DEU	KIR	12
TULV	S segment	KU139582	DEU	BAL	12
TULV	S segment	KU139581	DEU	BAL	12
TULV	S segment	KU139580	DEU	BAL	12
TULV	S segment	KU139579	DEU	TRE	09
TULV	S segment	KU139576	DEU	TRE	09
TULV	S segment	KU139573	DEU	SCH	06
TULV	S segment	KU139572	DEU	GOT	08
TULV	S segment	KU139571	DEU	GOT	07
TULV	S segment	KU139570	DEU	GOT	05
TULV	S segment	KU139569	DEU	GOT	05
TULV	S segment	KU139567	DEU	GOT	08
TULV	S segment	KU139566	DEU	GOT	05
TULV	S segment	KU139565	DEU	SIE	05
TULV	S segment	KU139564	DEU	SIE	08
TULV	S segment	KU139562	DEU	LOH	09

TULV	S segment	KU139561	DEU	KOE	08
TULV	S segment	KU139559	DEU	CUN	06
TULV	S segment	KU139558	DEU	GAT	11
TULV	S segment	KU139557	DEU	MUC	10
TULV	S segment	KU139555	DEU	HUE	09
TULV	S segment	KU139554	DEU	HUE	09
TULV	S segment	KU139553	DEU	GRO	07
TULV	S segment	KU139549	DEU	BIE	09
TULV	S segment	KU139548	DEU	LUG	10
TULV	S segment	KU139547	DEU	CRA	09
TULV	S segment	KU139546	DEU	WAL	04
TULV	S segment	KU139545	DEU	MOR	08
TULV	S segment	KU139544	DEU	MOR	07
TULV	S segment	KU139543	DEU	MOR	07
TULV	S segment	KU139542	DEU	HAU	05
TULV	S segment	KU139541	DEU	HAU	05
TULV	S segment	KU139540	DEU	WOL	08
TULV	S segment	KU139539	DEU	WOL	08
TULV	S segment	KU139538	DEU	WES	08
TULV	S segment	KU139537	DEU	WES	06
TULV	S segment	KU139536	DEU	GOE	10
TULV	S segment	KU139535	DEU	SCH	12
TULV	S segment	KU139534	DEU	SCH	12
TULV	S segment	KU139533	DEU	TRE	07
TULV	S segment	KU139532	DEU	LAU	07
TULV	S segment	KU139531	DEU	HTX	09
TULV	S segment	KU139530	DEU	HTX	09
TULV	S segment	KU139529	DEU	HTX	09
TULV	S segment	KU139528	DEU	HTX	09
TULV	S segment	KU139527	DEU	FRA	07
TULV	S segment	KT946591	FRA	CHE	15
TULV	S segment	KP013578	RUS	KRA	09
TULV	S segment	KP013577	RUS	KRA	11
TULV	S segment	KP013576	RUS	KRA	11
TULV	S segment	KP013575	RUS	KRA	11
TULV	S segment	KP013574	RUS	KRA	11
TULV	S segment	KP013573	RUS	KRA	08
TULV	S segment	KP013572	RUS	KRA	08
TULV	S segment	KP013571	RUS	KRA	08
TULV	S segment	KP013570	RUS	KRA	11
TULV	S segment	KP013569	RUS	KRA	11
TULV	S segment	KP013568	RUS	KRA	08
TULV	S segment	KJ742928	RUS	CRI	09
TULV	S segment	KJ742927	RUS	CRI	09
TULV	S segment	KF776875	SLO	LJU	13

TULV	S segment	KF557547	SRB	RAV	07
TULV	S segment	KF184328	AUT	SAN	08
TULV	S segment	KF184327	AUT	SAN	08
TULV	S segment	HQ697357	DEU	HEU	08
TULV	S segment	HQ697355	DEU	HEU	08
TULV	S segment	HQ697354	DEU	HEU	08
TULV	S segment	HQ697353	DEU	HEU	08
TULV	S segment	HQ697352	DEU	BIE	09
TULV	S segment	HQ697351	DEU	SIE	08
TULV	S segment	HQ697350	DEU	WIN	99
TULV	S segment	HQ697349	DEU	WIE	99
TULV	S segment	HQ697348	DEU	ROE	99
TULV	S segment	HQ697347	DEU	ECK	09
TULV	S segment	HQ697346	DEU	DUE	09
TULV	S segment	HQ697345	SWZ	NOF	09
TULV	S segment	HQ697344	DEU	SCH	08
TULV	S segment	GU300137	DEU	GOT	06
TULV	S segment	GU300135	DEU	GOT	06
TULV	S segment	EU439952	DEU	GOT	05
TULV	S segment	EU439949	DEU	GOT	05
TULV	S segment	EU439948	DEU	GOT	05
TULV	S segment	EU439947	DEU	GOT	05
TULV	S segment	EU439946	DEU	GOT	05
TULV	S segment	DQ768143	DEU	BRA	05
TULV	S segment	DQ662094	DEU	BRA	04
TULV	S segment	DQ662087	DEU	BRA	04
TULV	S segment	AM945879	KAZ	TAL	03
TULV	S segment	AM945878	KAZ	KAR	03
TULV	S segment	AM945877	KAZ	KAR	03
TULV	S segment	AJ223601	SVK	KOZ	94
TULV	S segment	AJ223600	SVK	KOZ	94
TULV	S segment	AF442621	RUS	OMS	97
TULV	S segment	AF442620	RUS	OMS	97
TULV	S segment	AF442619	RUS	OMS	97
TULV	S segment	AF442618	RUS	OMS	98
TULV	S segment	AF289821	DEU	COT	98
TULV	S segment	AF289820	DEU	COT	98
TULV	S segment	AF289819	DEU	COT	98
TULV	S segment	AF164094	CRO	ZAG	95
TULV	S segment	AF164093	DEU	GRA	97
TULV	S segment	AF063892	POL	LOD	95
TULV	S segment	AF017659	SRB	BEL	87

BIOGRAPHY

Valentina (Slobodan) Ćirković was born on the 7th of May, 1985 in Čačak, where she finished Elementary and High School. She enrolled at the Faculty of Biology, University of Belgrade, study program Biology of Microorganisms in 2004/05 and graduated in 2010, with the average mark of 9.06/10.0. Her Master's thesis was a part of investigation of the genotoxic potential of Danube River.

Valentina Ćirković has enrolled at the PhD studies, study program "Molecular Medicine" at the Faculty of Medicine, University of Belgrade in 2010. From January 2011 she has been employed at the Institute of Microbiology and Immunology, Faculty of Medicine, University of Belgrade as PhD candidate and research assistant within the scientific project entitled "Phylogenetic analysis and molecular evolution in highly variable viruses: coinfections, host-pathogene interaction" funded by Ministry of Education, Science and Technological Development of the Republic of Serbia, grant No 175024.

Valentina Ćirković is the coauthor of 16 articles indexed in Current Contents-u (CC) or Science Citation Index (SCI). In four articles she is the first author.

BIOGRAFIJA

Valentina (Slobodan) Ćirković je rođena 7. maja 1985. godine u Čačku, gde je završila osnovnu i srednju školu. Biološki fakultet Univerziteta u Beogradu upisuje školske 2004/05. godine kao redovan student, a završava ga 2010. godine sa prosečnom ocenom studiranja 9.06/10. Njen diplomski rad bio je deo projekta koji se odnosio na genotoksični potencijal uzoraka Dunava.

Valentina Ćirković 2010. godine upisuje doktorske studije na Medicinskom fakultetu Univerziteta u Beogradu, na studijskom programu “Molekularna medicina”. Od januara 2011. godine zaposlena je na Institutu za mikrobiologiju i imunologiju Medicinskog fakulteta, Univerziteta u Beogradu kao doktorand i istraživač saradnik na naučno istraživačkom projektu broj 175024 pod nazivom “Filogenetski pristup analizi molekularne evolucije visoko varijabilnih virusa – koinfekcije, interakcija virusa i domaćina” koji je finansiran od strane Ministarstva prosvete, nauke i tehnološkog razvoja Republike Srbije.

Valentina Ćirković je koautor 16 radova koji su koji je indeksirani u Current Contents–u (CC) ili Science Citation Index–u (SCI). Prvi je autor u četiri rada.

Prilog 1.

Izjava o autorstvu

Potpisani-a Valentina Ćirković

broj upisa MM03/10

Izjavljujem

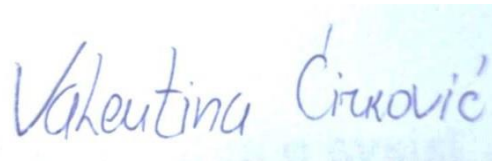
da je doktorska disertacija pod naslovom:

**„Filogenetska analiza molekularne evolucije hantavirusa u različitim
vrstama glodara”**

- rezultat sopstvenog istraživačkog rada,
- da predložena disertacija u celini ni u delovima nije bila predložena za dobijanje bilo koje diplome prema studijskim programima drugih visokoškolskih ustanova,
- da su rezultati korektno navedeni i
- da nisam kršio/la autorska prava i koristio intelektualnu svojinu drugih lica.

Potpis doktoranda

U Beogradu, 07.03.2018. godine



Valentina Ćirković

Prilog 2.

**Izjava o istovetnosti štampane i elektronske verzije
doktorskog rada**

Ime i prezime autora Valentina Ćirković

Broj upisa MM03/10

Studijski program Molekularna medicina

Naslov rada „Filogenetska analiza molekularne evolucije hantavirusa u različitim vrstama glodara“

Mentori Prof. dr Maja Stanojević

Dr Gorana Stamenković

Potpisani Valentina Ćirković

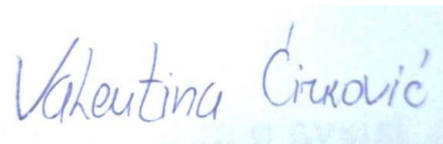
izjavljujem da je štampana verzija mog doktorskog rada istovetna elektronskoj verziji koju sam predao/la za objavljivanje na portalu **Digitalnog repozitorijuma Univerziteta u Beogradu.**

Dozvoljavam da se objave moji lični podaci vezani za dobijanje akademskog zvanja doktora nauka, kao što su ime i prezime, godina i mesto rođenja i datum odbrane rada.

Ovi lični podaci mogu se objaviti na mrežnim stranicama digitalne biblioteke, u elektronskom katalogu i u publikacijama Univerziteta u Beogradu.

Potpis doktoranda

U Beogradu, 07.03.2018. godine



Valentina Ćirković

Prilog 3.

Izjava o korišćenju

Ovlašćujem Univerzitetsku biblioteku „Svetozar Marković“ da u Digitalni repozitorijum Univerziteta u Beogradu unese moju doktorsku disertaciju pod naslovom:

„Filogenetska analiza molekularne evolucije hantavirusa u različitim vrstama glodara“

koja je moje autorsko delo.

Disertaciju sa svim priložima predao/la sam u elektronskom formatu pogodnom za trajno arhiviranje.

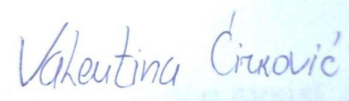
Moju doktorsku disertaciju pohranjenu u Digitalni repozitorijum Univerziteta u Beogradu mogu da koriste svi koji poštuju odredbe sadržane u odabranom tipu licence Kreativne zajednice (Creative Commons) za koju sam se odlučio/la.

1. Autorstvo
2. Autorstvo - nekomercijalno
- 3. Autorstvo – nekomercijalno – bez prerade**
4. Autorstvo – nekomercijalno – deliti pod istim uslovima
5. Autorstvo – bez prerade
6. Autorstvo – deliti pod istim uslovima

(Molimo da zaokružite samo jednu od šest ponuđenih licenci, kratak opis licenci dat je na poledini lista).

Potpis doktoranda

U Beogradu, 07.03.2018. godine



1. Autorstvo - Dozvoljavate umnožavanje, distribuciju i javno saopštavanje dela, i prerade, ako se navede ime autora na način određen od strane autora ili davaoca licence, čak i u komercijalne svrhe. Ovo je najslobodnija od svih licenci.
2. Autorstvo – nekomercijalno. Dozvoljavate umnožavanje, distribuciju i javno saopštavanje dela, i prerade, ako se navede ime autora na način određen od strane autora ili davaoca licence. Ova licenca ne dozvoljava komercijalnu upotrebu dela.
3. Autorstvo - nekomercijalno – bez prerade. Dozvoljavate umnožavanje, distribuciju i javno saopštavanje dela, bez promena, preoblikovanja ili upotrebe dela u svom delu, ako se navede ime autora na način određen od strane autora ili davaoca licence. Ova licenca ne dozvoljava komercijalnu upotrebu dela. U odnosu na sve ostale licence, ovom licencom se ograničava najveći obim prava korišćenja dela.
4. Autorstvo - nekomercijalno – deliti pod istim uslovima. Dozvoljavate umnožavanje, distribuciju i javno saopštavanje dela, i prerade, ako se navede ime autora na način određen od strane autora ili davaoca licence i ako se prerada distribuira pod istom ili sličnom licencom. Ova licenca ne dozvoljava komercijalnu upotrebu dela i prerada.
5. Autorstvo – bez prerade. Dozvoljavate umnožavanje, distribuciju i javno saopštavanje dela, bez promena, preoblikovanja ili upotrebe dela u svom delu, ako se navede ime autora na način određen od strane autora ili davaoca licence. Ova licenca dozvoljava komercijalnu upotrebu dela.
6. Autorstvo - deliti pod istim uslovima. Dozvoljavate umnožavanje, distribuciju i javno saopštavanje dela, i prerade, ako se navede ime autora na način određen od strane autora ili davaoca licence i ako se prerada distribuira pod istom ili sličnom licencom. Ova licenca dozvoljava komercijalnu upotrebu dela i prerada. Slična je softverskim licencama, odnosno licencama otvorenog koda.